PATENT
Docket No.: **34116/1051**

IN THE UNITED STATES PATENT AND TRADEMARK OFFICE

Applicants	:	Margolskee et al.	Examiner: Sharon L. Turner
Serial No.	:	09/834,792	
Cnfrm. No.	:	8395	Art Unit: 1649
Filed	:	April 13, 2001	
For	:	TRP8, A TRANSIENT RECEPTOR POTENTIAL CHANNEL EXPRESSED IN TASTE RECEPTOR CELLS	

DECLARATION OF ROBERT W. BRYANT, Ph.D., UNDER 37 CFR § 1.132

Mail Stop Amendment
Commissioner for Patents
P.O. Box 1450
Alexandria, VA 22313-1450

Dear Sir:

I, ROBERT W. BRYANT, Ph.D., pursuant to 37 CFR § 1.132, declare:

1. I hold a B.S. degree in polymer chemistry from SUNY College of Environmental Science and Forestry at Syracuse University, and a Ph.D. in biochemistry from Florida State University. I was a Postdoctoral Fellow in natural product biosynthesis at the University of Pittsburgh, and an Associate Research Professor of biochemistry at the George Washington University Medical School.

2. I spent 21 years directing research, assay design, and assay implementation for high-throughput screening in the New Leads Discovery and Allergy-Inflammation departments at the Schering-Plough Research Institute.

3. I am currently Vice President of Discovery Research at Linguagen Corporation, 2005 Eastpark Boulevard, Cranbury, New Jersey, 08512-3515.

4. Linguagen Corporation is a licensee of the above-identified patent application.

5. I am presenting this declaration to demonstrate that TRP8 is involved in bitter taste transduction and that membrane potential may be used to measure TRP8 activation.

6. Two groups of mice were tested for their aversion to denatonium and quinine, two bitter compounds, using a short access lickometer test, which measures the frequency with which the mice lick solutions containing varying concentrations of tastants. As shown in Figure 1 (left panel), the lick ratio of the wild type mice ("WT control") steadily decreased from 1.0 to 0.1 licks per interval as the concentration of denatonium increased from 0.1 mM to about 4 mM. The lick ratio of the TRP8 knockout mice ("TRP8 KO"), however, did not fall below 1.0 until the denatonium concentration reached about 10 mM. Similarly, as shown in Figure 1 (right panel) the lick ratio of the wild type mice steadily decreased from about 0.7 to about 0.1 licks per interval as the concentration of quinine hydrochloride increased from 0.01 mM to about 10 mM. The lick ratio of the TRP8 knockout mice, however, did not fall below 0.6 until the quinine hydrochloride concentration reached 1 mM, and never fell below 0.5. Thus, the TRP8 knockout mice showed a decreased aversion to both bitter compounds compared to the response of the wild-type mice. These data demonstrate that TRP8 is involved in bitter taste transduction.

Figure 1. TRP8 Knockout Mice Show Diminished Aversion to Bitter Compounds

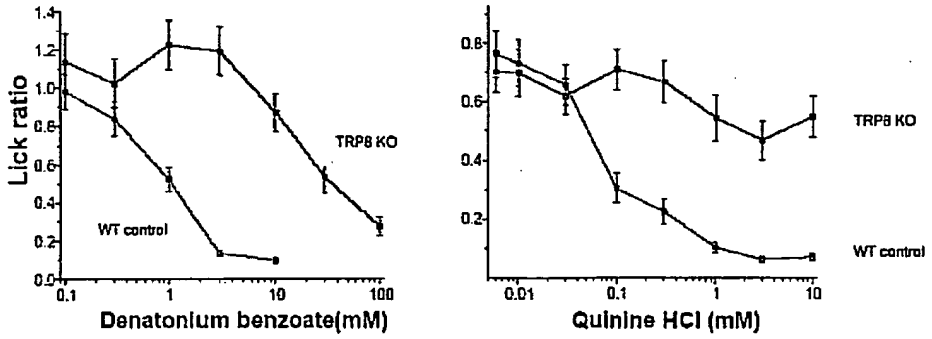

short access lickometer tests

7. Membrane potential is the electrical potential across the cell membrane resulting from the difference in the concentration of charged ions, *i.e.*, net charge, on each side of a membrane. ALBERTS ET AL., ESSENTIAL CELL BIOLOGY 376–377 (1997) (Exhibit 1). In mammalian cells, including taste cells, the cytoplasmic side of the plasma membrane is usually at a negative potential relative to the outside, *i.e.*, there is generally a net negative charge on the internal side of the membrane and a net positive charge external the membrane. *See* ALBERTS at 372–373; Kinnamon & Roper, "Passive and Active Membrane Properties of Mudpuppy Taste Receptor Cells," *J. Physiol.* 383:601–614 (1987) (Exhibit 2). Thus, an increase in intracellular cations, *e.g.*, calcium or others, would reduce the net negative charge inside the cell, thereby decreasing the membrane potential, *i.e.*, causing cell depolarization. Cell depolarization is also a process often associated with transmitter release in sensory cells. PRINCIPLES OF NEURAL SCIENCE 253–279 (Eric R. Kandel et al. eds., 4th ed. McGraw-Hill Co. 2000) (Exhibit 3). U.S. Patent Application No. 09/834,792 to Margolskee et al. ("Margolskee") teaches that TRP8 activation is associated with increased levels of intracellular calcium and with transmitter release. Margolskee ¶¶ [0011], [0060]. Thus, considering that TRP channels were known to be by and large non-selective cation channels, Zhang et al., "Increased Inwardly Rectifying Potassium Currents in HEK-293 Cells Expressing Murine Transient Receptor Potential 4," *Biochem. J.* 354(Pt 3):717–725 (2001) (Exhibit 4), and the known relationships between cation entry and membrane potential and between depolarization and transmitter release, this teaches that an increase in the level of TRP8 activation would be associated with a decrease in membrane potential.

8. The effect of carbachol (a surrogate bitter tastant) on membrane potential in wild type HEK 293 cells and HEK 293 cells transfected with TRP8 was evaluated. As illustrated in Figure 2, carbachol activates the M1 G-protein-coupled receptor ("M1 GPCR"), leading to activation of TRP8, which in turn results in an increase in the fluorescence signal of the membrane potential dye. This increased fluorescence signal is indicative of a decrease in the cell membrane potential caused by opening of a cation channel. As shown in Figure 3, after exposure to 30 μM carbachol ("Carb."), cells transfected with TRP8 ("TRP8 Transfectants") exhibited an increase from 0 to about 70,000 fluorescence units ("RFU"). This signal increase is indicative of cell depolarization where positive ions enter the cell and decrease the membrane potential. In contrast, wild type cells ("Sham Transfectants") exhibited very little change in fluorescence response and hence membrane

potential. These data demonstrate that membrane potential may be used to measure activation of TRP8.

Figure 2. TRP8 Activation by Bitter Compounds

Figure 3. A Cell-Based Assay Utilizing Cloned mTRP8: Sham vs. Transfectant Reponses

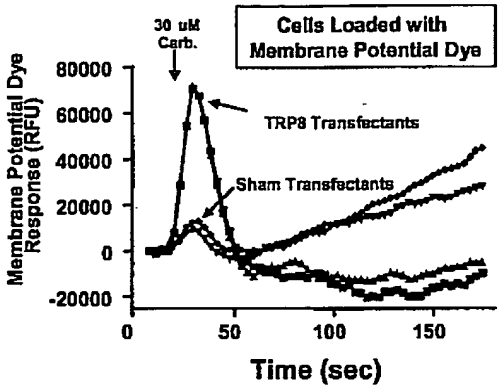

9. I hereby declare that all statements made herein of my own knowledge are true and that all statements made on information and belief are believed to be true; and further that these statements were made with the knowledge that willful false statements and the like so made are punishable by fine or imprisonment, or both, under section 1001 of Title 18 of the United States Code, and that such willful false statements may jeopardize the validity of the application or any patent issuing thereon.

9/20/2006
Date

R. W. Bryant
Robert W. Bryant

Essential Cell Biology

An Introduction to the Molecular Biology of the Cell

Bruce Alberts
Dennis Bray
Alexander Johnson
Julian Lewis
Martin Raff
Keith Roberts
Peter Walter

Garland Publishing, Inc.
New York & London

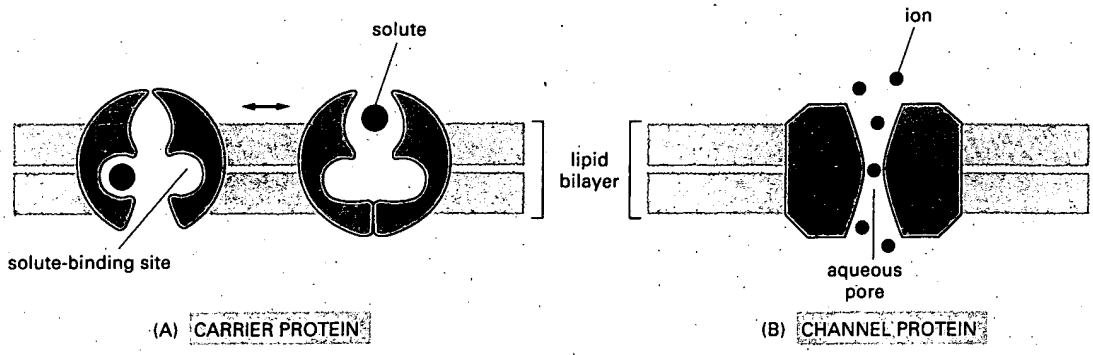

Figure 12–2 **A schematic view of the two classes of membrane transport proteins.** A carrier protein undergoes a series of conformational changes to transfer small water-soluble molecules across the lipid bilayer. In contrast, a channel protein forms a hydrophilic pore across the bilayer through which specific inorganic ions can diffuse. As would be expected, channel proteins transport at a much greater rate than carrier proteins. Ion channels can exist in either an open or a closed conformation and transport only in the open conformation, which is shown. Their opening and closing is usually controlled by an external stimulus or by conditions within the cell.

Two major classes of membrane transport proteins can be distinguished. *Carrier proteins* bind a solute on one side of the membrane and deliver it to the other side through a change in the conformation of the carrier protein. The solutes transported in this way can be either small organic molecules or inorganic ions. *Channel proteins*, by contrast, form tiny hydrophilic pores in the membrane, through which solutes can pass by diffusion (Figure 12–2). Most channel proteins let through inorganic ions only and are therefore called *ion channels*. Cells can also selectively transfer macromolecules such as proteins across their membranes, but this requires more elaborate machinery, which is discussed in Chapter 14.

In the first section of this chapter we discuss carrier proteins and their functions in solute transport. In the second section we consider the behavior and functions of ion channels. Because ions are electrically charged, their movements can create powerful electric forces across the membrane. These forces enable nerve cells to carry out electrical signaling, as we discuss in the final section.

To provide a foundation for these discussions, we begin by considering the differences in intracellular ion composition between a cell and its environment. This will help make it clear why the transport of ions by both carrier proteins and ion channels is of such fundamental importance to cells.

The Ion Concentrations Inside a Cell Are Very Different from Those Outside

Ion transport across cell membranes is of central importance in biology. Cells maintain an internal ion composition that is very different from that in the fluid around them, and these differences are crucial for a cell's survival and function. Inorganic ions such as Na^+, K^+, Ca^{2+}, Cl^-, and H^+ (protons) are the most plentiful of all the solutes in a cell's environment, and their movements across cell membranes play an essential part in many cell processes. Animal cells, for example, pump Na^+ outward across their plasma membrane to keep the internal concentration of Na^+ low. This pumping helps balance the osmotic pressures on the two sides of the membrane: if the pumping fails, water flows into the cell by osmosis and causes it to swell and burst. Ion movements across cell membranes also play fundamental roles in the functioning of nerve cells, as we discuss later, and in the production of ATP by all cells, as we discuss in Chapter 13.

The ion concentrations inside and outside a typical mammalian cell are shown in Table 12–1. Na^+ is the most plentiful positively charged ion

Table 12–1 **Comparison of Ion Concentrations Inside and Outside a Typical Mammalian Cell**

Component	Intracellular Concentration (mM)	Extracellular Concentration (mM)
Cations		
Na^+	5–15	145
K^+	140	5
Mg^{2+}*	0.5	1–2
Ca^{2+}*	10^{-7}	1–2
H^+	7×10^{-5} ($10^{-7.2}$ M or pH 7.2)	4×10^{-5} ($10^{-7.4}$ M or pH 7.4)
Anions		
Cl^-	5–15	110
Fixed anions**	high	0

*The concentrations of Ca^{2+} and Mg^{2+} given are for the free ions in the cytosol. There is a total of about 20 mM Mg^{2+} and 1–2 mM Ca^{2+} in cells, but this is mostly bound to proteins and other substances and thus cannot leave the cell. Much of the total cell Ca^{2+} is stored within various organelles.

**The fixed anions are the negatively charged small and large organic molecules that are trapped inside the cell, being unable to cross the plasma membrane.

(cation) outside the cell, while K^+ is the most plentiful inside. If a cell is not to be torn apart by electrical forces, the quantity of positive charge inside the cell must be balanced by an almost exactly equal quantity of negative charge, and the same is true for the charge in the surrounding fluid. (Tiny excesses of positive or negative charge, concentrated in the neighborhood of the plasma membrane, are allowed and have important electrical effects, as we discuss later.)

The high concentration of Na^+ outside the cell is balanced chiefly by extracellular Cl^-. The high concentration of K^+ inside is balanced by a variety of negatively charged intracellular ions (anions). In fact, most intracellular constituents are negatively charged: in addition to Cl^-, cells contain inorganic ions such as bicarbonate (HCO_3^-) and phosphate (PO_4^{3-}), organic metabolites carrying negatively charged phosphate and carboxyl (COO^-) groups, and macromolecules such as proteins and nucleic acids that also carry numerous phosphate and carboxyl groups. The negatively charged organic molecules are sometimes called "fixed anions" because they are unable to escape from the cell by crossing the plasma membrane.

Carrier Proteins and Their Functions

Carrier proteins are required for the transport of almost all small organic molecules across cell membranes, with the exception of fat-soluble molecules and small uncharged molecules that can pass directly through the lipid bilayer by *simple diffusion*. Each carrier protein is highly selective, often transporting just one type of molecule. To guide and propel the complex traffic of small molecules into and out of the cell and between the cytosol and the different membrane-bounded organelles, each cell membrane contains a set of different carrier proteins appropriate to that particular membrane. Thus in the plasma membrane there are carriers to import nutrients such as sugars, amino

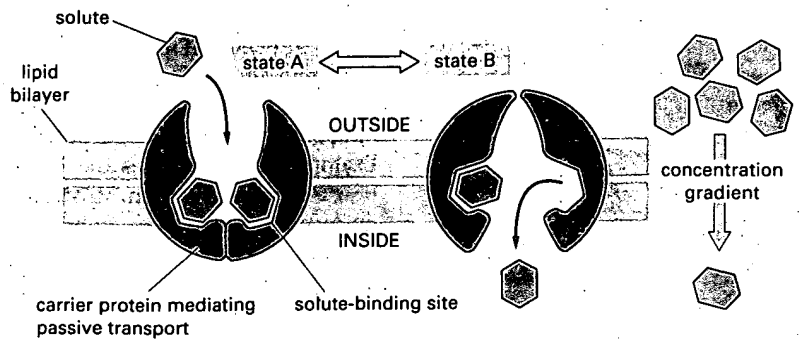

Figure 12–6 **A hypothetical model showing how a conformational change in a carrier protein could mediate the passive transport of a solute like glucose.** The carrier protein can exist in two conformational states: in state A the binding sites for the solute are exposed on the outside of the membrane; in state B the same sites are exposed on the other side of the membrane. The transition between the two states is proposed to occur randomly and independently of whether the solute is bound and to be completely reversible. If the concentration of the solute is higher on the outside of the membrane, it will be more often caught up in A → B transitions that carry it into the cell than in B → A transitions that carry it out, and there will be a net transport of the solute down its concentration gradient.

adopt at least two conformations and switches reversibly and randomly between them. In one conformation the carrier exposes binding sites for glucose to the exterior of the cell; in the other it exposes this site to the interior of the cell (Figure 12–6).

When glucose is plentiful outside the liver cell (after a meal), glucose molecules bind to the externally displayed binding sites; when the protein switches conformation, it carries these molecules inward and releases them into the cytosol, where the glucose concentration is low. Conversely, when blood sugar levels are low (when you are hungry), the hormone glucagon stimulates the liver cell to produce large amounts of glucose by the breakdown of glycogen. As a result, the glucose concentration is higher inside the cell than outside, and glucose binds to any internally displayed binding sites on the carrier protein; when the protein switches conformation in the opposite direction, the glucose is transported out of the cell. The flow of glucose can thus go either way, according to the direction of the glucose *concentration gradient* across the membrane—inward if glucose is more concentrated outside the cell than inside, and outward if the opposite is true. Transport proteins of this type, which permit a flux of solute but play no part in determining its direction, carry out passive transport. Although passive, the transport is highly selective: the binding sites in the glucose transporter bind only D-glucose and not, for example, its mirror image L-glucose, which the cell cannot use for glycolysis.

For glucose, which is an uncharged molecule, the direction of passive transport is determined simply by the concentration gradient. For electrically charged molecules, either small organic ions or inorganic ions, an additional force comes into play. For reasons we explain later, most cell membranes have a voltage across them, a difference in the electrical potential on each side of the membrane, which is referred to as the *membrane potential*. This exerts a force on any molecule that carries

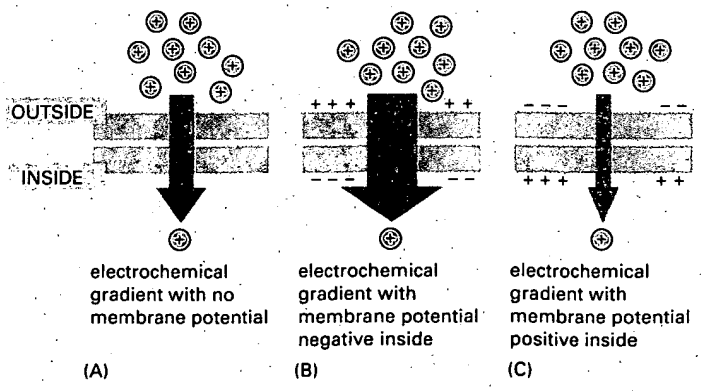

Figure 12–7 **The two components of the electrochemical gradient.** The net driving force (the electrochemical gradient) tending to move a charged solute (ion) across the membrane is the sum of the concentration gradient of the solute and the voltage across the membrane (the membrane potential). The width of the *green arrow* represents the magnitude of the electrochemical gradient for the same positively charged solute in three different situations. In (A), there is only a concentration gradient. In (B), the concentration gradient is supplemented by a membrane potential that increases the driving force. In (C), the membrane potential decreases the driving force that is caused by the concentration gradient.

an electric charge. The cytoplasmic side of the plasma membrane is usually at a negative potential relative to the outside, and this tends to pull positively charged solutes into the cell and drive negatively charged ones out. At the same time, a charged solute will also tend to move down its concentration gradient.

The net force driving a charged solute across the membrane is therefore a composite of two forces, one due to the concentration gradient and the other due to the voltage across the membrane. This net driving force is called the **electrochemical gradient** for the given solute. It is this gradient that determines the direction of passive transport across the membrane. For some ions, voltage and concentration gradient work in the same direction, creating a relatively steep electrochemical gradient (Figure 12–7B). This is the case with Na^+, for example, which is positively charged and at a higher concentration outside cells than inside. Na^+ therefore tends to enter cells if given a chance. If the voltage and concentration gradients have opposing effects, the resulting electrochemical gradient can be small (Figure 12–7C). This is the case for K^+, a positively charged ion that is present at a much higher concentration inside cells than outside. Because of opposing effects, K^+ has a small electrochemical gradient across the membrane, despite its large concentration gradient, and therefore there is little net movement of K^+ across the membrane.

$Na^+ \Rightarrow$ steep electrochemical gradient
$K^+ \Rightarrow$ small electro- gradient.

Question 12–1 A simple enzyme reaction can be described by the equation $E + S \rightleftharpoons ES \rightarrow E + P$, where E is the enzyme, S the substrate, P the product, and ES the enzyme-substrate complex.

A. Write a corresponding equation describing the workings of a carrier protein (CP) that mediates the transport of a solute (S) down its concentration gradient.

B. What does this equation tell you about carrier protein function?

C. Why would this equation be an inappropriate description of channel protein function?

Active Transport Moves Solutes Against Their Electrochemical Gradients

Cells cannot rely solely on passive transport. Active transport of solutes against their electrochemical gradient is essential to maintain the intracellular ionic composition of cells and to import solutes that are at a lower concentration outside the cell than inside. Cells carry out active transport in three main ways (Figure 12–8): (1) *Coupled transporters* couple the uphill transport of one solute across the membrane to the downhill transport of another. (2) *ATP-driven pumps* couple uphill transport to the hydrolysis of ATP. (3) *Light-driven pumps*, which are found mainly in bacterial cells, couple uphill transport to an input of energy from light, as mentioned earlier for bacteriorhodopsin.

Since a substance has to be carried uphill before it can flow downhill, the different forms of active transport are necessarily linked. Thus in the plasma membrane of an animal cell, an ATP-driven pump transports Na^+ out of the cell against its electrochemical gradient, and the Na^+ then

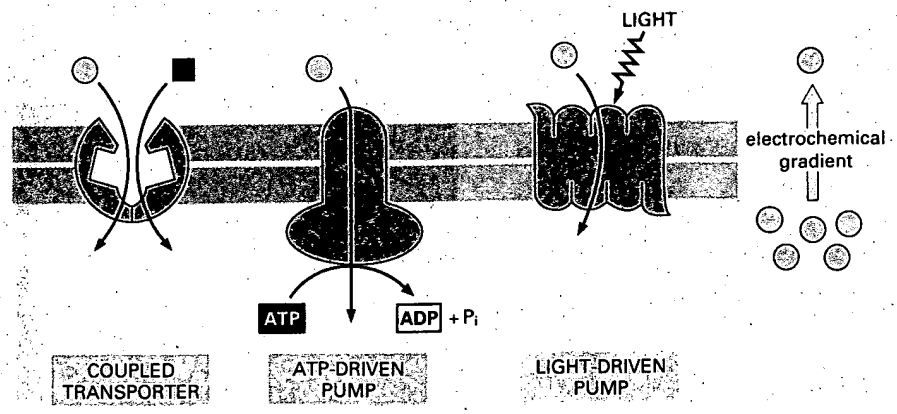

Figure 12–8 Three ways of driving active transport. The actively transported molecule is shown in *yellow*, and the energy source is shown in *red*.

J. Physiol. (1987), **383**, *pp.* 601–614
With 8 text-figures
Printed in Great Britain

PASSIVE AND ACTIVE MEMBRANE PROPERTIES OF MUDPUPPY TASTE RECEPTOR CELLS

BY S. C. KINNAMON AND S. D. ROPER

From the Rocky Mountain Taste and Smell Center, University of Colorado Health Sciences Center, 4200 East 9th Avenue, Denver, CO 80262, and the Department of Anatomy, Colorado State University, Fort Collins, CO 80523, U.S.A.

(*Received 17 March 1986*)

SUMMARY

1. Intracellular recordings were obtained from taste receptor cells and surface epithelial cells of isolated mudpuppy lingual epithelium.

2. Surface epithelial cells had a mean resting potential of $-40{\cdot}2 \pm 8{\cdot}9$ mV, a mean input resistance of $40{\cdot}3 \pm 11{\cdot}3$ MΩ, and a linear current–voltage (I–V) relationship. Taste receptor cells had a mean resting potential of $-61{\cdot}7 \pm 15$ mV, a mean input resistance of $380{\cdot}3 \pm 177{\cdot}2$ MΩ, and the I–V relationship showed pronounced outward rectification; the outward rectification persisted in high-K^+ saline, but was abolished by tetraethylammonium bromide (TEA).

3. Surface epithelial cells responded to depolarizing current injection with only passive membrane potential changes. Taste receptor cells responded to brief pulses of depolarizing current injection with regenerative action potentials characterized by an abrupt rising phase, an inflexion on the falling phase, and a prolonged after-potential.

4. The abrupt rising phase of the action potential was blocked by tetrodotoxin (TTX), suggesting that voltage-gated Na^+ currents are responsible for the rising phase.

5. Long-duration action potentials were elicited from cells treated with TEA to block outward K^+ currents and with TTX to block Na^+ currents, and from cells bathed in isotonic $CaCl_2$. These results suggest that the active membrane response contains a significant Ca^{2+} component.

6. The after-potential was blocked or greatly reduced by the addition of Ca^{2+} channel blockers to the bathing medium. In contrast, addition of TEA to the bathing medium greatly enhanced the after-potential. These data suggest that a significant portion of the after-potential is Ca^{2+} mediated.

7. The mean reversal potential for the after-potential ($-76{\cdot}8 \pm 6{\cdot}0$ mV) was significantly different from the mean reversal potential for the undershoot of the action potential ($-86 \pm 5{\cdot}6$ mV). Superfusion with TEA reduced the reversal potential of the after-potential to $-42{\cdot}3 \pm 8{\cdot}2$ mV and abolished the undershoot. These results suggest that the after-potential results from at least two conductances, one which is blocked by TEA and the other which is Ca^{2+} dependent and involves ions other than, or in addition to K^+.

8. Our data suggest that taste receptor cells, unlike surface epithelial cells, possess voltage-gated Na^+, Ca^{2+}, and K^+ channels, as well as Ca^{2+}-mediated channels. The role of the Ca^{2+} channels may be in part to regulate release of transmitter onto nerve terminals. The role of the other conductances in taste transduction is unknown.

INTRODUCTION

Intracellular recordings from individual sensory receptors have provided important information concerning mechanisms of sensory transduction. In many sensory cells it has been possible to record generator currents, receptor potentials and membrane conductance changes during sensory stimulation. From a number of studies in a variety of tissues it is becoming clear that many sensory receptors have voltage-gated and Ca^{2+}-activated conductances, and can generate action potentials under appropriate conditions (Lewis & Hudspeth, 1983; Corey, Dubinsky & Schwartz, 1984; Ohmori, 1984; Fuchs & Mann, 1986). In addition, there is evidence that these conductances play roles in sensory transduction. For example, pharmacological studies of rod photoreceptor cells have revealed that voltage-sensitive Ca^{2+} and K^+ channels, as well as Ca^{2+}-activated K^+ and Cl^- channels may be important in modulating the light-evoked receptor potential (Bader, Bertrand & Schwartz, 1982). Similar studies of isolated cochlear hair cells suggest that voltage-sensitive Ca^{2+} channels and Ca^{2+}-activated K^+ channels are involved in the electrical tuning mechanism of the hair cell membrane (Lewis & Hudspeth, 1983).

Much less is known about the ionic mechanisms underlying taste transduction. The lack of information concerning taste receptor cells is due in part to the difficulty in recording from the small taste cells of most species. Although intracellular recordings have been made from taste receptor cells in catfish (Teeter & Kare, 1974), frogs (Sato & Beidler, 1975; Akaike, Noma & Sato, 1976; Kashiwayanagi, Miyake & Kurihara, 1983; Sato, Sugimoto, Okada & Miyamoto, 1984), mudpuppies (West & Bernard, 1978), rats (Ozeki, 1971; Ozeki & Sato, 1972) and mice (Tonosaki & Funakoshi, 1984), what has been reported to date is that taste receptor cells generally have low resting potentials (less than -40 mV), low input resistances (17–80 MΩ), linear current–voltage (I–V) relationships and strictly passive membrane properties (however, cf. Roper, 1983; Kashiwayanagi *et al.* 1983). Taste receptor cells respond to a variety of chemical stimuli with depolarizing or hyperpolarizing membrane potential changes, but the ionic conductances underlying these receptor potentials are unknown (Sato, 1980).

We have re-examined the properties of taste receptor cells, using the large taste bud cells of *Necturus maculosus*. By stabilizing the isolated lingual epithelium in a vibration-free chamber and impaling single taste receptor cells under direct visual control, we have obtained data which differ significantly from the results of previous investigators. We report here that taste receptor cells have high resting potentials, high input resistances, non-linear I–V relationships, and most importantly that they produce regenerative action potentials when electrically excited. A preliminary report of these findings has been published (Roper, 1983).

METHODS

Mudpuppies (*Necturus maculosus*) were obtained from commercial suppliers and maintained at 4–10 °C in fresh water aquaria. They were fed minnows or earthworms bi-weekly.

Dissecting and recording procedures were those described by Roper (1983). To recapitulate, animals were rapidly decapitated and the upper jaw removed to expose the tongue. The lingual epithelium was gently freed from the dorsal anterior portion of the tongue by blunt dissection, and then stretched flat in a shallow chamber which had a glass bottom. The chamber was attached to the stage of a fixed-stage microscope equipped with a 40 × water immersion objective and Nomarski differential interference contrast optics. When viewed in this manner (400 ×), entire taste buds, individual taste cells, and even apical processes of single taste cells could be observed. Taste cells were clearly distinguishable from the surrounding epithelial cells by the following criteria: (1) taste cells were long and cylindrical, whereas epithelial cells were cuboidal in shape and (2) taste cells were always contained within the confines of the taste bud, which was clearly visible at 400 ×. Several taste cells have been filled with the dye Lucifer Yellow; dye-filled cells were always within the confines of the taste bud (Yang & Roper, 1986).

The preparation was perfused with an amphibian physiological saline (APS) solution (112 mM-NaCl, 2 mM-KCl, 8 mM-$CaCl_2$, 5 mM-HEPES (*N*-2-hydroxyethylpiperazine-*N'*-ethanesulphonic acid) buffered to pH 7·2 with NaOH) unless otherwise indicated. The elevated Ca^{2+} concentration facilitated stable intracellular impalements. Preparations remained viable for several hours under these conditions, and for up to two days if stored at 4 °C. Tetrodotoxin (TTX) was obtained from Sigma Chemical Corporation; apamin was obtained from Serva Biochemicals; charybdotoxin was a generous gift from Dr Christopher Miller, Brandeis University. All experiments were performed at room temperature (approximately 20 °C).

Micropipettes for intracellular recording had resistances of 50–150 MΩ (filled with 2·5 M-KCl). An agar–APS bridge connected to a AgCl pellet served as a reference electrode. Micro-electrodes were manipulated under visual control at 400 × and inserted into taste receptor cells (through the taste pore) or into surface epithelial cells. Stable impalements could be maintained for several minutes during constant perfusion of the bathing medium (approximately 1 ml/min).

Current was passed through the micro-electrode after carefully balancing the bridge circuit (WPI M4A electrometer with bridge) to obtain *I–V* relationships and to stimulate taste cells. Amplifier leakage currents were frequently checked and nulled to avoid artifacts during membrane potential measurements. Resting potentials were measured at the end of the impalement when the micro-electrode was abruptly and cleanly withdrawn from the cell.

RESULTS

Taste receptor cells (taste cells) of the mudpuppy are found within taste buds located on papillae which are usually spaced 2–3 mm apart on the anterior portion of the tongue. Non-gustatory epithelial cells comprise the remaining lingual epithelium. Since taste cells comprise a renewing neuroepithelial tissue which is derived from the surrounding lingual epithelium, it was of interest to compare membrane properties of taste cells with membrane properties of non-gustatory epithelial cells.

Passive membrane properties

Epithelial cells

Resting potentials obtained from micro-electrode impalements of surface epithelial cells varied from −22 to −60 mV, with a mean value of $-40{\cdot}2 \pm 8{\cdot}9$ mV ($n = 11$). The *I–V* relationship of a typical epithelial cell, obtained by passing a series of hyperpolarizing and depolarizing current pulses through the recording micro-electrode, is shown in Fig. 1*A*. In all cells examined, the *I–V* relationship was linear

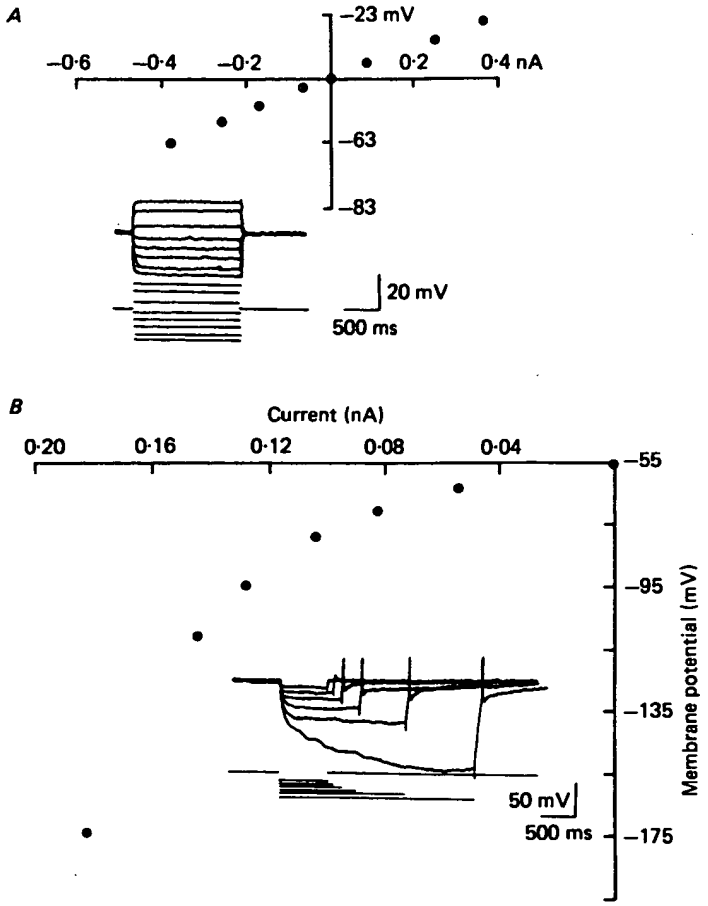

Fig. 1. Typical *I–V* relationships of: *A*, a surface epithelial cell and *B*, a taste cell, obtained by passing current through the micro-electrode. Abscissa, current. Ordinate, membrane potential. Insets: top traces, membrane potential; bottom traces, current monitor. Note that the *I–V* relationship for the epithelial cell is linear, whereas the *I–V* relationship for the taste cell shows outward rectification. In a few experiments, measurements were made with depolarizing currents as well as hyperpolarizing currents. Such cells showed linear *I–V* relationships with depolarizing current pulses until threshold was reached.

at all membrane potentials. The mean input resistance, calculated from the slopes of the individual *I–V* relationships was $40{\cdot}3 \pm 11{\cdot}3$ MΩ ($n = 9$). With an average cell radius of $13{\cdot}7 \times 10^{-4} \pm 7{\cdot}2 \times 10^{-4}$ cm ($n = 15$) (measured from enzymatically dissociated epithelial cells which become spherical after isolation: S. C. Kinnamon, T. Cummings & S. D. Roper, in preparation), the specific membrane resistance was calculated to be 926 Ω cm². The average membrane time constant was $1{\cdot}68 \pm 0{\cdot}66$ ms ($n = 5$) which yields a specific capacitance for the epithelial cell membrane of $1{\cdot}8 \times 10^{-6}$ F/cm².

Taste cells

In contrast to epithelial cells, taste cells had high resting potentials: values varied from −41 to −110 mV. In one series where resting potentials were carefully measured after a brief impalement, we obtained a mean value of $-61{\cdot}7 \pm 15{\cdot}0$ mV ($n = 21$). We attribute the large variability in resting potentials to unavoidable damage accompanying impalement of these long, spindle-shaped cells. The input resistances (measured from the linear portion of the *I–V* relationship) were unexpectedly high, with a mean value of $380{\cdot}3 \pm 177{\cdot}2$ MΩ ($n = 8$). From a measured cell radius of $12{\cdot}6 \times 10^{-4} \pm 1{\cdot}3 \times 10^{-4}$ cm (taste cells, like epithelial cells, become spherical when enzymatically dissociated: S. C. Kinnamon, T. Cummings & S. D. Roper, in preparation) and a measured membrane time constant (measured from the linear portion of the *I–V* relationship) of $61{\cdot}7 \pm 31{\cdot}2$ ms ($n = 8$), we calculated a mean specific membrane resistance of 7600 Ω cm² and a mean specific membrane capacitance of $8{\cdot}3 \times 10^{-6}$ F/cm² for taste cells. The large value obtained for specific membrane capacitance of taste cells could reflect an underestimate of membrane area of individual taste cells, such as microvillar membrane or membrane folds that would not be detected in the light microscope. Alternatively, it could reflect electrotonic coupling between taste cells *in situ* (West & Bernard, 1978; Yang & Roper, 1986).

The *I–V* relationship of taste cells, unlike epithelial cells, showed a pronounced non-linearity with increasing hyperpolarization (Fig. 1*B*); in particular, the non-linearity appeared when the membrane was hyperpolarized in excess of −60 mV. Since rectification can occur simply because of unequal concentrations of permeant ions, especially K^+, across the membrane (Jack, Noble & Tsien, 1975), we repeated experiments in APS containing 60 mM-KCl (NaCl was replaced with KCl) so that K^+ concentrations would be similar across the membrane. Under these conditions, the membrane potential depolarized to approximately −20 mV and the *I–V* relationship became even more non-linear (Fig. 2*A*). Superfusion with the K^+ channel blocker tetraethylammonium bromide (TEA; 5 mM) increased the input resistance of taste cells and caused the *I–V* relationship to become linear (Fig. 2*B*). In addition, when taste cells were exposed to TEA in normal APS (2 mM-KCl), there was a 20–30 mV depolarization of the resting membrane potential and a concomitant increase in input resistance. These results indicate that taste receptor cells have a voltage-sensitive, non-inactivating resting K^+ conductance that closes with hyperpolarization.

Active membrane properties

Surface epithelial cells responded to depolarizing current pulses with only passive potential changes. In sharp contrast, *taste receptor cells* produced regenerative action potentials when depolarized with brief current pulses (Fig. 3*A*; cf. Roper, 1983). These impulses had several characteristic features: First, there was a distinct threshold for regenerative excitability. This threshold varied with the quality of micro-electrode impalement (i.e. the resting potential and the input resistance), but was usually 10–30 mV positive to the resting potential. Secondly, the falling phase of the impulse often had a noticeable inflexion or plateau, suggestive of a Ca^{2+} component to the underlying currents (Fig. 3*A*, arrow). Thirdly, only a single action potential was elicited even when the depolarizing current was maintained for several

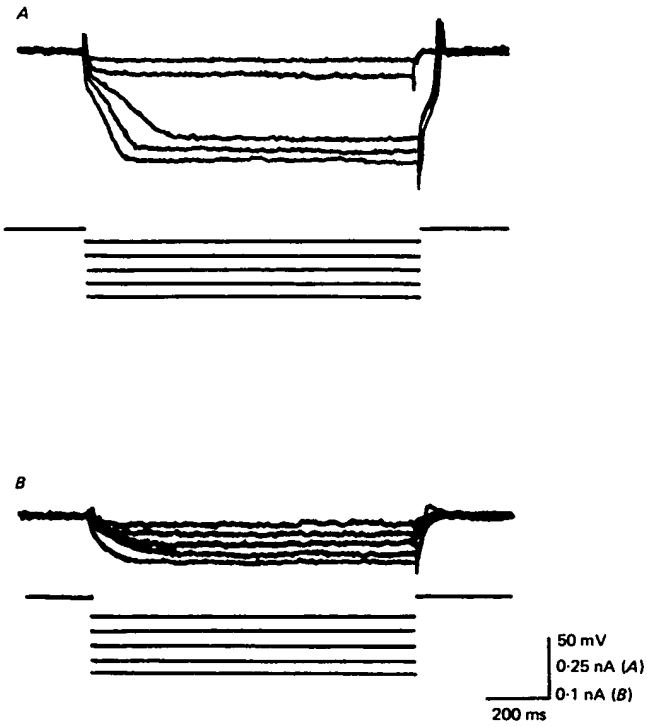

Fig. 2 Effect of elevated external K^+ and of TEA on the $I-V$ relationship in taste cells. *A*, during exposure of taste cell to 60 mM-K^+; resting potential was −20 mV. Note that the non-linearity was enhanced by the elevated K^+. *B*, during exposure of taste cell to 60 mM-K^+ plus 5 mM-TEA. Note that TEA completely blocked the non-linearity and increased the input resistance of the cell.

seconds (Fig. 3*B*). Finally, most action potentials were followed by a prolonged after-potential. A hyperpolarizing after-potential occurred when an impulse was elicited at resting potential (−60 mV; Fig. 4*A*) and a depolarizing after-potential occurred when an impulse was elicited from a cell hyperpolarized approximately 40 mV by direct current injection (Fig. 4*B*). Although most cells were capable of generating action potentials, there was a large variability in the *duration* of impulses and after-potentials in cells within a taste bud.

Ionic basis of the rising phase of impulses

We superfused the preparation with TTX while recording from a single taste cell to determine if Na^+ currents are involved in impulses of taste cells. Action potentials were reversibly blocked in 1 μM-TTX (Fig. 5); lower doses of TTX were ineffective. These data suggest that the rising phase of the impulse in taste cells is produced by voltage-gated Na^+ channels and that the channels are somewhat less sensitive than Na^+ channels in nerve and intact muscle cells to the blocking action of TTX, as are Na^+ channels of denervated skeletal muscle (Pappone, 1980).

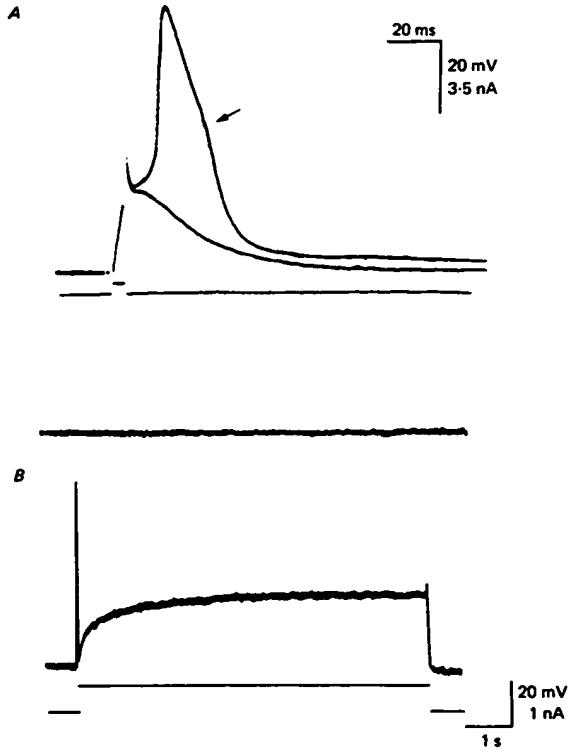

Fig. 3. Action potential elicited by depolarizing current injection in taste cells. *A*, sub- and suprathreshold responses to brief pulses of depolarizing current. Upper trace, membrane potential (resting potential = −58 mV); bottom trace, current through the micro-electrode. The arrow represents an inflexion on the falling phase of the impulse. *B*, response of a taste cell to prolonged current injection: top trace, zero potential; middle trace, intracellular membrane potential; bottom trace, current through the micro-electrode. Note that only a single action potential was elicited by prolonged electrical stimulation.

Ionic basis of the inflexion and falling phase of impulses

The inflexion on the falling phase of the impulse in taste cells suggests the presence of Ca^{2+} currents. To determine if Ca^{2+} currents are involved in taste cell action potentials, we blocked Na^+ currents with TTX and outward K^+ currents with TEA. Fig. 6*A* illustrates that taste cells were excitable under these conditions, and that impulses had a longer duration and a higher threshold than normal. Furthermore, impulses could be evoked even in the absence of Na^+; Fig. 6*B* illustrates an impulse elicited in the presence of 85 mM-$CaCl_2$. We conclude from these experiments that the regenerative membrane response contains a significant Ca^{2+} component in addition to the aforementioned Na^+ current.

TEA also blocked the undershoot of the action potential (Fig. 6*A*). TEA has been found to block a variety of voltage- and Ca^{2+}-dependent K^+ conductances in different cell types, including the delayed rectifier, Ca^{2+}-mediated K^+ conductance, and the sarcoplasmic reticulum K^+ channel (Latorre & Miller, 1983). Although our data

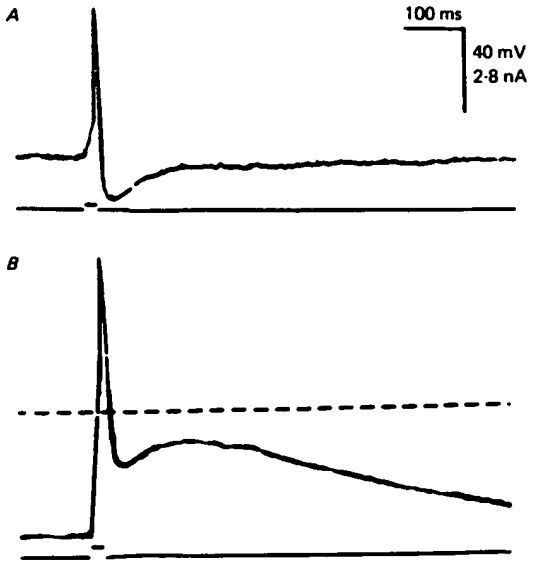

Fig. 4. After-potentials following an impulse in a taste cell. *A*, at the resting potential (−77 mV) and *B*, when the cell was hyperpolarized approximately 40 mV by passing current through the micro-electrode. The dashed line in *B* represents the resting potential of the cell. Note that the after-potential was hyperpolarizing at the resting potential and depolarizing when the cell was hyperpolarized.

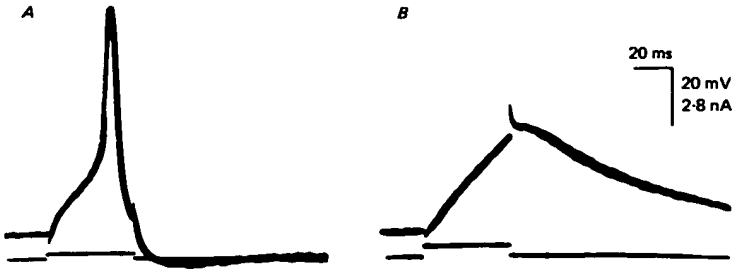

Fig. 5. Response of a taste cell to depolarizing current injection before (*A*) and after (*B*) superfusion with 1 μM-TTX. Note that most of the active membrane response was blocked by the TTX.

indicate that outward K^+ currents are important in repolarizing the membrane following an action potential, we do not know which type(s) of K^+ channel(s) is involved. It is possible that the voltage-sensitive K^+ conductance which is open at the resting potential (Figs. 1*B* and 2*A*, *B*) is the main conductance responsible for action potential repolarization.

Ionic basis of the after-potential

The after-potentials following impulses, an example of which is shown in Fig. 4*B*, sometimes lasted for several seconds. Since such after-potentials in many neurones are produced by Ca^{2+}-dependent conductances, and also because action potentials in

taste cells have a Ca^{2+} component, we examined the Ca^{2+} dependence of taste cell after-potentials by replacing Ca^{2+} with either 5 mM-$CdCl_2$, 8 mM-$CoCl_2$ or 8 mM-$MnCl_2$, which block Ca^{2+} channels in other tissues. After-potentials were either completely blocked or reduced in amplitude and duration by replacement of Ca^{2+} with these

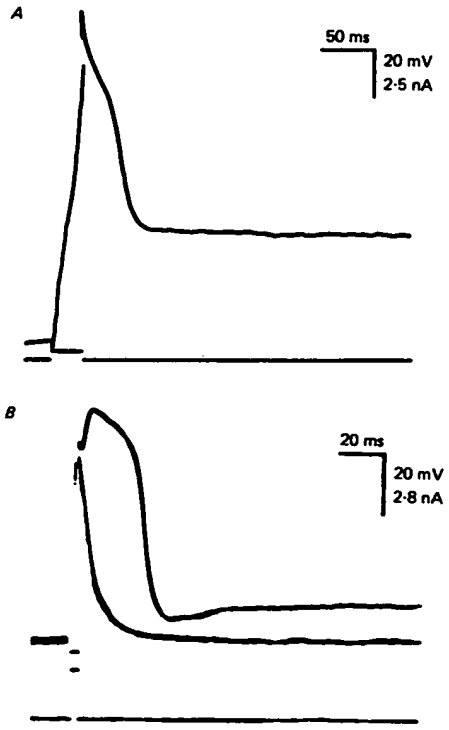

Fig. 6. Ca^{2+} action potentials in taste cells. *A*, action potential recorded from a taste cell superfused with 1 μM-TTX to block Na^+ currents and 5 mM-TEA to block outward K^+ currents; resting potential = −90 mV. *B*, action potential recorded from a taste cell bathed in isotonic (85 mM) $CaCl_2$; resting potential = −85 mV.

compounds (Fig. 7). In some experiments the effect of Ca^{2+} replacement could be reversed; however, reversal usually took several minutes and during this time the recording often deteriorated. In contrast, TEA greatly enhanced the amplitude and duration of the after-potential (Fig. 6*A*), presumably by prolonging the duration of Ca^{2+} influx during an action potential. These data suggest that a significant portion of the after-potential is Ca^{2+} mediated, either directly by a prolonged increase in Ca^{2+} conductance or indirectly by Ca^{2+}-activated permeability increases to other ions.

We measured the reversal potential of the after-potential to determine what ions are responsible for the after-potential. Fig. 8 illustrates impulses recorded at different membrane potential levels which had been established by injecting constant current through the micro-electrode. The after-potential reversed polarity at −76 mV in this example, which was similar to the mean value obtained from ten cells ($-76{\cdot}8 \pm 6$ mV). This value is much more negative than the Ca^{2+} equilibrium potential; therefore, the

after-potential is likely produced by a Ca^{2+}-mediated conductance rather than a prolonged increase in the conductance to Ca^{2+}. Superfusion with TEA (5 mM) shifted the reversal potential of the after-potential from -76 ± 6 to $-42{\cdot}3 \pm 8{\cdot}2$ mV.

The reversal potential of the after-potential differed significantly from the reversal

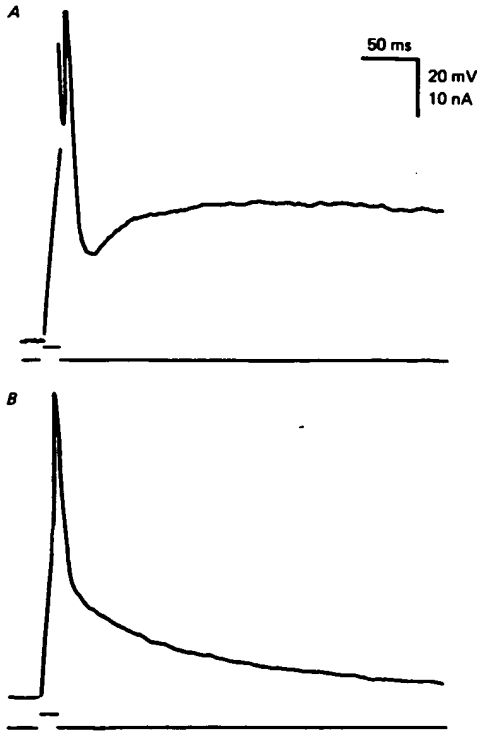

Fig. 7. Action potentials elicited from a taste cell before (*A*) and after (*B*) replacing $CaCl_2$ with 5 mM-$CdCl_2$. The cell was hyperpolarized by steady current injection to -100 mV to enhance the depolarizing after-potential. Note that the after-potential was greatly reduced, but not completely abolished by $CdCl_2$.

potential for the impulse undershoot (mean = $-86{\cdot}5 \pm 5{\cdot}6$ mV), which presumably reflects the K^+ equilibrium potential. The difference between the reversal potentials for the undershoot and the after-potential suggests a portion of the after-potential is mediated by ions other than K^+. Ca^{2+}-dependent Cl^- (Mayer, 1985) as well as Ca^{2+}-dependent non-specific cation conductances (Yellen, 1982; Petersen & Maruyama, 1984) have been found in a variety of tissues, and it is possible that these ions are involved in taste cell after-potentials.

The effect of TEA on the reversal potential suggests that either a voltage-dependent K^+ leak (Fig. 2) contributes significantly to the reversal potential of the after-potential, or that there is a Ca^{2+}-mediated K^+ conductance that is blocked by TEA, or that the delayed rectifier K^+ conductance is still active, as is true for hair cells (Lewis & Hudspeth, 1983). To determine if taste cells have a Ca^{2+}-dependent K^+ conductance, we examined the effects of toxins which have been shown to block

Ca^{2+}-dependent K^+ conductances in a variety of other tissues, namely apamin (Romey & Lazdunski, 1984) and charybdotoxin (Miller, Moczydlowski, Latorre & Phillips, 1985). Neither apamin (5 mM) nor charybdotoxin (100 nM) had any measurable effect on taste cell after-potentials.

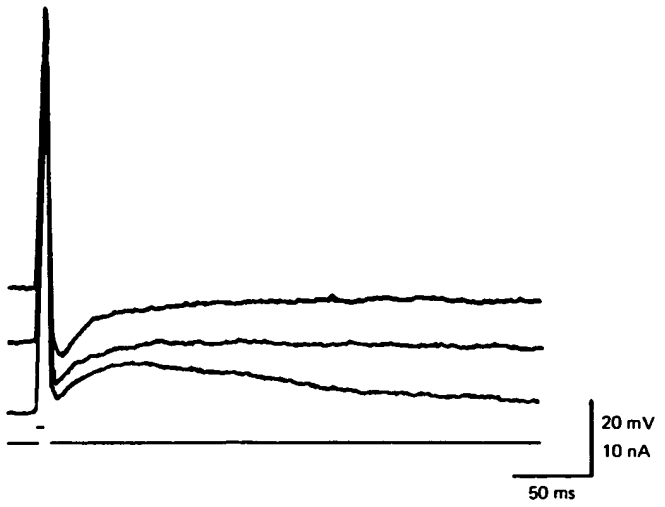

Fig. 8. Reversal potential for the after-potential. Action potentials were elicited at three different holding potentials which were established by passing steady current through the micro-electrode: top trace, resting potential (−60 mV); middle trace, holding potential = −76 mV; bottom trace, holding potential = −100 mV. Note that the after-potential reversed polarity at −76 mV.

In summary, the data suggest that the after-potential is produced by at least two conductances, one that is blocked by TEA and the other which is Ca^{2+} mediated and involves ions other than, or in addition to K^+.

DISCUSSION

The data presented here show that the membrane properties of taste receptor cells differ quite strikingly from surrounding epithelial cells. Most notably, taste cells in the mudpuppy are electrically excitable and possess voltage-gated Na^+, Ca^{2+}, and K^+ channels, as well as Ca^{2+}-mediated channels. Our findings were unexpected, since with the exception of one other investigation (Kashiwayanagi *et al.* 1983), these data are unprecedented. We attribute our findings to the improved recording conditions, namely a vibration-free environment for intracellular micro-electrode impalement. In addition, the large size of mudpuppy taste cells facilitates stable micro-electrode impalement. Although we cannot rule out the possibility that taste cells in the mudpuppy are fundamentally different from those of other species, we believe this is unlikely. Taste cells in the mudpuppy respond to the same basic stimuli as do taste cells of other species, with the exception that the mudpuppy lacks a response to sweet taste (McPheeters & Roper, 1985). Furthermore, we were able to replicate very closely

many of the findings from previous investigations in other species: when there were clear signs of cell damage during micro-electrode impalement, we obtained passive membrane properties identical to those reported by others and the taste cells were unexcitable. Voltage-gated channels similar to those in taste cells have been found recently in other non-neuronal cells, including Schwann cells (Gray & Ritchie, 1985), lymphocytes (Yellen, 1984), pancreatic islet of Langerhans cells (Ashcroft, Harrison & Ashcroft, 1984), cochlear hair cells (Lewis & Hudspeth, 1983; Ohmori, 1984; Fuchs & Mann, 1986), and photoreceptor cells (Corey *et al.* 1984).

The resting properties of taste cells are unusual, in that the so-called leak (resting) K^+ conductance appears to be voltage-sensitive. Voltage-dependent K^+ channels that can be open at the resting potential include Ca^{2+}-dependent K^+ channels (for review, Latorre & Miller, 1983) and the K^+ channels which mediate the M-current in amphibian sympathetic neurones (Adams, Brown & Constanti, 1982).

In this report we have emphasized properties of taste cells which were common to the majority of taste cells impaled. Nevertheless, there were large deviations from the mean values for several of the parameters measured. There are two possibilities for the variability in measured values. First, although taste cells in *Necturus* are large compared to taste cells of other species, they are still small relative to many excitable cells which have been studied with micro-electrodes. Thus, it is probable that we damaged the membrane of some taste cells during micro-electrode impalement. A second more intriguing possibility is that the different classes of taste cells have different properties (see West & Bernard, 1978). For example, there are at least four morphological classes of taste cells which are believed to represent different stages in the growth of taste receptor cells (Kinnamon, Taylor, Delay & Roper, 1985; Delay, Kinnamon & Roper, 1986). Thus, it is possible that membrane properties of taste cells vary with age of the cell, as has been found for muscle cells and several types of neurones (for review see Spitzer, 1979). Such a variability in basic membrane properties could influence the response of the taste cell to chemosensory stimulation.

A critical question is: what role do the passive and active membrane properties play in chemosensory transduction? In this paper we have not addressed the observations that chemosensory stimulation can also produce action potentials in taste cells (Kinnamon, McPheeters & Roper, 1985). It is possible that the Ca^{2+} influx associated with action potentials potentiates transmitter release from taste cells onto gustatory terminals (Kashiwayanagi *et al.* 1983). However, it is unlikely that action potentials would be *required* for transmitter release, since the length constant of the taste cell membrane is sufficient to allow subthreshold potentials to spread from the apical region to the basal region of the cell with little decrement (S. D. Roper, unpublished observation). It is also unlikely that action potentials serve to code stimulus intensity under normal conditions, since we rarely see repetitive impulses to either a sustained electrical depolarization (Fig. 3*B*) or a sustained chemical stimulation (S. C. Kinnamon & S. D. Roper, in preparation). One possibility is that voltage-gated channels are modulated by an electrogenic Na^+ pump. Electrogenic Na^+ pumps are commonly found in many transporting epithelia (Petersen, 1980). The presence of low concentrations of NaCl might be expected to hyperpolarize the basolateral membrane of taste cells by activating an electrogenic Na^+ pump. This hyperpolarization would in turn affect voltage-sensitive membrane channels and influence the receptivity to other substances.

An intriguing possibility is that the voltage-gated and Ca^{2+}-mediated channels are modulated by the taste stimulus and therefore directly cause chemosensory transduction. Modulation of ion channels could occur by direct interaction of the taste stimulus with ion channels on the apical membrane, or by indirect action on ion channels throughout the cell through the release of intracellular second messengers. Ionic channels in other systems have been found to be modulated by neurotransmitters acting through second messengers. For example, serotonin closes K^+ channels in sensory neurones of *Aplysia* (Siegelbaum, Camardo & Kandel, 1982), and noradrenaline increases the mean open time of cardiac Ca^{2+} channels (Reuter, Stevens, Tsien & Yellen, 1982). In addition, and of greater relevance to taste transduction, K^+ channels of pancreatic cells are closed in response to glucose (Ashcroft *et al.* 1984), and K^+ channels derived from sarcoplasmic reticulum of muscle are closed in response to protons (Bell, 1985). The precise role of the membrane conductances described in this report to taste transduction awaits more detailed investigations of the response of taste cells to chemical stimuli.

We thank Dr Paul Fuchs for a critical reading of the manuscript and Dr William Betz for the use of his digitizer and computer. This study was supported by N.I.H. grants NS20382, PO1NS20486-02, and AG03340 to S.D.R.

REFERENCES

ADAMS, P. R., BROWN, D. A. & CONSTANTI, A. (1982). M-currents and other potassium currents in bull-frog sympathetic neurones. *Journal of Physiology* **330**, 537–572.

AKAIKE, N., NOMA, A. & SATO, M. (1976). Electrical responses of frog taste cells to chemical stimuli. *Journal of Physiology* **254**, 87–107.

ASHCROFT, F. M., HARRISON, D. E. & ASHCROFT, S. J. H. (1984). Glucose induces closure of single potassium channels in isolated rat pancreatic b-cells. *Nature* **312**, 446–448.

BADER, C. R., BERTRAND, D. & SCHWARTZ, E. A. (1982). Voltage-activated and calcium-activated currents studied in solitary rod inner segments from the salamander retina. *Journal of Physiology* **331**, 253–284.

BELL, J. (1985). Protons decrease the single channel conductance of the sarcoplasmic reticulum K^+ channel in neutral and negatively charged bilayers. *Biophysical Journal* **48**, 349–353.

COREY, D. P., DUBINSKY, J. M. & SCHWARTZ, E. A. (1984). The calcium current in inner segments of rods from the salamander *Ambystoma tigrinum* retina. *Journal of Physiology* **354**, 557–575.

DELAY, R. J., KINNAMON, J. C. & ROPER, S. D. (1986). Ultrastructure of mouse vallate taste buds: II. Cell types and cell lineage. *Journal of Comparative Neurology* (in the Press).

FUCHS, P. A. & MANN, A. C. (1986). Voltage oscillations and ionic currents in hair cells isolated from the apex of the chick's cochlea. *Journal of Physiology* **371**, 31*P*.

GRAY, P. T. A. & RITCHIE, J. M. (1985). Ion channels in Schwann and glial cells. *Trends in Neurosciences* **87**, 411–415.

JACK, J. J. B., NOBLE, D. & TSIEN, R. W. (1975). *Electric Current Flow in Excitable Cells*, p. 235. Oxford: Oxford University Press.

KASHIWAYANAGI, M., MIYAKE, M. & KURIHARA, K. (1983). Voltage-dependent Ca^{2+} channel and Na^+ channel in frog taste cells. *American Journal of Physiology* **244**, C82–88.

KINNAMON, J. C., TAYLOR, B. J., DELAY, R. J. & ROPER, S. D. (1985). Ultrastructure of mouse vallate taste buds I. Taste cells and their associated synapses. *Journal of Comparative Neurology* **235**, 48–60.

KINNAMON, S. C., MCPHEETERS, M. & ROPER, S. (1985). Electrophysiology of isolated taste cells from the mudpuppy. *Neuroscience Abstracts* **11**, 1131.

LATORRE, R. & MILLER, C. (1983). Conduction and selectivity in potassium channels. *Journal of Membrane Biology* **71**, 11–30.

LEWIS, R. S. & HUDSPETH, A. J. (1983). Voltage- and ion-dependent conductances in solitary vertebrate hair cells. *Nature* **304**, 538–541.

MAYER, M. L. (1985). A calcium-activated chloride current generates the after-depolarization of rat sensory neurones in culture. *Journal of Physiology* **364**, 217–239.

MILLER, C. MOCZYDLOWSKI, E., LATORRE, R. & PHILLIPS, M. (1985). Charybdotoxin, a protein inhibitor of single Ca^{2+}-activated K^+ channels from mammalian skeletal muscle. *Nature* **313**, 316–318.

MCPHEETERS, M. & ROPER, S. D. (1985). Amiloride does not block taste transduction in the mudpuppy, *Necturus maculosus*. *Chemical Senses* **10**, 341–352.

OHMORI, H. (1984). Studies of ionic currents in the isolated vestibular hair cell of the chick. *Journal of Physiology* **350**, 561–581.

OZEKI, M. (1971). Conductance change associated with receptor potentials of gustatory cells in rat. *Journal of General Physiology* **58**, 688–699.

OZEKI, M. & SATO, M. (1972). Responses of gustatory cells in the tongue of rat to stimuli representing four taste qualities. *Comparative Biochemistry and Physiology* **41A**, 391–407.

PAPPONE, P. A. (1980). Voltage-clamp experiments in normal and denervated mammalian skeletal muscle fibres. *Journal of Physiology* **306**, 377–410.

PETERSEN, O. H. (1980). *The Electrophysiology of Gland Cells*. London: Academic Press.

PETERSEN, O. H. & MARUYAMA, Y. (1984). Calcium-activated potassium channels and their role in secretion. *Nature* **307**, 693–696.

REUTER, H., STEVENS, C. F., TSIEN, R. W. & YELLEN, G. (1982). Properties of single calcium channels in cardiac cell culture. *Nature* **297**, 501–504.

ROMEY, G. & LAZDUNSKI, M. (1984). The coexistence in rat muscle cells of two distinct classes of Ca^{2+}-dependent K^+ channels with different pharmacological properties and different physiological functions. *Biochemical and Biophysical Research Communications* **118**, 669–674.

ROPER, S. (1983). Regenerative impulses in taste cells. *Science* **220**, 1311–1312.

SATO, T. (1980). Recent advances in the physiology of taste cells. *Progress in Neurobiology* **14**, 25–67.

SATO, T. & BEIDLER, L. M. (1975). Membrane resistance change of the frog taste cells in response to water and NaCl. *Journal of General Physiology* **66**, 735–763.

SATO. T., SUGIMOTO, K., OKADA, Y. & MIYAMOTO, T. (1984). Ionic basis of the resting membrane potential in frog taste cells. *Japanese Journal of Physiology* **34**, 973–983.

SIEGELBAUM, S. A., CAMARDO, J. S. & KANDEL, E. R. (1982). Serotonin and cyclic AMP close single K^+ channels in *Aplysia* sensory neurones. *Nature* **299**, 413–417.

SPITZER, N. C. (1979). Ion channels in development. *Annual Review of Neuroscience* **2**, 363–397.

TEETER, J. & KARE, M. R. (1974). Passive electrical properties and responses to chemical stimulation of cutaneous taste bud cells. *Federation Proceedings* **33**, 416.

TONOSAKI, K. & FUNAKOSHI, M. (1984). Intracellular taste cell responses of mouse. *Comparative Biochemistry and Physiology* **78A**, 651–656.

WEST, C. H. K. & BERNARD, R. A. (1978). Intracellular characteristics and responses of taste bud and lingual cells of the mudpuppy. *Journal of General Physiology* **72**, 305–326.

YANG, J. & ROPER, S. D. (1986). Dye-coupling in the lingual epithelium in the mudpuppy, *Necturus maculosus*. *Chemical Senses* (in the Press).

YELLEN, G. (1982). Single Ca^{2+}-activated nonselective cation channels in neuroblastoma. *Nature* **296**, 357–359.

YELLEN, G. (1984). The immune system uses ion channels, too. *Trends in Neurosciences* **7**, 179–181.

PRINCIPLES OF NEURAL SCIENCE

Fourth Edition

Edited by

ERIC R. KANDEL

JAMES H. SCHWARTZ

THOMAS M. JESSELL

Center for Neurobiology and Behavior
College of Physicians & Surgeons of Columbia University
and
The Howard Hughes Medical Institute

Art direction by
Sarah Mack and Jane Dodd

McGraw-Hill
Health Professions Division

New York St. Louis San Francisco Auckland Bogotá Caracas Lisbon London
Madrid Mexico City Milan Montreal New Delhi San Juan
Singapore Sydney Tokyo Toronto

McGraw-Hill

A Division of The McGraw-Hill Companies

Principles of Neural Science, 4/e

1234567890 DOWDOW 99

ISBN 0–8385–7701–6

This book was set in Palatino by Clarinda Prepress, Inc.
The editors were John Butler and Harriet Lebowitz.
The production supervisor was Shirley Dahlgren.
The art manager was Eve Siegel.
The illustrators were Precision Graphics.
The designer was Joellen Ackerman.
The index was prepared by Judy Cuddihy.
R. R. Donnelley & Sons, Inc. was printer and binder.

This book is printed on acid-free paper.

Cataloging-in-Publication Data is on file for this title at the Library of Congress.

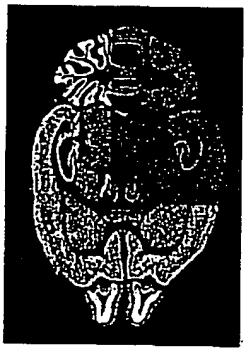

Cover image: The autoradiograph illustrates the widespread localization of mRNA encoding the NMDA-R1 receptor subtype determined by in situ hybridization. Areas of high NMDA receptor expression are shown as light regions in this horizontal section of an adult rat brain.

From Moriyoshi K, Masu M, Ishi T, Shigemoto R, Mizuno N, Nakanishi S. 1991. Molecular cloning and characterization of the rat NMDA receptor. Nature 354:31–37.

14

Transmitter Release

SOME OF THE BRAIN'S MOST remarkable feats, such as learning and memory, are thought to emerge from the elementary properties of chemical synapses. The distinctive feature of these synapses is that action potentials in the presynaptic terminals lead to the release of chemical transmitters. In the past three chapters we saw how postsynaptic receptors for these transmitters control the ion channels that generate the postsynaptic potential. Now we return to the presynaptic cell and consider how electrical events in the terminal are coupled to the secretion of neurotransmitters. In the next chapter we shall examine the chemistry of the neurotransmitters themselves.

Transmitter Release Is Regulated by Depolarization of the Presynaptic Terminal

How does an action potential in the presynaptic cell lead to the release of transmitter? The importance of depolarization of the presynaptic membrane was demonstrated by Bernard Katz and Ricardo Miledi using the giant synapse of the squid. This synapse is large enough to permit the insertion of two electrodes into the presynaptic terminal (one for stimulating and one for recording) and an electrode into the postsynaptic cell for recording the synaptic potential, which provides an index of transmitter release.

The presynaptic cell typically produces an action potential with an amplitude of 110 mV, which leads to transmitter release and the generation of a large synaptic potential in the postsynaptic cell. The action potential is produced by voltage-gated Na^+ influx and K^+ efflux. Katz and Miledi found that when the voltage-gated Na^+ channels are blocked upon application of tetrodotoxin, successive presynaptic action potentials become progressively smaller, owing to the progressive blockade of Na^+ channels during the onset of tetrodotoxin's effect. The postsynaptic potential is reduced accordingly. When the Na^+ channel blockade becomes so profound as to reduce the amplitude of the presynaptic spike below 40 mV, the synaptic potential disappears altogether (Figure 14-1B). Thus, transmitter release (as measured by the size of the postsynaptic potential) shows a steep dependence on presynaptic depolarization.

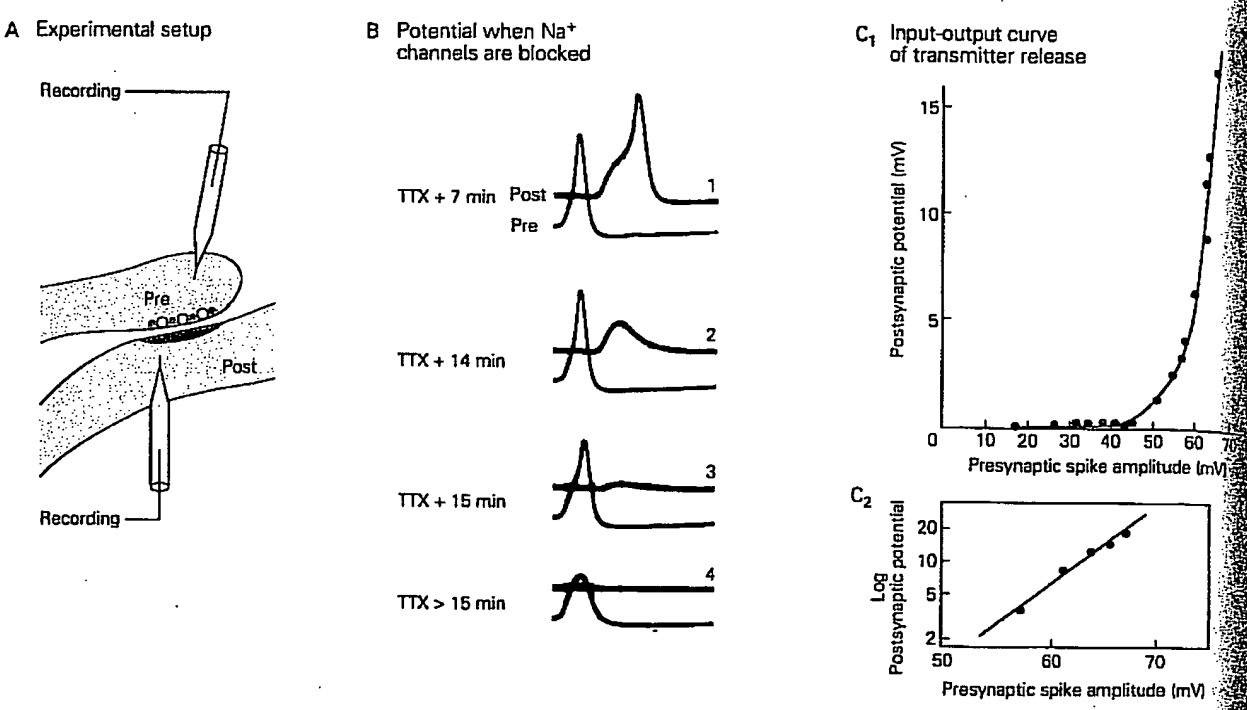

Figure 14-1 The contribution of voltage-gated Na^+ channels to transmitter release is tested by blocking the channels and measuring the amplitude of the presynaptic action potential and the resulting postsynaptic potential. (Adapted from Katz and Miledi 1967a.)

A. Recording electrodes are inserted in both the pre- and postsynaptic fibers of the giant synapse in the stellate ganglion of a squid.

B. Tetrodotoxin (TTX) is added to the solution bathing the cell in order to block the voltage-gated Na^+ channels. The amplitudes of both the presynaptic action potential and the postsynaptic potential gradually decrease. After 7 min the presynaptic action potential can still produce a suprathreshold synaptic potential that triggers an action potential in the postsynaptic cell (1). After 14 and 15 min the presynaptic spike gradually becomes smaller and produces smaller synaptic potentials (2 and 3). When the presynaptic spike is reduced to 40 mV or less, it fails to produce a synaptic potential (4).

C. An input-output curve for transmitter release can be inferred from the dependence of the amplitude of the synaptic potential on the amplitude of the presynaptic action potential. This is obtained by stimulating the presynaptic nerve as the Na^+ channels for the presynaptic action potential are progressively blocked. 1. A 40 mV presynaptic depolarization is required to produce a synaptic potential. Beyond this threshold there is a steep increase in amplitude of the synaptic potential in response to small changes in the amplitude of the presynaptic potential. 2. The semilogarithmic plot of the data in the input-output curve illustrates that the relationship between the presynaptic spike and the postsynaptic potential is logarithmic. A 10 mV increase in the presynaptic spike produces a 10-fold increase in the synaptic potential.

How does membrane depolarization cause transmitter release? One possibility, suggested by the above experiment, is that Na^+ influx may be the important factor. However, Katz and Miledi were able to show that such influx is not necessary. While the Na^+ channels were still fully blocked by tetrodotoxin, Katz and Miledi directly depolarized the presynaptic membrane by passing depolarizing current through the second intracellular microelectrode. Beyond a threshold of about 40 mV from the resting potential, progressively greater amounts of transmitter are released (as judged by the appearance and amplitude of the postsynaptic potential). In the range of depolarization at which chemical transmitter is released (40–70 mV above the resting level), a 10 mV increase in depolarization produces a 10-fold increase in transmitter release. Thus, the presynaptic terminal is able to release transmitter without influx of Na^+. The Na^+ influx is important only insofar as it depolarizes the membrane enough to generate the action potential necessary for transmitter release.

Might the voltage-gated K^+ efflux triggered by the action potential be responsible for release of transmitter? To examine the contribution of K^+ efflux to transmitter release, Katz and Meledi blocked the voltage-gated K^+ channels with tetraethylammonium at the same time they blocked the voltage-sensitive Na^+

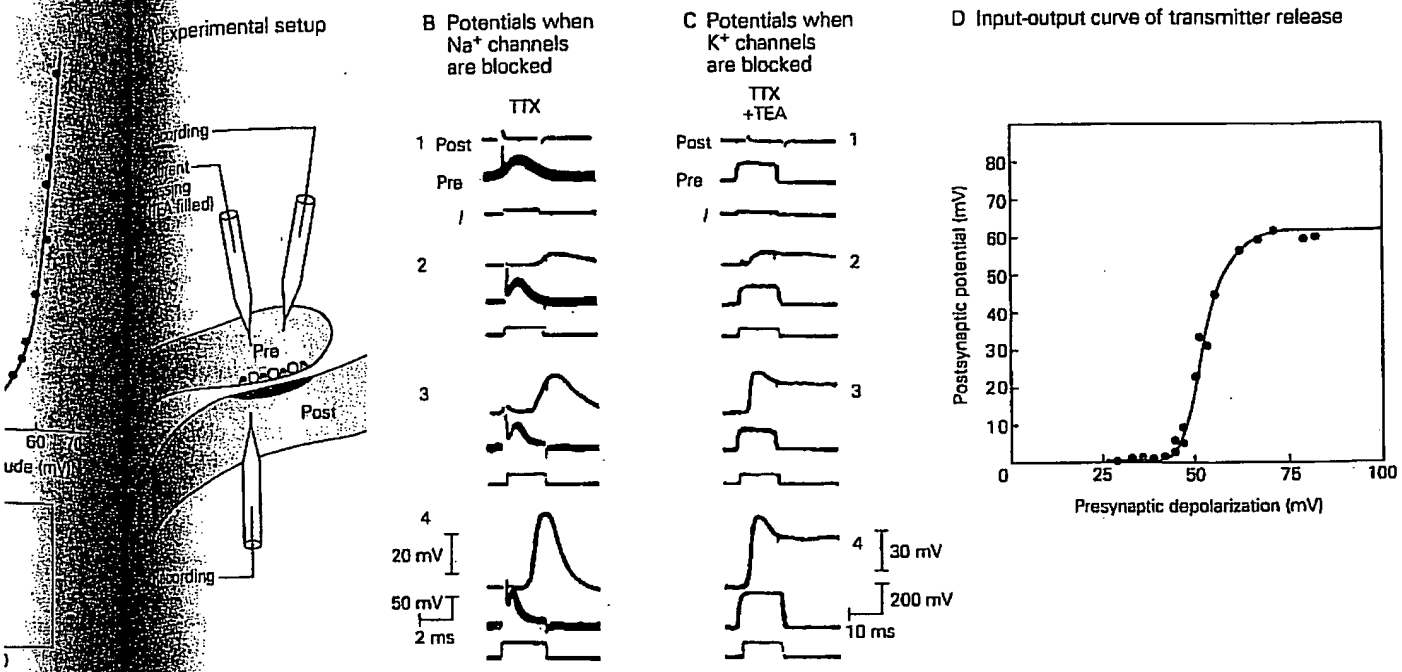

Figure 14-2 Blocking the voltage-sensitive Na^+ channels and K^+ channels in the presynaptic terminals affects the amplitude and duration of the presynaptic action potential and the resulting postsynaptic potential, but does not block the release of transmitter. (Adapted from Katz and Miledi 1967a.)

A. The experimental arrangement is the same as in Figure 14-1 except that a current-passing electrode has been inserted into the presynaptic cell. (TEA = tetraethylammonium.)

B. The voltage-gated Na^+ channels are completely blocked by adding tetrodotoxin (TTX) to the cell-bathing solution. Each set of three traces represents (from bottom to top) the depolarizing current pulse injected into the presynaptic terminal (*I*), the resulting potential in the presynaptic terminal (Pre), and the postsynaptic potential generated as a result of transmitter release onto the postsynaptic cell (Post). Progressively stronger current pulses are applied to produce correspondingly greater depolarizations of the presynaptic terminal (2–4). These presynaptic depolarizations cause postsynaptic potentials even in the absence of Na^+ flux. The greater the presynaptic depolarization, the larger the postsynaptic potential, indicating that membrane potential exerts a direct control over transmitter release. The presynaptic depolarizations are not maintained throughout the duration of the depolarizing current pulse because of the delayed activation of the voltage-gated K^+ channels, which causes repolarization.

C. After the voltage-gated Na^+ channels of the action potential have been blocked, tetraethylammonium (TEA) is injected into the presynaptic terminal to block the voltage-gated K^+ channels as well. Each set of three traces represents current pulse, presynaptic potential, and postsynaptic potential as in part B. Because the presynaptic K^+ channels are blocked, the presynaptic depolarization is maintained throughout the current pulse. The large sustained presynaptic depolarizations produce large sustained postsynaptic potentials (2–4). This indicates that neither Na^+ nor K^+ channels are required for effective transmitter release.

D. Blocking both the Na^+ and K^+ channels permits the measurement of a more complete input-output curve than that in Figure 14-1. In addition to the steep part of the curve, there is now a plateau. Thus, beyond a certain level of presynaptic depolarization, further depolarization does not cause any additional release of transmitter. The initial level of the presynaptic membrane potential was about −70 mV.

with tetrodotoxin. They then passed a depolarizing current through the presynaptic terminals and found that the postsynaptic potentials nonetheless were of normal size, indicating that normal transmitter release occurred (Figure 14-2). Indeed, under the conditions of this experiment, the presynaptic potential is maintained throughout the current pulse because the K^+ current that normally repolarizes the presynaptic membrane is blocked. As a result, transmitter release is sustained (Figure 14-2C). Increases in the presynaptic potential above an upper limit produce no further increase in postsynaptic potential (Figure 14-2D). Thus, neither Na^+ nor K^+ flux is required for transmitter release.

Transmitter Release Is Triggered by Calcium Influx

Katz and Miledi then turned their attention to Ca^{2+} ions. Earlier, José del Castillo and Katz had found that

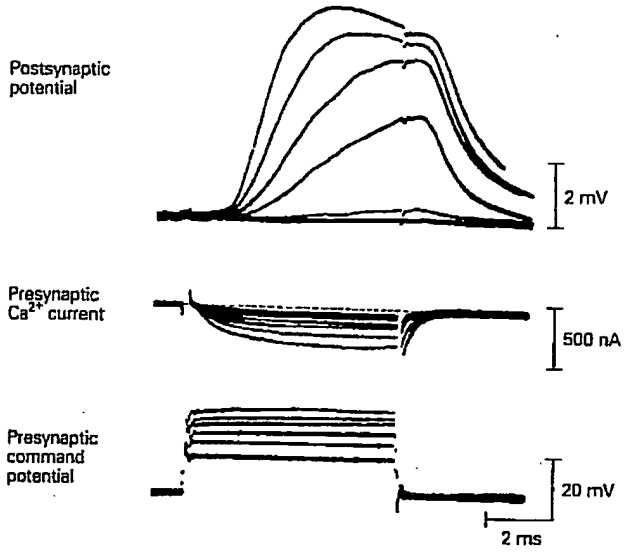

Figure 14-3 A simple experiment demonstrates that transmitter release is a function of Ca^{2+} influx into the presynaptic terminal. The voltage-sensitive Na^+ and K^+ channels in a squid giant synapse are blocked by tetrodotoxin and tetraethylammonium. The presynaptic terminal is voltage-clamped and the membrane potential is stepped to six different command levels of depolarization (bottom traces). The amount of presynaptic inward Ca^{2+} current (middle traces) that accompanies the depolarization correlates with the amplitude of the resulting postsynaptic potential (top traces). This is because the amount of Ca^{2+} current through voltage-gated channels determines the amount of transmitter released, which in turn determines the size of the postsynaptic potential. The notch in the postsynaptic potential trace is an artifact that results from turning off the presynaptic command potential. (Adapted from Llinás and Heuser 1977.)

increasing the extracellular Ca^{2+} concentration enhanced transmitter release; lowering the extracellular Ca^{2+} concentration reduced and ultimately blocked synaptic transmission. However, since transmitter release is an intracellular process, these findings implied that Ca^{2+} must enter the cell to influence transmitter release.

Previous work on the squid giant axon had identified a class of voltage-gated Ca^{2+} channels. As there is a very large inward electrochemical driving force on Ca^{2+}—the extracellular Ca^{2+} concentration is normally four orders of magnitude greater than the intracellular concentration—opening of voltage-gated Ca^{2+} channels would result in a large Ca^{2+} influx. These Ca^{2+} channels are, however, sparsely distributed along the main axon. Katz and Miledi proposed that the Ca^{2+} channels might be much more abundant at the presynaptic terminal and that Ca^{2+} might serve dual functions: as a carrier of depolarizing charge during the action potential (like Na^+) and as a special signal conveying information about changes in membrane potential to the intracellular machinery responsible for transmitter release.

Direct evidence for the presence of a voltage-gated Ca^{2+} current at the squid presynaptic terminal was provided by Rodolfo Llinás and his colleagues. Using a microelectrode voltage clamp, Llinás depolarized the terminal while blocking the voltage-gated Na^+ and K^+ channels with tetrodotoxin and tetraethylammonium, respectively. He found that graded depolarizations activated a graded inward Ca^{2+} current, which in turn resulted in graded release of transmitter (Figure 14-3). The Ca^{2+} current is graded because the Ca^{2+} channels possess voltage-dependent activation gates, like the voltage-gated Na^+ and K^+ channels. The Ca^{2+} channels in the squid terminals differ from Na^+ channels, however, in that they do not inactivate quickly but stay open as long as the presynaptic depolarization lasts. One striking feature of transmitter release at all synapses is its steep and nonlinear dependence on Ca^{2+} influx—a two-fold increase in Ca^{2+} influx can increase transmitter release up to 16-fold. This relationship indicates that at some site—called the *calcium sensor*—the binding of up to four Ca^{2+} ions is required to trigger release.

Even in the axon terminal Ca^{2+} currents are small and are normally masked by Na^+ and K^+ currents, which are 10–20 times larger. However, in the region of the active zone (the site of transmitter release) Ca^{2+} influx is 10 times greater than elsewhere in the terminal. This localization is consistent with the distribution of intramembranous particles seen in freeze-fracture electron micrographs and thought to be the Ca^{2+} channels (see Figure 14-7 in Box 14-2).

The localization of Ca^{2+} channels at active zones provides a high, local rise in Ca^{2+} concentration at the site of transmitter release during the action potential. Indeed, during an action potential the Ca^{2+} concentration at the active zone can rise more than a thousandfold (to ~100 μM) within a few hundred microseconds. This large and rapid increase is required for the rapid synchronous release of transmitter. The calcium sensor responsible for fast transmitter release is thought to have a low affinity for Ca^{2+}. On the order of 50–100 μM intracellular Ca^{2+} is required to trigger release, whereas only ~1 μM of Ca^{2+} is required for many enzymatic reactions. Because of the low-affinity calcium sensor, release only takes place in a narrow region surrounding the intracellular mouth of a Ca^{2+} channel, the only location where the Ca^{2+} concentration is sufficient to trigger release. The requirement for a high concentration of Ca^{2+} also ensures that release will be rapidly terminated upon repolarization. Once the Ca^{2+} channels close

high local Ca^{2+} concentration dissipates rapidly (within 1 ms) because of diffusion.

Calcium channels open somewhat more slowly than the Na^+ channels and therefore Ca^{2+} influx does not occur until the action potential in the presynaptic cell has begun to repolarize (Figure 14-4). The delay that is characteristic of chemical synaptic transmission—the time from the onset of the action potential in the presynaptic terminals to the onset of the postsynaptic potential—is due in large part to the time required for Ca^{2+} channels to open in response to depolarization. However, because the voltage-dependent Ca^{2+} channels are located very close to the transmitter release sites, Ca^{2+} needs to diffuse only a short distance, permitting transmitter release to occur within 0.2 ms of Ca^{2+} entry!

As we shall see later in this chapter, the duration of the action potential is an important determinant of the amount of Ca^{2+} that flows into the terminal. If the action potential is prolonged, more Ca^{2+} flows into the cell and therefore more transmitter is released, causing a greater postsynaptic potential.

Calcium channels are found in all nerve cells as well as in cells outside the nervous system, such as skeletal and cardiac muscle cells, where the channels are important for excitation-contraction coupling, and endocrine cells, where they mediate release of hormones. There are many types of Ca^{2+} channels—called L, P/Q, N, R, and T—with specific biophysical and pharmacological properties and different physiological functions. The distinct properties of these channel types are determined by the identity of their pore-forming subunit (termed the α1-subunit), which is encoded by a family of related genes (Table 14-1). Calcium channels also have associated subunits (termed α2, β, γ, and δ) that modify the properties of the channel formed by the α1-subunits. All α1-subunits are homologous to the voltage-gated Na^+ channel α-subunits, consisting of four repeats of a basic domain containing six transmembrane segments (including an S4 voltage-sensor) and a pore-lining P region (see Figure 9-14).

Most nerve cells contain more than one type of Ca^{2+} channel. Channels formed from the different α1-subunits can be distinguished by their different voltage-dependent gating properties, their distinctive sensitivity to pharmacological blockers, and their specific physiological function. The *L-type channels* are selectively blocked by the dihydropyridines, a class of clinically important drugs used to treat hypertension. The *P/Q-type channels* are selectively blocked by ω-agatoxin IVA, a component of the venom of the funnel web spider. The *N-type channels* are blocked selectively by a toxin obtained from the venom of the marine cone snail, the ω-conotoxin GVIA. The L-type, P/Q-type, N-type, and R-type channels all require fairly strong depolarizations for their activation (voltages positive to −40 to −20 mV are required), and are thus often referred to as *high-voltage-activated* Ca^{2+} channels. In contrast, T-type Ca^{2+} channels are *low-voltage-activated* Ca^{2+} channels that open in reponse to small depolarizations around the threshold for generating an action potential (−60 to −40 mV). Because they are activated by small changes in membrane potential, the T-type channels help control

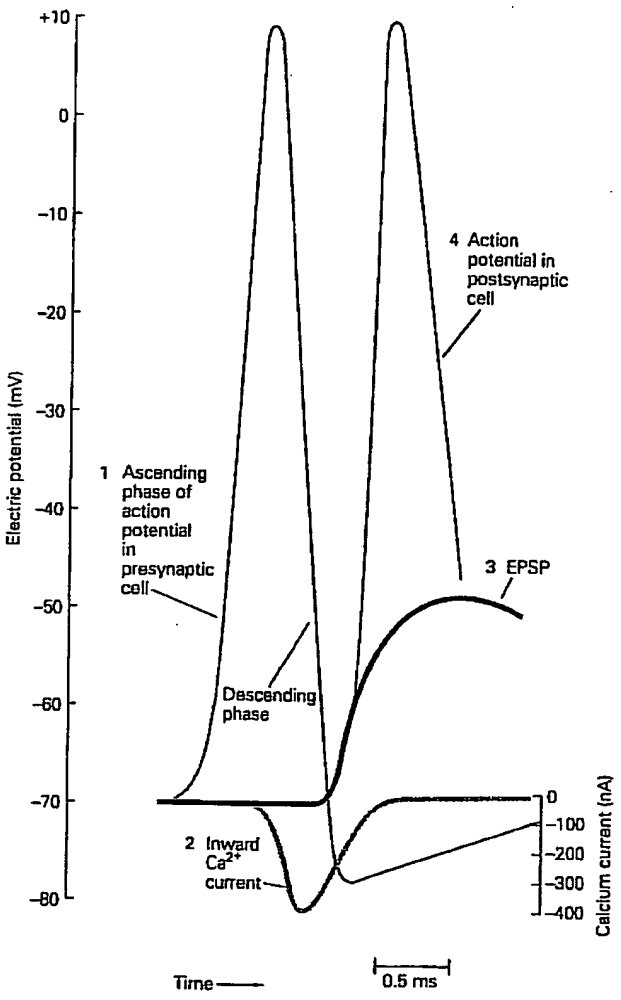

Figure 14-4 The time course of Ca^{2+} influx in the presynaptic cell determines the onset of synaptic transmission. An action potential in the presynaptic cell (1) causes voltage-gated Ca^{2+} channels in the terminal to open and a Ca^{2+} current (2) to flow into the terminal. (Note that the Ca^{2+} current is turned on during the descending phase of the presynaptic action potential owing to delayed opening of the Ca^{2+} channels.) The Ca^{2+} influx triggers release of neurotransmitter. The postsynaptic response to the transmitter begins soon afterward (3) and, if sufficiently large, will trigger an action potential in the postsynaptic cell (4). (EPSP = excitatory postsynaptic potential.) (Adapted from Llinás 1982.)

Table 14-1 Molecular Bases for Calcium Channel Diversity

Gene[1]	Ca^{2+} channel type	Tissue	Selective blockers	Function
A	P/Q	Neurons	ω-agatoxin (spider venom)	Fast rele
B	N	Neurons	ω-conotoxin (snail venom)	Fast rele
C/D/S	L	Neurons, endocrine	Dihydropyridines	Slow rele
		Heart, skeletal muscle		(Peptides)
E	R	Neurons	?	Fast rele
G/H	T	Neurons, heart	?	Excitabili

[1]The gene for the main pore-forming type of α1-subunit.

excitability at the resting potential and are an important source of the excitatory current that drives the rhythmic pacemaker activity of certain cells, both in the brain and the heart.

In neurons the rapid release of conventional transmitters associated with fast synaptic transmission is mediated by three main classes of Ca^{2+} channels: the P/Q-type, the N-type, and R-type channels. The L-type channels do not contribute to fast transmitter release but are important for the slower release of neuropeptides from neurons and of hormones from endocrine cells. The fact that Ca^{2+} influx through only certain types of Ca^{2+} channels, can control transmitter release is presumably due to the fact that these channels are concentrated at active zones. Localization of the N-type Ca^{2+} channels at the active zones has been visualized with fluorescently labeled ω-conotoxin at the frog neuromuscular junction (Figure 14-5). By contrast, L-type channels may be excluded from active zones, limiting their participation to slow synaptic transmission.

Transmitter Is Released in Quantal Units

How and where does Ca^{2+} influx trigger release? To answer that question we must first consider how transmitter substances are released. Even though the release of synaptic transmitter appears smoothly graded, it is actually released in discrete packages called *quanta*. Each quantum of transmitter produces a postsynaptic potential of fixed size, called the *quantal synaptic potential*. The total postsynaptic potential is made up from an integral number of quantal responses (Figure 14-6). Synaptic potentials seem smoothly graded in recordings only because each quantal (or unit) potential is small relative to the total potential.

Paul Fatt and Bernard Katz obtained the first clue to the quantal nature of synaptic transmission when they made recordings from the nerve-muscle synapse of the frog without presynaptic stimulation and observed small spontaneous postsynaptic potentials of about 0.5 mV. Like the nerve-evoked end-plate potentials, these small depolarizing responses were largest at the site of nerve-muscle contact and decayed electronically with distance (see Figure 11-5). Similar results have since been obtained in mammalian muscle and in central neurons. Because the synaptic potentials at vertebrate nerve-muscle synapses are called end-plate potentials, Fatt and Katz called these spontaneous potentials *miniature end-plate potentials*.

The time course of the miniature end-plate potentials and the effects of various drugs on them are indistinguishable from the properties of the end-plate potential evoked by nerve stimulation. Because acetylcholine (ACh) is the transmitter at the nerve-muscle synapse, the miniature end-plate potentials, like the end-plate potentials, are enhanced and prolonged by prostigmine, a drug that inhibits the hydrolysis of ACh by acetylcholinesterase. Likewise, the miniature end-plate potentials are reduced and finally abolished by agents that block the ACh receptor. In the absence of stimulation the miniature end-plate potentials occur at random intervals; their frequency can be increased by depolarizing the presynaptic terminal. They disappear if the presynaptic motor nerve degenerates but reappear when a new motor synapse is formed, indicating that these events represent small amounts of transmitter that are continuously released from the presynaptic nerve terminal.

What could account for the fixed size (around 0.5 mV) of the miniature end-plate potential? Del Castillo and Katz first tested the possibility that each quantum represented a fixed response due to the opening of a single ACh receptor-channel. By applying small amounts of

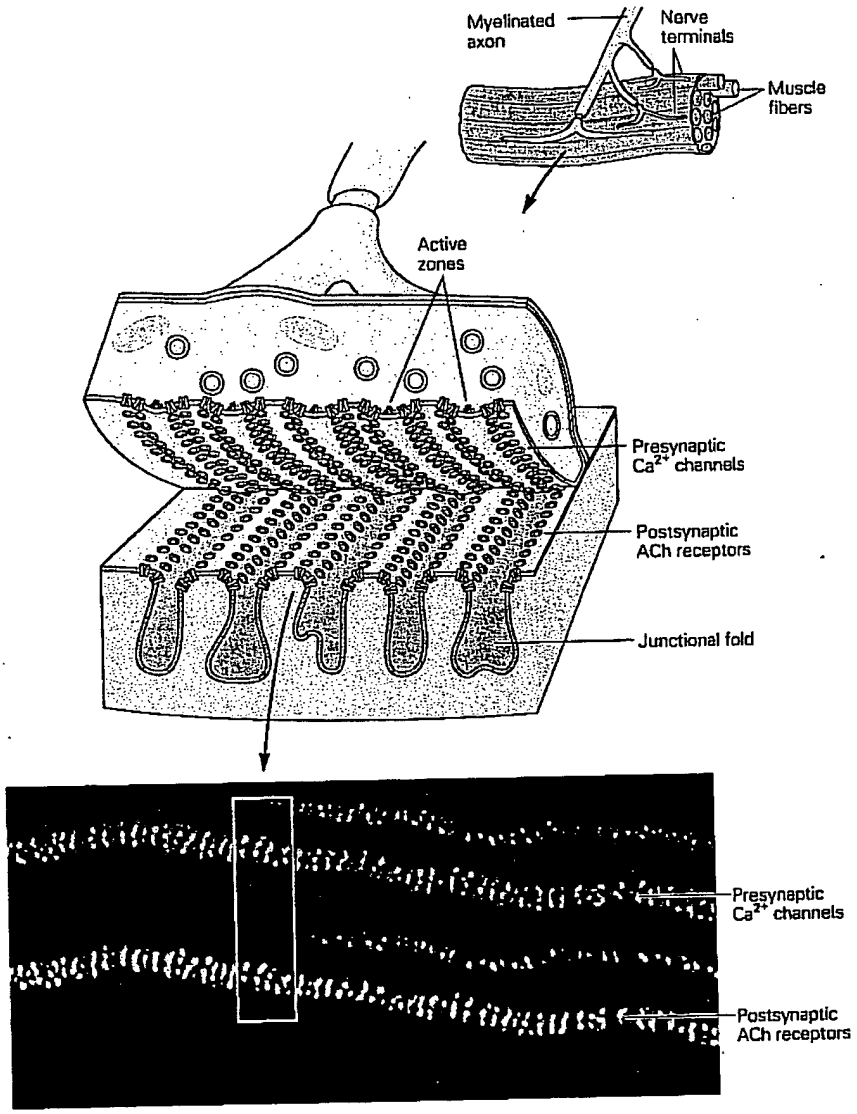

Figure 14-5 Calcium channels are concentrated at the neuromuscular junction in regions of the presynaptic nerve terminal opposite clusters of acetylcholine (ACh) receptors on the postsynaptic membrane. The fluorescent image shows the presynaptic Ca^{2+} channels stained red, after labeling with a Texas red–coupled marine snail toxin that binds to Ca^{2+} channels. Postsynaptic ACh receptors are labeled in green with boron-dipyromethane difluoride-labeled α-bungarotoxin, which binds selectively to ACh receptors. The two images are normally superimposed but have been separated for clarity. The patterns of labeling with both probes are in almost precise register, indicating that the active zone of the presynaptic neuron is in almost perfect alignment with the postsynaptic membrane containing the high concentration of ACh receptors. (From Robitaille et al., 1990.)

ACh to the frog muscle end-plate they were able to elicit depolarizing responses much smaller than 0.5 mV. From this it became clear that the miniature end-plate potential must reflect the opening of more than one ACh receptor-channel. In fact, Katz and Miledi were later able to estimate the elementary current through a single ACh receptor-channel as being only about 0.3 μV (see Chapter 6). This is about 1/2000 of the amplitude of a spontaneous miniature end-plate potential. Thus a miniature end-plate potential of 0.5 mV requires summation of the elementary currents of about 2000 channels. This estimate was later confirmed when the currents through single ACh-activated channels were measured directly using patch-clamp techniques (see Box 6-2).

Since the opening of a single channel requires the binding of two ACh molecules to the receptor (one molecule to each of the two α-subunits), and some of the released ACh never reaches the receptor molecules (either because it diffuses out of the synaptic cleft or is lost through hydrolysis), about 5000 molecules are needed to produce one miniature end-plate potential. This number has been confirmed by direct chemical measurement of the amount of ACh released with each quantal synaptic potential.

We can now ask some important questions. Is the normal postsynaptic potential evoked by nerve stimulation also composed of quantal responses that correspond to the quanta of spontaneously released transmit-

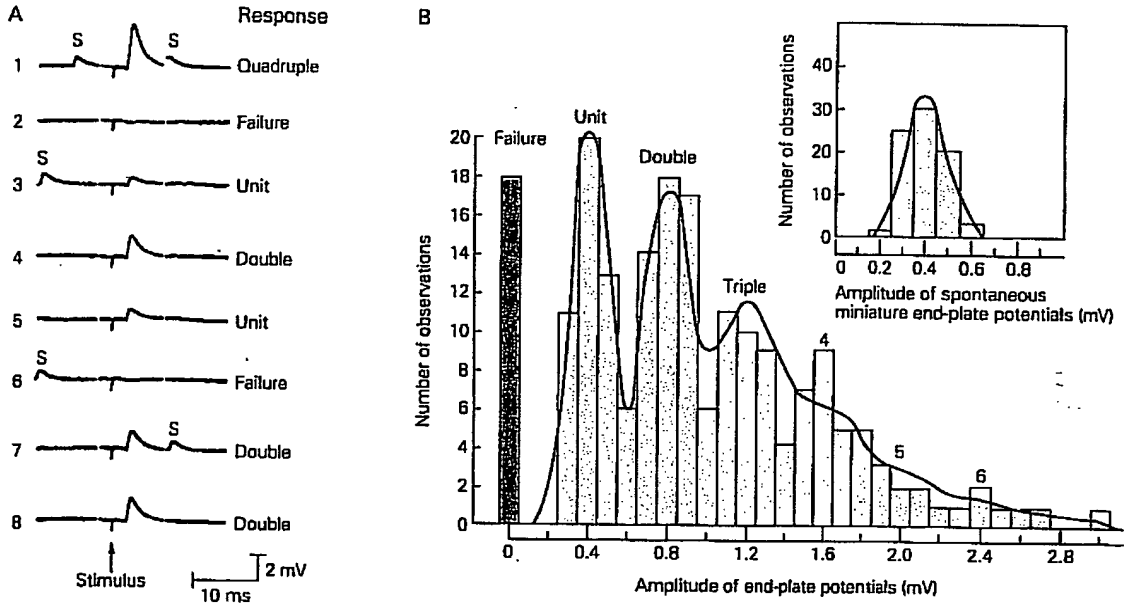

Figure 14-6 Neurotransmitter is released in fixed increments, or quanta. Each quantum of transmitter produces a unit postsynaptic potential of fixed amplitude. The amplitude of the postsynaptic potential evoked by nerve stimulation is equal to the unit amplitude multiplied by the number of quanta of transmitter released.

A. Intracellular recordings from a muscle fiber at the endplate show the postsynaptic change in potential when eight consecutive stimuli of the same size are applied to the motor nerve. To reduce transmitter output and to keep the end-plate potentials small, the tissue was bathed in a Ca^{2+}-deficient (and Mg^{2+}-rich) solution. The postsynaptic responses to the stimulus vary. Two presynaptic impulses elicit no postsynaptic response (failures); two produce unit potentials; and the others produce responses that are approximately two to four times the amplitude of the unit potential. Note that the spontaneous miniature end-plate potentials (S) are the same size as the unit potential. (Adapted from Liley 1956.)

B. After many end-plate potentials were recorded, the number of responses at each amplitude was counted and then plotted in the histogram shown here. The distribution of responses falls into a number of peaks. The first peak, at 0 mV, represents failures. The first peak of responses, at 0.4 mV, represents the unit potential, the smallest elicited response. This unit response is the same amplitude as the spontaneous miniature end-plate potentials (inset). The other peaks in the histogram occur at amplitudes that are integral multiples of the amplitude of the unit potential. The red line shows a theoretical distribution composed of the sum of several Gaussian functions fitted to the data of the histogram. In this distribution each peak is slightly spread out, reflecting the fact that the amount of transmitter in each quantum, and hence the amplitude of the postsynaptic response, varies randomly about the peak. The number of events under each peak divided by the total number of events in the histogram is the probability that the presynaptic terminal releases the corresponding number of quanta. This probability follows a Poisson distribution (see Box 14-1). The distribution of amplitudes of the spontaneous miniature potentials, shown in the inset, is also fit by a Gaussian curve. (Adapted from Boyd and Martin 1956.)

ter? If so, what determines the number of quanta of transmitter released by a presynaptic action potential? Does Ca^{2+} alter the number of ACh molecules that make up each quantum or does it affect the number of quanta released by each action potential?

These questions were addressed by del Castillo and Katz in a study of synaptic signaling at the nerve-muscle synapse when the external concentration of Ca^{2+} is decreased. When the neuromuscular junction is bathed in a solution low in Ca^{2+}, the evoked end-plate potential (normally 70 mV in amplitude) is reduced markedly, to about 0.5–2.5 mV. Moreover, the amplitude of successively evoked end-plate potentials varies randomly from one stimulus to the next, and often no responses can be detected at all (termed *failures*). However, the minimum response above zero—the unit synaptic potential in response to a presynaptic potential—is identical in size (about 0.5 mV) and shape to the spontaneous miniature end-plate potentials. All end-plate potentials larger than the quantal synaptic potential are integral multiples of the unit potential (Figure 14-6).

Del Castillo and Katz could now ask: How does the rise of intracellular Ca^{2+} that accompanies each action potential affect the release of transmitter? They found

Box 14-1 Calculating the Probability of Transmitter Release

The release of a quantum of transmitter is a random event. The fate of each quantum of transmitter in response to an action potential has only two possible outcomes—a quantum is or is not released. This event resembles a binomial or Bernoulli trial (similar to tossing a coin in the air to determine whether it comes up heads or tails). The probability of a quantum being released by an action potential is independent of the probability of other quanta being released by that action potential. Therefore, for a population of releasable quanta, each action potential represents a series of independent binomial trials (comparable to tossing a handful of coins to see how many coins come up heads).

In a binomial distribution p stands for the average probability of success (ie, the probability that any given quantum will be released) and q (or $1 - p$) stands for the mean probability of failure. Both the average probability (p) that an individual quantum will be released and the store (n) of readily releasable quanta are assumed to be constant. (Any reduction in the store is assumed to be quickly replenished after each stimulus.) The product of n and p yields an estimate, m, of the mean number of quanta that are released to make up the end-plate potential. This mean is called the *quantal content* or *quantal output*.

Calculation of the probability of transmitter release can be illustrated with the following example. Let us consider a terminal that has a releasable store of five quanta ($n = 5$). If we assume that $p = 0.1$, then q (the probability that an individual quantum is not released from the terminals) is $1 - p$, or 0.9. We can now determine the probability that a stimulus will release no quanta (failure), a single quantum, two quanta, three quanta, or any number of quanta (up to n). The probability that none of the five available quanta will be released by a given stimulus is the product of the individual probabilities that each quantum will not be released: $q^5 = (0.9)^5$, or 0.59. We would thus expect to see 59 failures in a hundred stimuli. The probabilities of observing zero, one, two, three, four, or five quanta are represented by the successive terms of the binomial expansion:

$$(q + p)^5 = q^5(\text{failures}) + 5\,q^4p(1\text{ quantum}) + 10\,q^3p^2(2\text{ quanta}) + 10\,q^2p^3(3\text{ quanta}) + 5\,qp^4(4\text{ quanta}) + p^5(5\text{ quanta}).$$

Thus, in 100 stimuli the binomial expansion would predict 33 unit responses, 7 double responses, 1 triple response, and 0 quadruple and quintuple responses.

Values for m vary, from about 100–300 at the vertebrate nerve-muscle synapse, the squid giant synapse, and *Aplysia* central synapses, to as few as 1–4 in the synapses of the sympathetic ganglion and spinal cord of vertebrates. The probability of release p also varies, ranging from as high as 0.7 at the neuromuscular junction in the frog and 0.9 in the crab down to around 0.1 at some central synapses. Estimates for n range from 1000 (at the vertebrate nerve-muscle synapse) to 1 (at single terminals of central neurons).

The parameters n and p are statistical terms; the physical processes represented by them are not yet known. Although the parameter n is assumed to refer to the number of readily releasable (or available) quanta of transmitter, it may actually represent the number of *release sites* or *active zones* in the presynaptic terminals that are loaded with vesicles. Although the number of release sites is thought to be fixed, the fraction that is loaded with vesicles is thought to be variable. The parameter p probably represents a compound probability depending on at least two processes: the probability that a vesicle has been loaded or docked onto a release site (a process referred to as vesicle mobilization) and the probability that an action potential will discharge a quantum of transmitter from a docked active zone. The parameter p is thought to depend on the presynaptic Ca^{2+} influx during an action potential.

The quantal size (a) is the response of the postsynaptic membrane to a single quantum of transmitter. Quantal size depends largely on the properties of the postsynaptic cell, such as the input resistance and capacitance (which can be independently estimated) and the sensitivity of the postsynaptic membrane to the transmitter substance. This can also be measured by the postsynaptic membrane's response to the application of a constant amount of transmitter.

that when the external Ca^{2+} concentration is increased, the amplitude of the unit synaptic potential does not change. However, the number of failures decreases and the incidence of higher-amplitude responses (composed of multiple quantal units) increases. These observations illustrate that alterations in external Ca^{2+} concentration do not affect the *size* of a quantum of transmitter (the number of ACh molecules) but rather affect the average number of quanta that are released in response to a presynaptic action potential (Box 14-1). The greater the Ca^{2+} influx into the terminal, the larger the number of quanta released.

The findings that the amplitude of the end-plate potential varies in a stepwise manner at low levels of ACh release, that the amplitude of each step increase is an integral multiple of the unit potential, and that the unit

potential has the same mean amplitude as that of the spontaneous miniature end-plate potentials led del Castillo and Katz to conclude that transmitter is released in fixed packets or quanta. When the external Ca^{2+} concentration is normal, an action potential in the presynaptic terminal releases about 150 quanta, each about 0.5 mV in amplitude, resulting in a large end-plate potential. In the absence of an action potential, the rate of quantal release is very low—only one quantum per second is released spontaneously at the end-plate. The rate of quantal release increases 100,000-fold when Ca^{2+} enters the presynaptic terminal with an action potential, bringing about the synchronous release of about 150 quanta in one or two milliseconds.

Transmitter Is Stored and Released by Synaptic Vesicles

What morphological features of the cell might account for the quantum of transmitter? The physiological observations indicating that transmitter is released in fixed quanta coincided with the discovery, through electron microscopy, of accumulations of small vesicles in the presynaptic terminal. The electron micrographs suggested to del Castillo and Katz that the vesicles were organelles for the storage of transmitter. They also argued that each vesicle stored one quantum of transmitter (amounting to several thousand molecules) and that each vesicle releases its entire contents into the synaptic cleft when the vesicle fuses with the inner surface of the presynaptic terminal at specific release sites.

At these sites, *the active zones*, a band of synaptic vesicles cluster above a fuzzy electron-dense material attached to the internal face of the presynaptic membrane, directly above the junctional folds in the muscle (see Figure 11-1). As we saw in Chapter 11, the neuromuscular junction in frogs contains about 300 active zones with a total of about 10^6 vesicles. Here, and at central synapses, the vesicles are typically clear, small, and ovoid, with a diameter of about 50 nm.

Neuropeptides and certain transmitters released from neuroendocrine cells are packaged in larger vesicles that contain an electron-dense material. These large dense-core vesicles are not localized at active zones. They can be released from anywhere within a neuron, including the cell body. Release of transmitter from large dense-core vesicles is associated with slow modulatory synaptic actions (see Chapter 13).

Quantal transmission has been demonstrated at all chemical synapses so far examined, with one exception, in the retina, which we shall examine in Chapter 26. At most synapses in the central nervous system each action potential releases only between 1 and 10 quanta, many fewer than the 150 quanta released at the nerve-muscle synapse. Whereas the surface area of a presynaptic motor terminal ending on a muscle fiber is large (about 2000–6000 μm^2) and contains about 300 active zones, a typical excitatory afferent fiber from a dorsal root ganglion cell forms only about four synapses on a motor neuron, each of which is about 2 μm^2 and contains only one active zone.

Quantal analysis of transmitter release from these afferent neurons indicates that release from each active zone is all-or-none. That is, any given active zone releases either one quantum or none at all in response to a presynaptic action potential. The probability of release depends on the amount of Ca^{2+} influx during the action potential. Similar results have been obtained for other central synapses. Thus, variations in the response of a central neuron to a single presynaptic neuron result from the all-or-none release of one quantum from each of a few terminals, each usually with only one active zone.

Not all chemical signaling between neurons depends on vesicular storage and release. Some membrane-permeable substances, such as prostaglandins, other metabolites of arachidonic acid, and the gases CO and NO (see Chapter 13), can traverse the lipid bilayer of the membrane by diffusion. These substances may act at synapses either as chemical messengers or as retrograde signals that diffuse from the postsynaptic neuron back to the presynaptic neuron to regulate transmitter release. Other substances can be moved out of nerve endings by carrier proteins if their intracellular concentration is sufficiently high. In certain retinal glial cells, transporters for glutamate or GABA that normally take up transmitter into a cell from the extracellular space can reverse direction and release transmitter into the extracellular space. Still other substances simply leak out of nerve terminals at a low rate. For example, about 90% of the ACh that leaves the presynaptic terminal at the neuromuscular junction can be traced to continuous leakage. However, because this leakage is asynchronous and not targeted to receptors at the end-plate region, and because it is continuous and low level rather than synchronous and concentrated, it is ineffective functionally.

Synaptic Vesicles Discharge Transmitter by Exocytosis

Direct evidence that exocytosis of a single synaptic vesicle is responsible for the release of one quantum of transmitter was at first difficult to obtain, because the chance of finding a vesicle in the act of being discharged

Box 14-2 Freeze-Fracture Technique

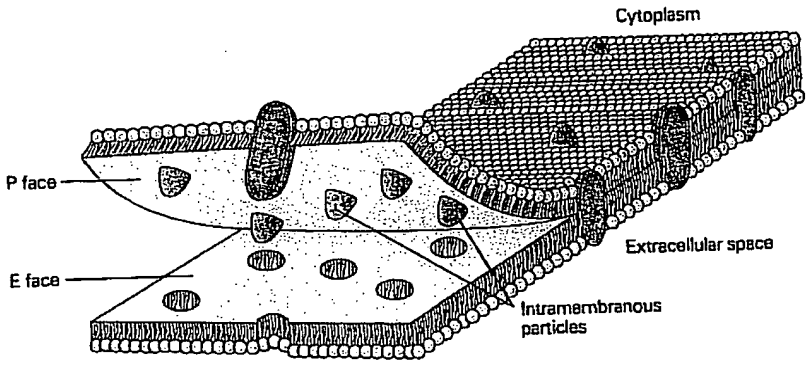

Figure 14-7A. Freeze-fracture exposes the intramembranous area to view. The path of membrane cleavage is along the hydrophobic interior of the lipid bilayer, resulting in two complementary fracture faces. The P face (corresponding to the protoplasmic-facing leaflet of the bilayer) contains most of the integral membrane proteins (particles), because these are anchored to cytoskeletal structures. The E face (corresponding to the extracellular-facing leaflet of the bilayer) shows pits complementary to the integral protein particles. (Adapted from Fawcett 1981.)

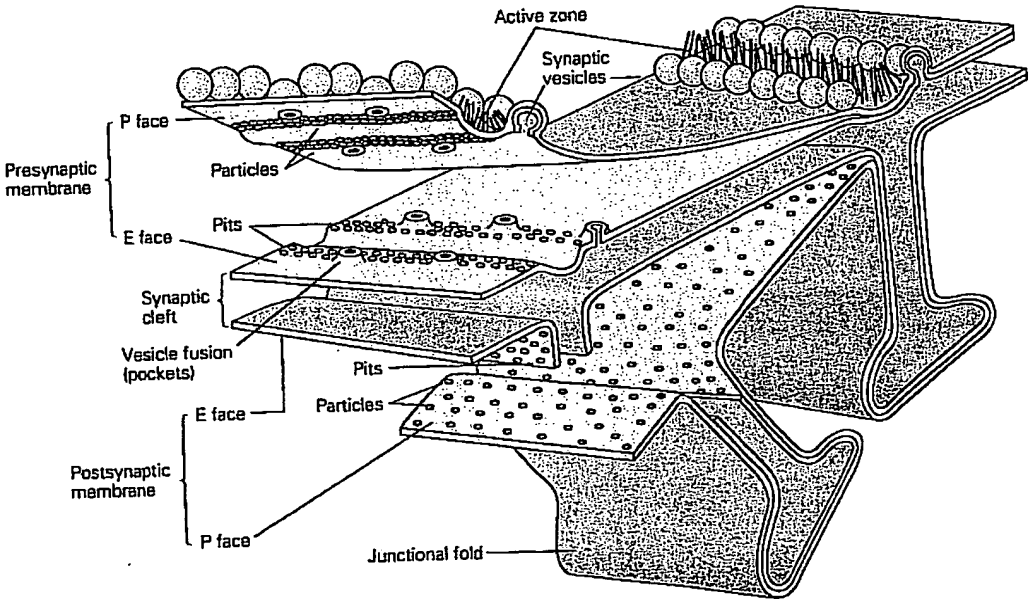

Figure 14-7B. This idealized three-dimensional view of pre- and postsynaptic membranes shows the active zones with adjacent rows of synaptic vesicles, as well as places where the vesicles are undergoing exocytosis. The rows of particles on either side of the active zone are intramembranous proteins thought to be Ca++ channels. (Adapted from Kuffler et al. 1984.)

Freeze-fracture reveals the structural details of synaptic membranes. In this technique frozen tissue is broken open under a high vacuum and coated with platinum and carbon. Frozen membrane tends to break at the weakest plane, which is between the two molecular layers of lipids. Two complementary faces of the membrane are thus exposed: The leaflet nearest the cytoplasm (the interior half) is the protoplasmic (P) face, while the leaflet that borders the extracellular space is the external (E) face (Figure 14-7A).

Freeze-fracture exposes a large expanse of the presynaptic intramembranous area (Figure 14-7B). Deformations of the membrane that occur at the active zone, where vesicles are attached, are readily apparent. The advantage of the freeze-fracture technique is best appreciated by comparing a freeze-fracture electron micrograph with a conventional thin-section electron micrograph of the active zone (see Figure 14-8).

is extremely small. A thin section through a conventionally fixed terminal at the neuromuscular junction of the frog shows only 1/4000 of the total presynaptic membrane. Moreover, the exocytotic opening of each small vesicle is of the same dimension as the thickness of the ultrathin (50–100 nm) sections required for transmission electron microscopy. To overcome such problems, freeze-fracture techniques began to be applied to the synapse in the 1970s (Box 14-2).

Using these techniques, Thomas Reese and John Heuser made three important observations. First, they found one or two rows of unusually large intramembranous particles along the presynaptic density, on both margins (Figure 14-8A). Although the function of these particles is not yet known, they are thought to be voltage-gated Ca^{2+} channels. Their density (about 1500 per μm^2) is approximately that of the voltage-gated Ca^{2+} channels essential for transmitter release. Moreover, the proximity of the particles to the release site is consistent with the short time interval between the onset of the Ca^{2+} current and the release of transmitter. Second, they noted the appearance of deformations alongside the rows of intramembranous particles during synaptic activity (Figure 14-8B). They interpreted these deformations as representing invaginations of the cell membrane during exocytosis. Finally, Reese and Heuser found that these deformations do not persist after the transmitter has been released; they seem to be transient distortions that occur only when vesicles are discharged.

To catch vesicles in the act of exocytosis, Heuser, Reese, and their colleagues had to quick-freeze the tissue with liquid helium at precisely defined intervals after the presynaptic nerve had been stimulated. The neuromuscular junction can thus be frozen just as the action potential invades the terminal and exocytosis occurs. In addition, they applied the drug 4-aminopyridine—a compound that blocks certain voltage-gated K^+ channels—to broaden the action potential and increase the number of quanta of transmitter discharged with each nerve impulse. These techniques provided clear images of synaptic vesicles during exocytosis.

The electron micrographs revealed a number of omega-shaped (Ω) structures that correspond to vesicles that have just fused with the membrane. Varying the concentration of 4-aminopyridine altered the amount of transmitter release. Moreover, there was an increase in the number of Ω-shaped structures that was directly correlated with the size of the postsynaptic response. These morphological studies therefore provide independent evidence that transmitter is released by exocytosis from synaptic vesicles.

The fusion of the synaptic vesicles with the plasma membrane during exocytosis increases the surface area of the plasma membrane. In certain favorable cell types this increase in area can be detected in electrical measurements as increases in membrane capacitance, providing further support for exocytosis. As we saw in Chapter 8, the capacitance of the membrane is proportional to its surface area. In adrenal chromaffin cells (which release epinephrine) and in mast cells of the rat peritoneum (which release histamine), individual large dense-core vesicles are large enough to permit measurement of the increase in capacitance associated with fusion of a single vesicle. Release of transmitter in these cells is accompanied by stepwise increases in capacitance, which in turn are followed somewhat later by stepwise decreases in capacitance, which presumably reflect the retrieval and recycling of the excess membrane (Figure 14-9B). Capacitance increases can be detected at fast synapses after a rise in Ca^{2+} due to the fusion of a large number of small synaptic vesicles (Figure 14-9C). However, the increase in capacitance associated with the fusion of a single small synaptic vesicle is too small to resolve.

Exocytosis Involves the Formation of a Fusion Pore

Exactly how fusion of the synaptic vesicle membrane with the plasma membrane occurs and the role that Ca^{2+} plays in catalyzing this reaction is under intensive study. Morphological studies from mast cells using rapid freezing suggested that exocytosis depends on the temporary formation of a *fusion pore* that spans the membranes of the vesicle and plasma membrane. Subsequent studies of capacitance increases in mast cells showed that prior to complete fusion a channel-like fusion pore could be detected in the electrophysiological recordings (Figure 14-10). This fusion pore starts out with a single-channel conductance of around 200 pS, similar to that of gap-junction channels, which also bridge two membranes. During exocytosis the pore rapidly dilates, probably from around 1 nm to 50 nm, and the conductance increases dramatically (Figure 14-10A). In some instances the fusion pore flickers open and closed several times prior to complete fusion (Figure 14-10B).

Since transmitter release is so fast, fusion must occur within a fraction of a millisecond. Therefore, the proteins that fuse synaptic vesicles to the plasma membrane are most likely preassembled into a fusion pore that bridges the vesicle and plasma membranes before fusion occurs. Much like the gap-junction channels we learned about in Chapter 10, the fusion pore may consist of two hemichannels, one each in the vesicle membrane and the plasma membrane, which then join in the course of vesicle docking (Figure 14-10C). Calcium influx would then simply cause the preexisting pore to

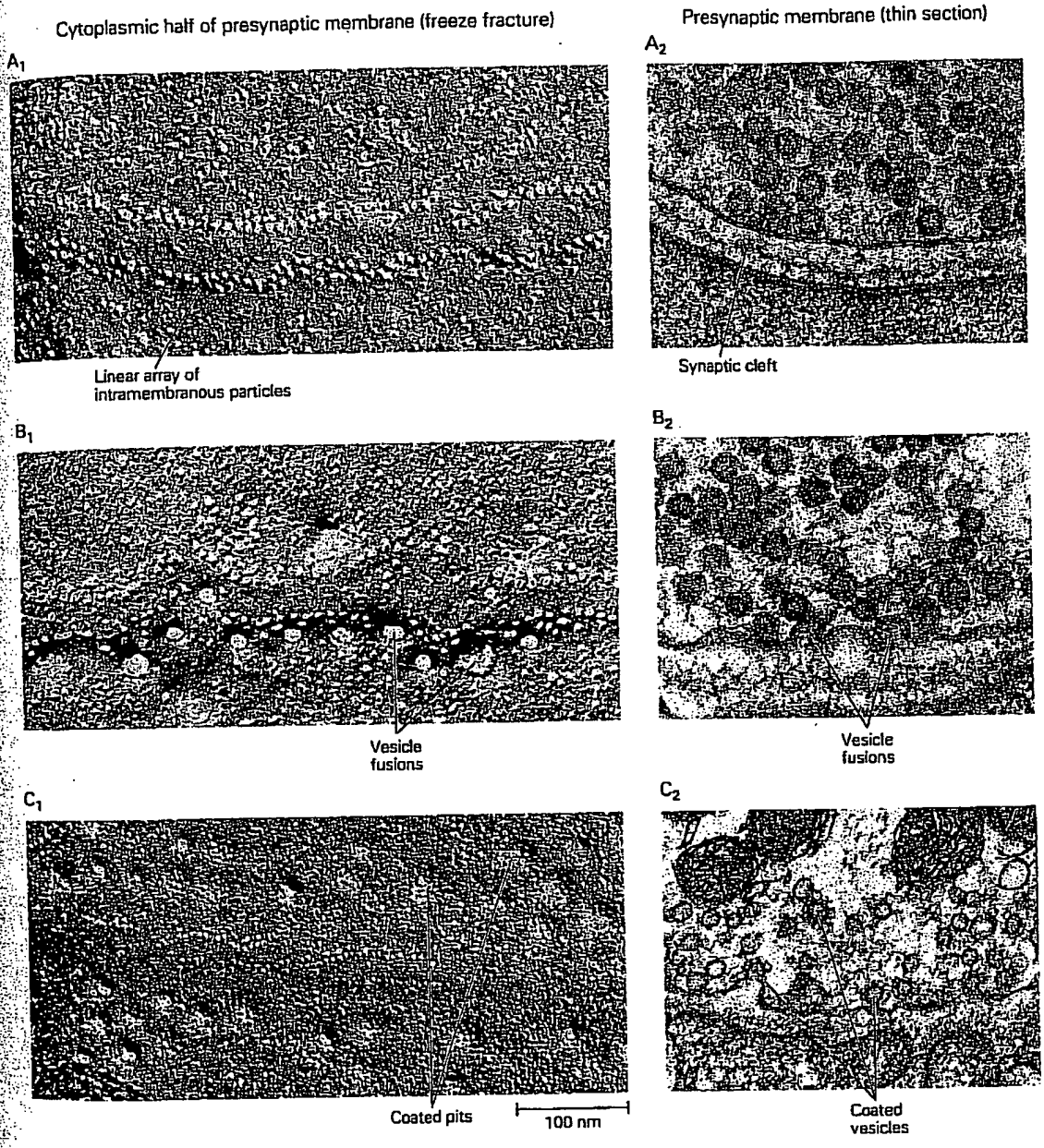

Figure 14-8 The events of exocytosis at the presynaptic terminal are revealed by electron microscopy. The images on the left are freeze-fracture electron micrographs of the cytoplasmic half (P face) of the presynaptic membrane (compare figure 14-7). Thin-section electron micrographs of the presynaptic membrane are shown on the right. (Adapted from Alberts et al. 1989.)

A. Parallel rows of intramembranous particles arrayed on either side of an active zone may be the voltage-gated Ca^{2+} channels essential for transmitter release.

B. Synaptic vesicles begin fusing with the plasma membrane within 5 ms after the stimulus. Fusion is complete within another 2 ms. Each opening in the plasma membrane represents the fusion of one synaptic vesicle. In thin-section electron micrographs, vesicle fusion events are observed in cross section as Ω-shaped structures.

C. Membrane retrieval becomes apparent as coated pits form within about 10 s after fusion of the vesicles with the presynaptic membrane. After another 10 s the coated pits begin to pinch off by endocytosis to form coated vesicles. These vesicles include the original membrane proteins of the synaptic vesicle and also contain molecules captured from the external medium. The vesicles are recycled at the terminals or are transported to the cell body, where the membrane constituents are degraded or recycled (see Chapter 4).

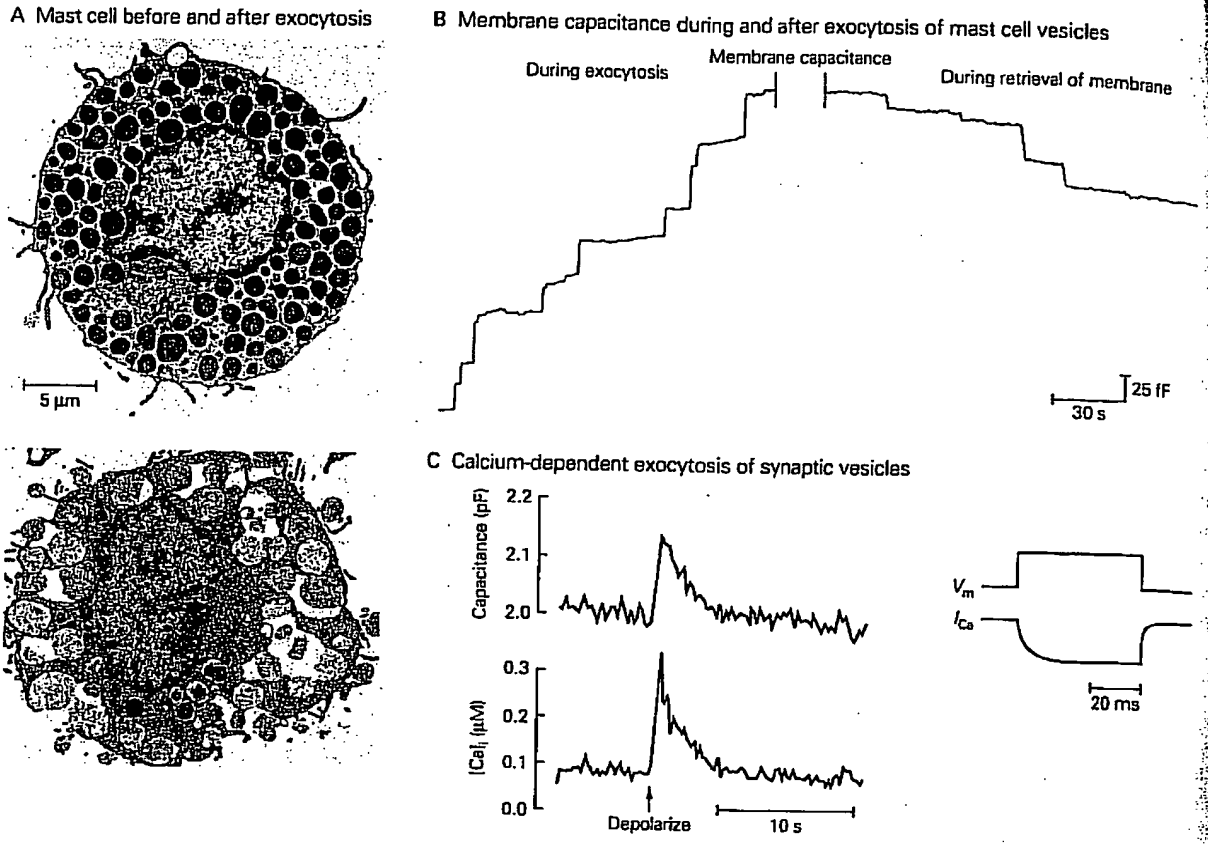

Figure 14-9 Capacitance measurements allow direct study of exocytosis and endocytosis.

A. Exocytosis from mast cells. Electron micrographs of a mast cell before (top) and after (bottom) inducing exocytosis. Mast cells are secretory cells of the immune system that contain large dense-core vesicles filled with the transmitter histamine. Exocytosis of mast cell secretory vesicles is normally triggered by the binding of antigen complexed to an immunoglobulin (IgE). Under experimental conditions massive exocytosis can be triggered by the inclusion of a nonhydrolyzable analog of GTP in an intracellular recording electrode. (From Lawson et al., 1977.)

B. Stepwise increases in capacitance reflect the successive fusion of individual secretory vesicles with the cell membrane. The step increases are unequal because of a variability in the diameter (and thus membrane area) of the vesicles. After exocytosis the membrane added through fusion is retrieved through endocytosis. Endocytosis of individual vesicles gives rise to the stepwise decreases in membrane capacitance. In this way the cell maintains a constant size. (The units are in femtofarads, fF, where 1 fF = 0.1 μm^2 of membrane area.) (Adapted from Fernandez et al. 1984.)

C. Exocytosis and membrane retrieval from a neuronal presynaptic terminal. Recordings were obtained from isolated synaptic terminals of bipolar neurons in the retina of the goldfish. Transmitter release was triggered by a depolarizing voltage-clamp step (applied at arrow), which elicited a large sustained Ca^{2+} current (inset). The Ca^{2+} influx causes a transient rise in the cytoplasmic Ca^{2+} concentration (bottom trace). This results in the exocytosis of several thousand small synaptic vesicles, leading to an increase in total capacitance (top trace). The increments in capacitance due to fusion of a single small synaptic vesicle are too small to resolve. As the internal Ca^{2+} concentration falls back to its resting level upon repolarization, the extra membrane area is rapidly retrieved and capacitance returns to its baseline value. (Adapted from von Gersdorff and Matthews 1994.)

open and then dilate, allowing the release of transmitter.

Recent advances in chemical detection suggest that transmitter may be released through the fusion pore itself, prior to full dilation and vesicle fusion (Figure 14-10C). An electrochemical method termed *voltammetry* permits the detection of certain amine-containing transmitters, such as serotonin, using an extracellular carbon-fiber electrode (Figure 14-11). A large voltage is applied to the electrode, which leads to the oxidation of the released transmitter. This oxidation reaction releases free electrons, which can be detected as a transient electrical current that is proportional to the amount of transmitter released. In response to action potentials large transient increases in transmitter release are observed

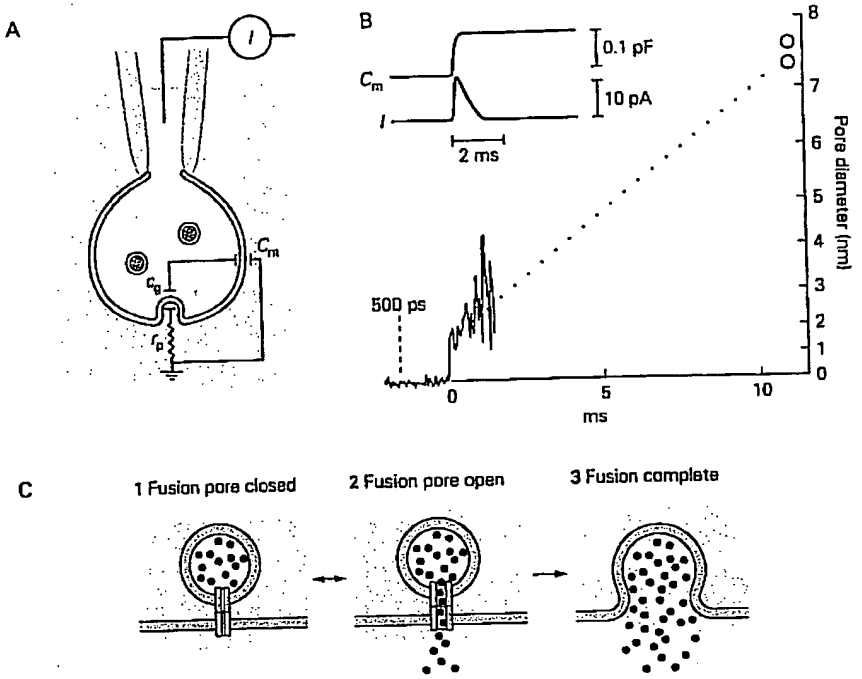

Figure 14-10 Transmitter is released from synaptic vesicles through the opening of a fusion pore that connects a secretory vesicle with the presynaptic membrane.

A. Patch-clamp recording setup for recording current through the fusion pore. As a vesicle fuses with the plasma membrane, the capacitance of the vesicle (C_g) is initially connected to the capacitance of the rest of the cell (C_m) through the high resistance (r_p) of the fusion pore. (From Monck and Fernandez 1992.)

B. Electrical events associated with the opening of the fusion pore. Since the membrane potential of the vesicle (lumenal side negative) is normally much more negative than the membrane potential of the cell, there will be a transient flow of charge (current) from the vesicle to the cell membrane associated with fusion. This generates a transient current (I) associated with the increase in membrane capacitance (C_m). The magnitude of the conductance of the fusion pore (g_p) can be calculated from the time constant of the transient current according to $\tau = C_g r_p = C_g / g_p$. The fusion pore diameter can be calculated from the fusion pore conductance, assuming that the pore spans two lipid bilayers and is filled with a solution whose resistivity is equal to that of the cytoplasm. The fusion pore shows an initial conductance of around 200 pS, similar to the conductance of a gap-junction channel, corresponding to a pore diameter of around 2 nm. The conductance rapidly increases within a few milliseconds as the pore dilates to around 7–8 nm (dotted line). (From Spruce et al. 1990.)

C. Steps in exocytosis through a fusion pore. 1. A docked vesicle contains a preassembled fusion pore ready to open. 2. During the initial stages of exocytosis the fusion pore rapidly opens, allowing transmitter to leak out of the vesicle. 3. In most cases the fusion pore rapidly dilates as the vesicle undergoes complete fusion with the plasma membrane.

corresponding to the exocytosis of the contents of a single large dense-core vesicle. Often, these large transient increases are preceded by a smaller longer-lasting signal, corresponding to a period of release at a low rate (Figure 14-11C). Such events are thought to reflect leakage of transmitter through the fusion pore, prior to complete exocytotic fusion. A good deal of fast transmitter release may involve release through fusion pores without the requirement for complete fusion.

Synaptic Vesicles Are Recycled

If there were no process to compensate for the fusion of successive vesicles to the plasma membrane during continued nerve activity, the membrane of a synaptic terminal would enlarge and the number of synaptic vesicles would decline. This does not occur, however, because the vesicle membrane added to the terminal membrane is retrieved rapidly and recycled, generating new synaptic vesicles (Figure 14-12).

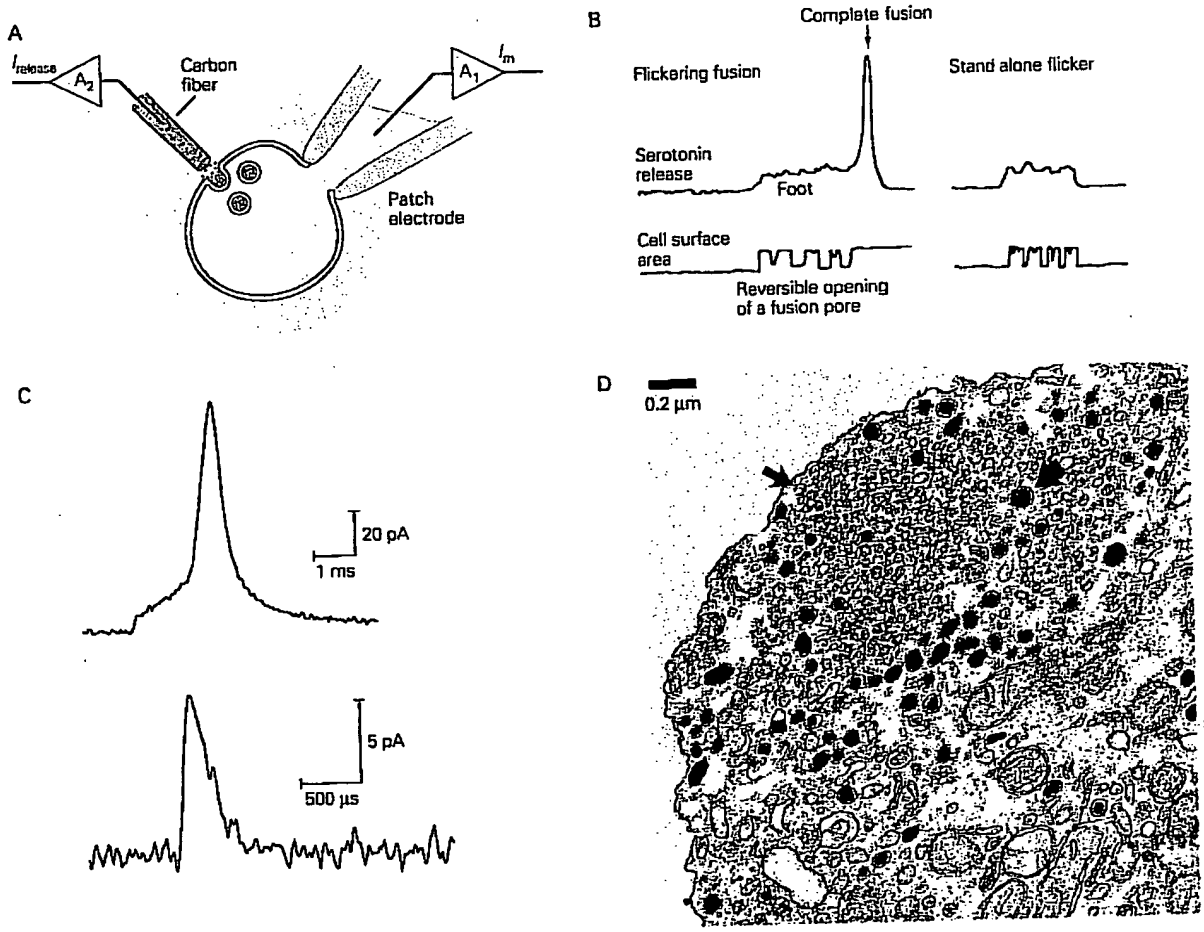

Figure 14-11 Transmitter release through the fusion pore can be measured using electrochemical detection methods.

A. Setup for recording transmitter release by voltametry. A cell is voltage-clamped with an intracellular patch electrode while an extracellular carbon fiber is pressed against the cell surface. A large voltage applied to the tip of the electrode oxidizes certain amine-containing transmitters (such as serotonin or norepinephrine). This oxidation reaction generates one or more free electrons, which results in an electrical current that can be recorded through an amplifier (A_2) connected to the carbon electrode. The current is proportional to the amount of transmitter release. Membrane current and capacitance are recorded through the intracellular patch electrode amplifier (A_1).

B. Recordings of transmitter release and capacitance measurements from mast cell secretory vesicles indicate that the fusion pore may "flicker" (open and close several times) prior to complete membrane fusion. During these brief openings transmitter can diffuse out through the pore, producing a "foot" of low-level release that precedes a large spike of transmitter release upon a full fusion event. Sometimes the reversible fusion pore opening and closing is not followed by full fusion, resulting in "stand alone flicker" in which transmitter is released only by diffusion through the fusion pore. (From Neher 1993.)

C–D. Similar patterns of release of the transmitter serotonin are observed from Retzius neurons of the leech. The electron micrograph shows that these neurons package serotonin in both large, dense-core vesicles and small, clear synaptic vesicles (arrow). Amperometry measurements show that Ca^{2+} elevation triggers both large spikes of serotonin release (top trace) and smaller release events (bottom trace) (note the difference in current scales). These correspond to fusion of the large dense-core vesicles and synaptic vesicles, respectively. The synaptic vesicles release their contents rapidly, in less than 1 ms. This rapid time course is consistent with the expected rate of diffusion of transmitter through a fusion pore of 300 pS. Each large vesicle contains around 15,000–300,000 molecules of serotonin. Each small vesicle contains approximately 5000 molecules of serotonin. (From Bruns and Jahn 1995.)

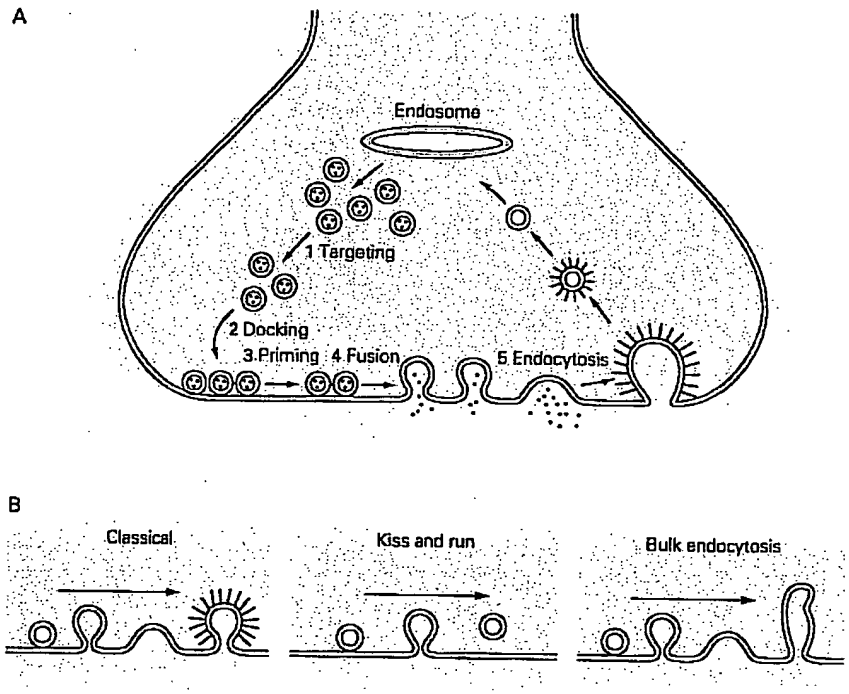

Figure 14-12 The cycling of synaptic vesicles at nerve terminals involves several distinct steps.

A. Free vesicles must be *targeted* to the active zone (1) and then dock at the active zone (2). The docked vesicles must become primed so that they can undergo exocytosis (3). In response to a rise in Ca^{2+} the vesicles undergo fusion and release their contents (4). The fused vesicle membrane is taken up into the interior of the cell by endocytosis (5). The endocytosed vesicles then fuse with the endosome, an internal membrane compartment. After processing, new synaptic vesicles bud off the endosome, completing the recycling process.

B. Retrieval of vesicles after exocytosis is thought to occur via three distinct mechanisms. In the first, classical pathway excess membrane is retrieved by means of clathrin-coated pits. These coated pits concentrate certain intramembranous particles into small packages. The pits are found throughout the terminal except at the active zones. As the plasma membrane enlarges during exocytosis, more membrane invaginations are coated on the cytoplasmic surface. (The path of the coated pits is shown by arrows after step 5.) This pathway may be important at normal to high rates of release. In the kiss-and-run pathway the vesicle does not completely integrate itself into the plasma membrane. This corresponds to release through the fusion pore. This pathway may predominate at lower to normal release rates. In the bulk endocytosis pathway excess membrane reenters the terminal by budding from uncoated pits. These uncoated cisternae are formed primarily at the active zones. This pathway may be reserved for retrieval after very high rates of release and may not be used during the usual functioning of the synapse. (Adapted from Schweizer et al. 1995.)

Although the number of vesicles in a nerve terminal does decrease transiently during release, the total amount of membrane in vesicles, cisternae, and plasma membrane remains constant, indicating that membrane is retrieved from the surface membrane into the internal organelles. How the synaptic vesicles are recycled has not yet been resolved, but the process is known to involve clathrin-coating of the vesicle and the protein dynamin (Chapter 4 and below) and is thought to be similar to known mechanisms in epithelial cells (Figure 14-12). According to this view, the excess membrane from synaptic vesicles that have undergone exocytosis is recycled through endocytosis into an intracellular organelle called the endosome. Endocytosis and recycling takes about 30 seconds to one minute to be completed.

More rapid components of membrane recovery have been detected with capacitance measurements. Importantly, the rate of membrane recovery appears to depend on the extent of stimulation and exocytosis. With relatively weak stimuli that release only a few vesicles, membrane retrieval is rapid and occurs within a few seconds (for example, see Figure 14-9B). Stronger stimuli that release more vesicles lead to a slowing of membrane recovery. The fastest form of vesicle cycling in-

volves the release of transmitter through the transient opening and closing of the fusion pore without full membrane fusion. The advantage of such "kiss-and-run" release is that it rapidly recycles the vesicle for subsequent release because it requires only closure of the fusion pore. Thus, different types of retrieval processes may operate under different conditions (Figure 14-12).

A Variety of Proteins Are Involved in the Vesicular Release of Transmitter

What is the nature of the molecular machinery that drives vesicles to cluster near synapses, to dock at active zones, to fuse with the membrane in response to Ca^{2+} influx, and then to recycle? Proteins have been identified that are thought to (1) restrain the vesicles so as to prevent their accidental mobilization, (2) target the freed vesicles to the active zone, (3) dock the targeted vesicles at the active zone and prime them for fusion, (4) allow fusion and exocytosis, and (5) retrieve the fused membrane by endocytosis (Figure 14-13).

We first consider proteins involved in restraint and mobilization. The vesicles outside the active zone represent a reserve pool of transmitter. They do not move about freely in the terminal but rather are restrained or anchored to a network of cytoskeletal filaments by the *synapsins*, a family of four proteins (Ia, Ib, IIa, and IIb). Of these four, synapsins Ia and Ib are the best studied. These two proteins are substrates for both the cAMP-dependent protein kinase and the Ca^{2+}/calmodulin-dependent kinase. When synapsin I is not phosphorylated, it is thought to immobilize synaptic vesicles by linking them to actin filaments and other components of the cytoskeleton. When the nerve terminal is depolarized and Ca^{2+} enters, synapsin I is thought to become phosphorylated by the Ca^{2+}/calmodulin-dependent protein kinase. Phosphorylation frees the vesicles from the cytoskeletal constraint, allowing them to move into the active zone (Figure 14-14).

The targeting of synaptic vesicles to docking sites for release may be carried out by Rab3A and Rab3C, two members of a class of small proteins, related to the *ras* proto-oncogene superfamily, that bind GTP and hydrolyze it to GDP and inorganic phosphate (Figure 14-14B). These Rab proteins bind to synaptic vesicles through a hydrophobic hydrocarbon group that is covalently attached to the carboxy terminus of the Rab protein. Hydrolysis of the GTP bound to Rab, converting it to GDP, may be important for the efficient targeting of synaptic vesicles to their appropriate sites of docking. During exocytosis the Rab proteins are released from the synaptic vesicles into the cytoplasm.

Following the targeting of a vesicle to its release site, a complex set of interactions occurs between proteins in the synaptic vesicle membrane and proteins in the presynaptic membrane. Such interactions are thought to complete the docking of vesicles and to prime them so they are ready to undergo fusion in response to Ca^{2+} influx. Similar interactions are important for exocytosis in all cells, not only in the synaptic terminals of neurons.

As we have seen in Chapter 4, all secretory proteins are synthesized on ribosomes and injected into the lumen of the endoplasmic reticulum (ER). When these proteins leave the ER they are targeted to the Golgi apparatus in vesicles formed from the membrane of the ER. The vesicles then dock and fuse with the Golgi membrane, discharging their protein into the lumen of the Golgi, where the protein is modified. Other vesicles shuttle the secretory protein between the *cis* and the *trans* compartments (the different cisternae) of the Golgi apparatus until the protein becomes fully modified and mature. The mature protein is packaged in vesicles that bud off the Golgi and migrate to the cell surface, where the protein is released through exocytosis. This type of release is *constitutive* (that is the release is continuous and occurs independently of Ca^{2+}) in contrast to *regulated* release, which occurs at synapses in response to Ca^{2+} entry into the presynaptic terminal.

One prominent hypothesis for how membrane vesicles are docked and readied for exocytosis has been proposed by James Rothman, Richard Scheller, and Reinhard Jahn. According to this theory, specific integral proteins in the vesicle membrane (vesicle-SNARES, or v-SNARES) bind to specific receptor proteins in the target membrane (target membrane or t-SNARE) (Figure 14-15). In the brain two t-SNARES have been identified: *syntaxin*, a nerve terminal integral membrane protein, and SNAP-25, a peripheral membrane protein of 25 kDa mass. In the synaptic vesicle the integral membrane protein VAMP (or synaptobrevin) has been identified as the v-SNARE.

The importance of the SNARE proteins in synaptic transmission is emphasized by the finding that all three proteins are targets of various clostridial neurotoxins. All of these toxins act by inhibiting synaptic transmission. One such toxin, tetanus toxin, a zinc endoprotease, specifically cleaves VAMP. Three other zinc endoproteases, botulinum toxins A, B, and C, specifically cleave SNAP-25, VAMP, and syntaxin, respectively. VAMP has the additional feature that it resembles a viral fusion peptide.

Reconstitution studies of purified proteins in lipid vesicles indicate that VAMP, syntaxin, and SNAP-25 may form the minimal functional unit that mediates membrane fusion. Moreover a detailed structural model

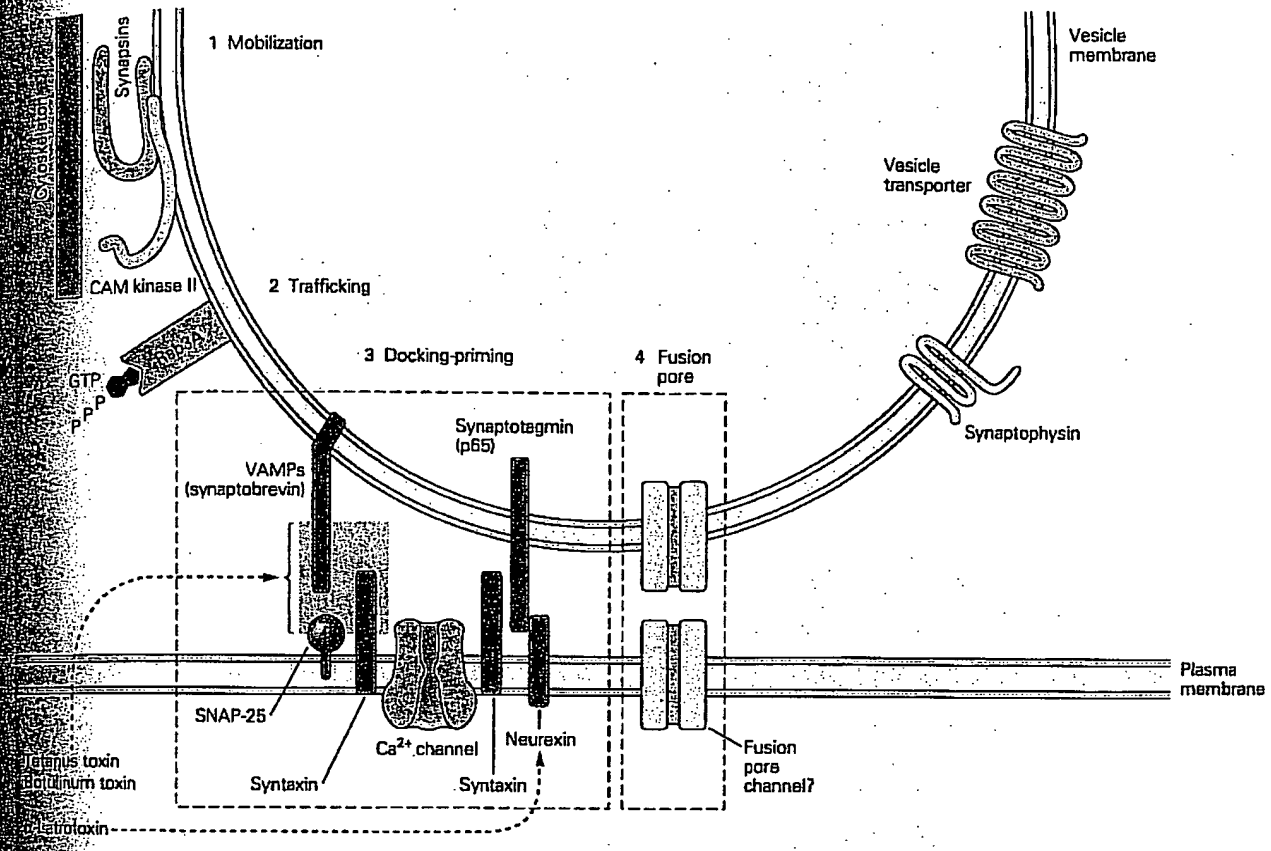

Figure 14-13 This diagram depicts characterized synaptic vesicle proteins and some of their postulated receptors and functions. Separate compartments are assumed for (1) storage (where vesicles are tethered to the cytoskeleton), (2) trafficking and targeting of vesicles to active zones, (3) the docking of vesicles at active zones and their priming for release, and (4) release. Some of these proteins represent the targets for neurotoxins that act by modifying transmitter release. VAMP (synaptobrevin), SNAP-25, and syntaxin are the targets for tetanus and botulinum toxins, two zinc-dependent metalloproteases, and are cleaved by these enzymes. α-Latrotoxin, a spider toxin that generates massive vesicle depletion and transmitter release, binds to the neurexins. **1.** Synapsins are vesicle-associated proteins that are thought to mediate interactions between the synaptic vesicle and the cytoskeletal elements of the nerve terminal. **2.** The Rab proteins (see Figure 14-14B) appear to be involved in vesicle trafficking within the cell and also in targeting of vesicles within the nerve terminal. **3.** The docking, fusion, and release of vesicles appears to involve distinct interactions between vesicle proteins and proteins of the nerve terminal plasma membrane: VAMP (synaptobrevin) and synaptotagmin (p65) on the vesicle membrane, and syntaxins and neurexins on the nerve terminal membrane. Arrows indicate potential interactions suggested on the basis of in vitro studies. **4.** The identity of the vesicle and plasma membrane proteins that comprise the fusion pore remains unclear. Synaptophysin, an integral membrane protein in synaptic vesicles, is phosphorylated by tyrosine kinases and may regulate release. Vesicle transporters are involved in accumulation of neurotransmitter within the synaptic vesicle (see Chapter 15).

has been proposed for how these proteins interact to promote membrane fusion (Figure 14-15B).

The ternary complex of VAMP, syntaxin, and SNAP-25 is extraordinarily stable. For efficient vesicle recycling to occur this complex must be disassembled by the binding of two soluble cytoplasmic proteins: the *N*-ethylmaleimide-sensitive fusion (NSF) protein and the soluble NSF attachment protein (SNAP—this protein is unrelated to SNAP-25; the similar names are coincidental). The v-SNARES and t-SNARES serve as receptors for SNAP (hence their name *SNAP receptors*), which then binds NSF. The NSF is an ATPase, utilizing the energy released upon hydrolysis of ATP to unravel the SNARE assembly.

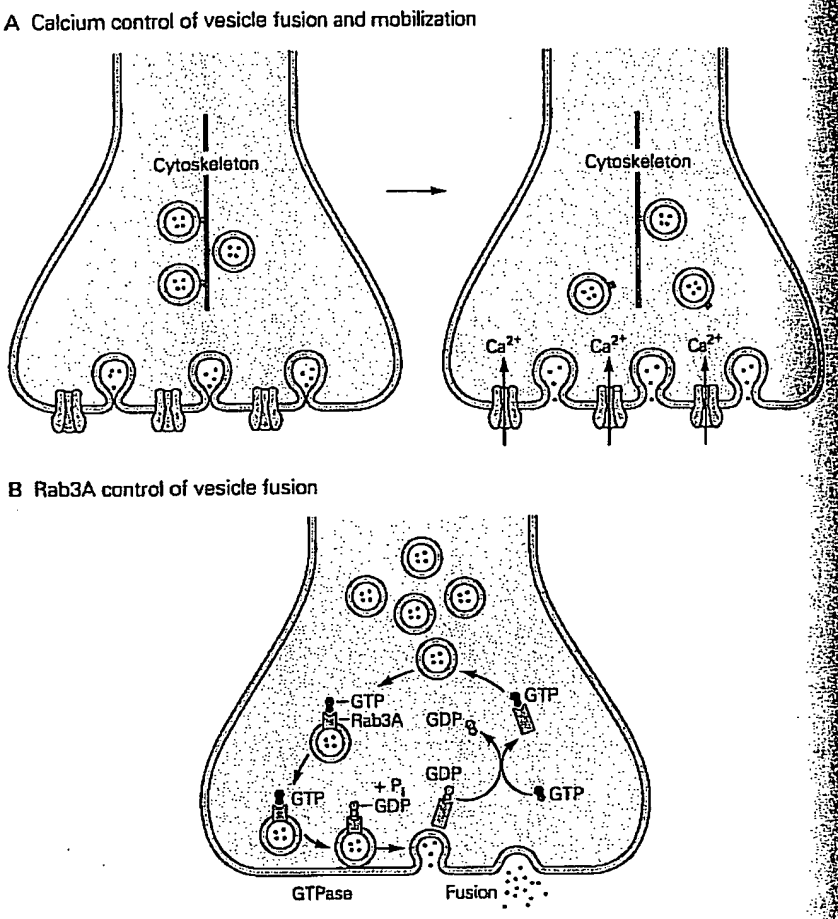

Figure 14-14 The mobilization, docking, and function of synaptic vesicles are controlled by Ca^{2+} and low-molecular-weight GTP-binding proteins.

A. Synaptic vesicles in nerve terminals are sequestered in a *storage compartment* where they are tethered to the cytoskeleton, as well as in a *releasable* compartment where they are docked to the presynaptic membrane. Entry of Ca^{2+} into the nerve terminal leads to the opening of the fusion pore complex and neurotransmitter release. Calcium entry also frees vesicles from the storage compartment through phosphorylation of synapsins, thus increasing the availability of vesicles for docking at the presynaptic plasma membrane.

B. The Rab3A cycle targets vesicles to their release sites. Rab3A complexed to GTP binds to synaptic vesicles. During the targeting of synaptic vesicles to the active zone, Rab3A hydrolyzes its bound GTP to GDP. GTP hydrolysis may serve to make a reversible reaction irreversible, preventing vesicles from leaving the active zone once they arrive. During fusion and exocytosis, Rab3A-GDP dissociates from the vesicle. There is then an exchange of GTP for GDP. This is followed by the association of Rab3A-GTP with a new synaptic vesicle, thus completing the cycle.

One additional integral membrane protein of the synaptic vesicle, thought to be important for exocytosis, is *synaptotagmin* (or p65). Synaptotagmin contains two domains (the C2 domains) homologous to the regulatory region of protein kinase C. The C2 domains bind to phospholipids in a calcium-dependent manner. This property suggests that synaptotagmin might insert into the presynaptic phospholipid bilayer in response to Ca^{2+} influx, thus serving as the calcium sensor for exocytosis (see Figure 14-12). Synaptotagmin may also function as a v-SNARE since it binds syntaxin and a SNAP isoform.

Several mutant animals that lack synaptotagmin have been created to test this protein's role in synaptic transmission. Based on these experiments two models have been proposed for the role of synaptotagmin. According to one view synaptotagmin acts as a fusion clamp or negative regulator of release (preventing exocytosis in the absence of Ca^{2+}). In this view, the influx of Ca^{2+} rapidly frees this clamp, allowing synchronous release. This hypothesis is attractive since the same machinery involved in synaptic vesicle fusion (the SNAP-SNARE complex) also functions in constitutive release that is independent of external Ca^{2+}. This model is based on results from experiments with *Drosophila* and nematode mutants lacking synaptotagmin, which show greatly impaired synaptic transmission in response to an action potential in the presynaptic terminal. Moreover, in *Drosophila* the rate of spontaneous miniature end-plate potentials is increased, suggesting that synaptotagmin has an inhibitory role.

The second hypothesis is that synaptotagmin serves as a positive regulator of release, actively promoting vesicle fusion. This view is based on the observation that in mutant mice that lack a major isoform of synaptotagmin, fast synaptic transmission is blocked without an increase in spontaneous release. Since there are several isoforms of synaptotagmin in mammals, but only one isoform in invertebrates, it is possible that the different mammalian isoforms have different roles: One

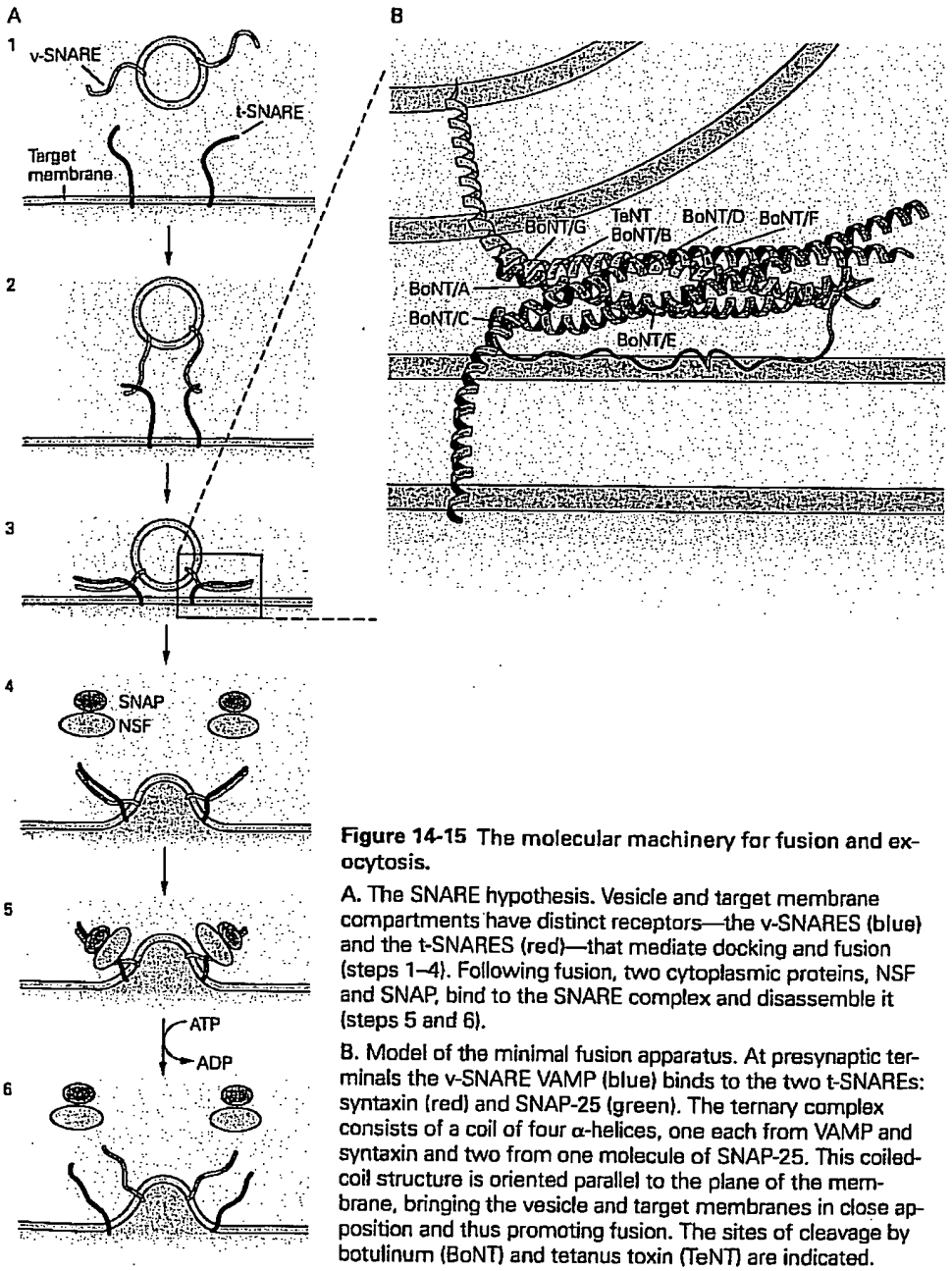

Figure 14-15 The molecular machinery for fusion and exocytosis.

A. The SNARE hypothesis. Vesicle and target membrane compartments have distinct receptors—the v-SNARES (blue) and the t-SNARES (red)—that mediate docking and fusion (steps 1–4). Following fusion, two cytoplasmic proteins, NSF and SNAP, bind to the SNARE complex and disassemble it (steps 5 and 6).

B. Model of the minimal fusion apparatus. At presynaptic terminals the v-SNARE VAMP (blue) binds to the two t-SNAREs: syntaxin (red) and SNAP-25 (green). The ternary complex consists of a coil of four α-helices, one each from VAMP and syntaxin and two from one molecule of SNAP-25. This coiled-coil structure is oriented parallel to the plane of the membrane, bringing the vesicle and target membranes in close apposition and thus promoting fusion. The sites of cleavage by botulinum (BoNT) and tetanus toxin (TeNT) are indicated.

...mediate regulated fast release and another may ...ntrol constitutive release.

...Synaptotagmin may also play an additional role in ...ndocytosis. Following exocytosis the fused membrane ...hieved by endocytosis. Excess membrane anywhere ...terminal except at the active zone leads to the for... ...of a pit that is coated with clathrin. The binding ...clathrin to the membrane is enhanced by certain ...tor proteins. Synaptotagmin serves as a receptor for the clathrin adaptor protein AP-2. The clathrin coat forms a regular lattice around the pit, which finally pinches off as a small coated vesicle. The pinching off of the vesicle depends on a cytoplasmic GTPase called dynamin, which forms a constricting helical ring around the neck of the vesicle during endocytosis. A *Drosophila* mutant defective in dynamin is impaired in synaptic transmission owing to an inhibition of vesicle recycling.

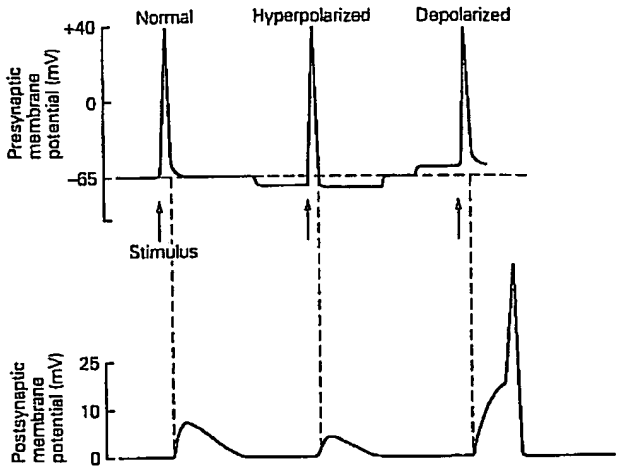

Figure 14-16 Changes in membrane potential of the presynaptic terminal affect the intracellular concentration of Ca^{2+} and thus the amount of transmitter released. When the presynaptic membrane is at its normal resting potential, an action potential (top trace) produces a postsynaptic potential of a given size (bottom). Hyperpolarizing the presynaptic terminal by 10 mV prior to an action potential decreases the steady state Ca^{2+} influx, so that the same-size action potential produces a smaller postsynaptic potential. In contrast, *depolarizing* the presynaptic neuron by 10 mV *increases* the steady state Ca^{2+} influx, so that the same-size action potential produces a postsynaptic potential large enough to trigger an action potential in the postsynaptic cell.

The Amount of Transmitter Released Can Be Modulated by Regulating the Amount of Calcium Influx During the Action Potential

The effectiveness of chemical synapses can be modified for both short and long periods. This modifiability, or *synaptic plasticity*, is controlled by two types of processes: (1) processes within the neuron that result from changes in the resting potential or the firing of action potentials and (2) extrinsic processes, such as the synaptic input from other neurons.

Long-term changes in chemical synaptic action are crucial to development and learning, and we consider these changes in detail later in the book. Here we shall first discuss the short-term changes—changes in the amount of transmitter released due to either changes within the presynaptic terminal or extrinsic factors.

Intrinsic Cellular Mechanisms Regulate the Concentration of Free Calcium

As we saw at the beginning of this chapter, transmitter release depends strongly on the intracellular Ca^{2+} concentration. Thus, mechanisms within the presynaptic neuron that affect the concentration of free Ca^{2+} in the presynaptic terminal also affect the amount of transmitter released. In some cells there is a small steady influx of Ca^{2+} through the presynaptic terminal membrane even at the resting membrane potential. This Ca^{2+} flows through the L-type voltage-gated Ca^{2+} channels, which inactivate little, if at all.

The steady state Ca^{2+} influx is enhanced by depolarization and decreased by hyperpolarization. A slight depolarization of the membrane can increase the steady state influx of Ca^{2+} and thus enhance the amount of transmitter released by subsequent action potentials. A slight hyperpolarization has the opposite effect (Figure 14-16). By altering the amount of Ca^{2+} that flows into the terminal, small changes in the resting membrane potential can make an effective synapse inoperative or a weak synapse highly effective. Such changes in membrane potential can also be produced by other neurons releasing transmitter at axo-axonic synapses that regulate presynaptic ion channels, as described later. They can also be produced experimentally by injecting current.

Synaptic effectiveness can also be altered in most nerve cells by intense activity. In these cells a high-frequency train of action potentials is followed by a period during which action potentials produce successively larger postsynaptic potentials. High-frequency stimulation of the presynaptic neuron (which in some cells can generate 500–1000 action potentials per second) is called *tetanic stimulation*. The increase in size of the postsynaptic potentials during tetanic stimulation is called *potentiation;* the increase that persists after tetanic stimulation is called *posttetanic potentiation*. This enhancement usually lasts several minutes, but it can persist for an hour or more (Figure 14-17).

Posttetanic potentiation is thought to result from a transient saturation of the various Ca^{2+} buffering systems in the presynaptic terminals, primarily the smooth endoplasmic reticulum and mitochondria. This leads to a temporary excess of Ca^{2+}, called *residual* Ca^{2+}, the result of the relatively large influx that accompanies the train of action potentials. The increase in the resting concentration of free Ca^{2+} enhances synaptic transmission for many minutes or longer by activating certain enzymes that are sensitive to the enhanced levels of resting Ca^{2+}, for example, the Ca^{2+}/calmodulin-dependent protein kinase. Activation of such calcium-dependent enzymatic pathways is thought to increase the mobilization of synaptic vesicles in the terminals, for example through phosphorylation of the synapsins. Phosphorylation of synapsin allows synaptic vesicles to be freed from their cytoskeletal restraint and to be mobilized

docked at release sites. As a result, each action potential sweeping into the terminals of the presynaptic neuron will release more transmitter than before. Here then is a simple kind of cellular memory! The presynaptic cell stores information about the history of its activity in the form of residual Ca^{2+} in its terminals. The storage of biochemical information in the nerve cell, after a brief period of activity, leads to a strengthening of the presynaptic connection that persists for many minutes. In Chapter 62 we shall see how posttetanic potentiation at certain synapses is followed by an even longer-lasting process (also initiated by Ca^{2+} influx), called *long-term potentiation*, which can last for many hours or even days.

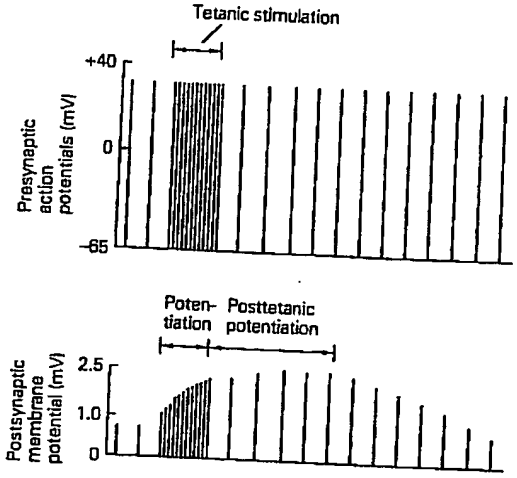

Figure 14-17 A high rate of stimulation of the presynaptic neuron produces a gradual increase in the amplitude of the postsynaptic potentials. This enhancement in the strength of the synapse represents storage of information about previous activity, an elementary form of memory. The time scale of the experimental record here has been compressed (each presynaptic and postsynaptic potential appears as a simple line indicating its amplitude). To establish a baseline (control), the presynaptic neuron is stimulated at a rate of 1 per second, producing a postsynaptic potential of about 1 mV. The presynaptic neuron is then stimulated for several seconds at a higher rate of 5 per second. During this *tetanic stimulation* the postsynaptic potential increases in size, a phenomenon known as *potentiation*. After several seconds of stimulation the presynaptic neuron is returned to the control rate of firing (1 per second). However, the postsynaptic potentials remain enhanced for minutes, and in some cells for several hours. This persistent increase is called *posttetanic potentiation*.

Axo-axonic Synapses on Presynaptic Terminals Regulate Intracellular Free Calcium

Synapses are formed on axon terminals as well as the cell body and dendrites of neurons (see Chapter 12). Whereas axosomatic synaptic actions affect all branches of the postsynaptic neuron's axon (because they affect the probability that the neuron will fire an action potential), axo-axonic actions selectively control individual branches of the axon. One important action of axo-axonic synapses is to control Ca^{2+} influx into the presynaptic terminals of the postsynaptic cell, either depressing or enhancing transmitter release.

As we saw in Chapter 12, when one neuron hyperpolarizes the cell body (or dendrites) of another, it decreases the likelihood that the postsynaptic cell will fire; this action is called *postsynaptic inhibition*. In contrast, when a neuron contacts the axon terminal of another cell, it can reduce the amount of transmitter that will be released by the second cell onto a third cell; this action is called *presynaptic inhibition* (Figure 14-18A). Likewise, axo-axonic synaptic actions can increase the amount of transmitter released by the postsynaptic cell; this action is called *presynaptic facilitation* (Figure 14-18B). For reasons that are not well understood, presynaptic modulation usually occurs early in sensory pathways.

The best-analyzed mechanisms of presynaptic inhibition and facilitation are in the neurons of invertebrates and in the mechanoreceptor neurons (whose cell bodies are in dorsal root ganglia) of vertebrates. Three mechanisms for presynaptic inhibition have been identified in these cells. One is mediated by activation of metabotropic receptors that leads to the simultaneous closure of Ca^{2+} channels and opening of voltage-gated K^+ channels, which both decreases the influx of Ca^{2+} and enhances repolarization of the cell. The second mechanism is mediated by activation of ionotropic GABA-gated Cl^- channels, resulting in an increased conductance to Cl^-, which decreases (or short-circuits) the amplitude of the action potential in the presynaptic terminal. As a result, less depolarization is produced and fewer Ca^{2+} channels are activated by the action potential. The third mechanism is also mediated by activation of metabotropic receptors and involves direct inhibition of the transmitter release machinery, independent of Ca^{2+} influx. This is thought to work by decreasing the Ca^{2+} sensitivity of one or more steps involved in the release process.

Presynaptic facilitation, in contrast, can be caused by an enhanced influx of Ca^{2+}. In certain molluscan neurons serotonin acts through cAMP-dependent protein phosphorylation to close K^+ channels, thereby broadening the action potential and allowing the Ca^{2+} influx to persist for a longer period (see Chapter 13). In

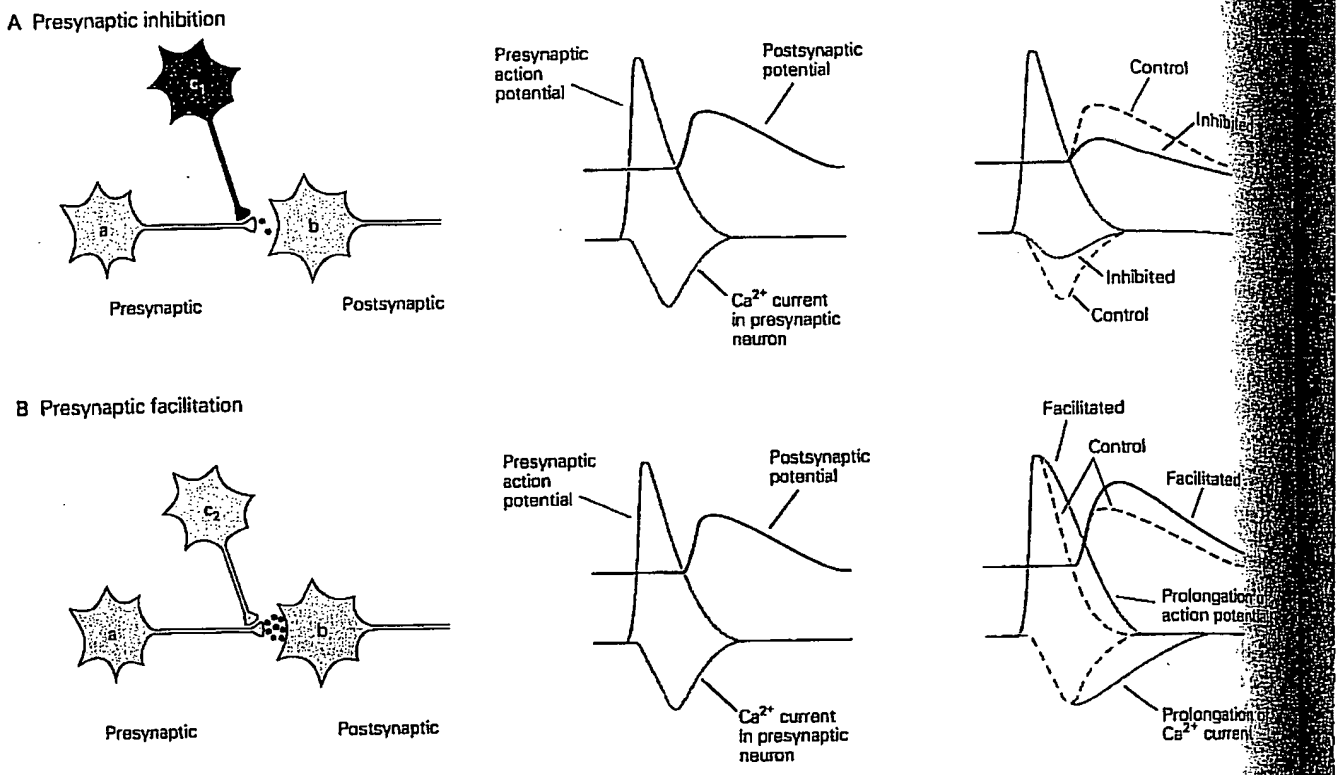

Figure 14-18 Axo-axonic synapses can inhibit or facilitate transmitter release by the postsynaptic cell.

A. An inhibitory neuron (c_1) contacts the terminal of a second presynaptic neuron (a). Release of transmitter by cell c_1 depresses the Ca^{2+} current in cell a, thereby reducing the amount of transmitter released by cell a. As a result, the postsynaptic potential in cell b is depressed.

B. A facilitating neuron (c_2) contacts the terminal of a second presynaptic neuron (a). Release of transmitter by cell c_2 depresses the K^+ current in cell a, thereby prolonging the action potential in cell a and increasing the Ca^{2+} influx through voltage-gated Ca^{2+} channels. As a result, the postsynaptic potential in cell b is increased.

addition, the cAMP-dependent protein kinase also acts directly on the machinery of exocytosis to enhance release in a manner that is independent of the amount of Ca^{2+} influx. In other cells activation of presynaptic ligand-gated channels, such as nicotinic ACh receptors or the kainate type of glutamate receptors, increases transmitter release, possibly by depolarizing the presynaptic terminals and enhancing Ca^{2+} influx.

Thus, regulation of the free Ca^{2+} concentration in the presynaptic terminal is an important factor in a variety of mechanisms that endow chemical synapses with plastic capabilities. Although we know a fair amount about short-term changes in synaptic effectiveness—changes that last minutes and hours—we are only beginning to learn about changes that persist days, weeks, and longer. These long-term changes often require alteration in gene expression and growth of synapses in addition to alteration in Ca^{2+} influx and enhancement of release from preexisting synapses.

An Overall View

In his book *Ionic Channels of Excitable Membranes*, Bertil Hille summarizes the importance of calcium in neuronal function:

Electricity is used to gate channels and channels are used to make electricity. However, the nervous system is not primarily an electrical device. Most excitable cells ultimately translate their electrical excitation into another form of activity. As a broad generalization, excitable cells translate their electricity into action by Ca^{2+} fluxes modulated by voltage-sensitive Ca^{2+} channels. Calcium ions are intracellular messengers

...le of activating many cell functions. Calcium channels... ...e as the only link to transduce depolarization into all the ...electrical activities controlled by excitation. Without Ca^{2+} ...nnels our nervous system would have no outputs.

...Neither Na^+ influx nor K^+ efflux is required to re... ...ase neurotransmitters at a synapse. Only Ca^{2+}, which ...ters the cell through voltage-gated channels in the ...esynaptic terminal, is essential. Synaptic delay—the ...time between the onset of the action potential and the ...lease of transmitter—largely reflects the time it takes ...voltage-gated Ca^{2+} channels to open and for Ca^{2+} to ...ger the discharge of transmitter from synaptic vesi...

...Transmitter is packaged in vesicles and each vesicle ...ntains approximately 5000 transmitter molecules. Re... ...ase of transmitter from a single vesicle results in a ...antal synaptic potential. Spontaneous miniature ...naptic potentials result from the spontaneous fusion ...single synaptic vesicles. Synaptic potentials evoked ...nerve stimulation are composed of integral multiples ...the quantal potential. Increasing the extracellular ...does not change the size of the quantal synaptic ...tential. Rather, it increases the probability that a vesi...will discharge its transmitter. As a result, there is an ...crease in the number of vesicles released and a larger ...ostsynaptic potential.

...Rapid freezing experiments have shown that the ...sicles fuse with the presynaptic plasma membrane in ...vicinity of the active zone. Freeze-fracture studies ...have also revealed rows of large intramembranous par...icles along the active zone that are thought to be Ca^{2+} ...annels. These highly localized channels may be re...ponsible for the rapid increase, as much as a thousand...old in the Ca^{2+} concentration of the axon terminal dur...ng an action potential. One hypothesis about how Ca^{2+} ...ggers vesicle fusion is that this ion permits the forma...tion of a fusion pore that traverses both the vesicle and ...plasma membrane. This pore allows the contents of ...vesicle to be released into the extracellular space and ...may further dilate so that the entire vesicle fuses with ...presynaptic plasma membrane.

...Calcium also regulates the mobilization of the ...naptic vesicles to the active zone. These vesicles ap...pear to be bound to the cytoskeleton by synapsin, and ...ions thought to free the vesicles by activating the ...calmodulin–dependent protein kinase, which ...phosphorylates the synapsins.

...Several molecular candidates have been identified ...that could account for the two other components of re...lease, targeting and docking. Targeting is thought to be ...mediated by the small GTP-binding Rab3A and Rab3C ...proteins. Docking and fusion is thought to involve the synaptic vesicle v-SNARE VAMP (or synaptobrevin) and the plasma membrane t-SNARES, syntaxin and SNAP-25. Calcium binding to synaptotagmin may actively promote vesicle fusion or remove an inhibitory clamp that normally blocks fusion.

Finally, the amount of transmitter released from a neuron is not fixed but can be modified by both intrinsic and extrinsic modulatory processes. High-frequency stimulation produces an increase in transmitter release called posttetanic potentiation. This (intrinsic) potentiation, which lasts a few minutes, is caused by Ca^{2+} left in the terminal after the large Ca^{2+} influx that occurs during the train of action potentials. Tonic depolarization or hyperpolarization of the presynaptic neuron can also modulate release by altering steady state Ca^{2+} influx. The extrinsic action of neurotransmitters on receptors in the axon terminal of another neuron can facilitate or inhibit transmitter release by altering the steady state level of resting Ca^{2+} or the Ca^{2+} influx during the action potential.

In the next chapter we shall carry our discussion of synaptic transmission further by examining the nature of the transmitter molecules that are used for chemical transmission.

Eric R. Kandel
Steven A. Siegelbaum

Selected Readings

Dunlap K, Luebke JI, Turner TJ. 1995. Exocytotic Ca^{2+} channels in mammalian central neurons. Trends Neurosci 18:89–98.

Hanson PI, Heuser JE, Jahn R. 1997. Neurotransmitter release—four years of SNARE complexes. Curr Opin Neurobiol 7(3):310–315.

Jessell TM, Kandel ER. 1993. Synaptic transmission: a bidirectional and self-modifiable form of cell-cell communication. Cell 72:1–30.

Katz B. 1969. *The Release of Neural Transmitter Substances.* Springfield, IL: Thomas.

Lindau M, Almers W. 1995. Structure and function of fusion pores in exocytosis and ectoplasmic membrane fusion. Curr Opin Cell Biol 7:509–517.

Matthews G. 1996. Synaptic exocytosis and endocytosis: capacitance measurements. Curr Opin Neurobiol 6(3): 358–364.

Schweizer FE, Betz H, Augustine GJ. 1995. From vesicle

docking to endocytosis: intermediate reactions of exocytosis. Neuron 14(4):689–696.

Smith SJ, Augustine GJ. 1988. Calcium ions, active zones and synaptic transmitter release. Trends Neurosci 11:458–464.

Südhof TC. 1995. The synaptic vesicle cycle: a cascade of protein-protein interactions. Nature 375:645–653.

References

Alberts B, Bray D, Lewis J, Raff M, Roberts K, Watson JD. 1994. *Molecular Biology of the Cell*, 3rd ed. New York: Garland.

Almers W, Tse FW. 1990. Transmitter release from synapses: Does a preassembled fusion pore initiate exocytosis? Neuron 4:813–818.

Bähler M, Greengard P. 1987. Synapsin I bundles F-actin in a phosphorylation-dependent manner. Nature 326:704–707.

Baker PF, Hodgkin AL, Ridgway EB. 1971. Depolarization and calcium entry in squid giant axons. J Physiol (Lond) 218:709–755.

Boyd IA, Martin AR. 1956. The end-plate potential in mammalian muscle. J Physiol (Lond) 132:74–91.

Breckenridge LJ, Almers W. 1987. Currents through the fusion pore that forms during exocytosis of a secretory vesicle. Nature 328:814–817.

Bruns D, Jahn R. 1995. Real-time measurement of transmitter release from single synaptic vesicles. Nature 377:62–65.

Couteaux R, Pecot-Dechavassine M. 1970. Vésicules synaptiques et poches au niveau des "zones actives" de la jonction neuromusculaire. C R Hebd Séances Acad Sci Sér D Sci Nat 271:2346–2349.

Del Castillo J, Katz B. 1954. The effect of magnesium on the activity of motor nerve endings. J Physiol (Lond) 124:553–559.

Erulkar SD, Rahamimoff R. 1978. The role of calcium ions in tetanic and post-tetanic increase of miniature end-plate potential frequency. J Physiol (Lond) 278:501–511.

Faber DS, Korn H. 1988. Unitary conductance changes at teleost Mauthner cell glycinergic synapses: a voltage-clamp and pharmacologic analysis. J Neurophysiol 60:1982–1999.

Fatt P, Katz B. 1952. Spontaneous subthreshold activity at motor nerve endings. J Physiol (Lond) 117:109–128.

Fawcett DW. 1981. *The Cell*, 2nd ed. Philadelphia: Saunders.

Fernandez JM, Neher E, Gomperts BD. 1984. Capacitance measurements reveal stepwise fusion events in degranulating mast cells. Nature 312:453–455.

Geppert M, Sudhof TC. 1998. RAB3 and synaptotagmin: the yin and yang of synaptic membrane fusion. Annu Rev Neurosci 21:75–95.

Heuser JE, Reese TS. 1977. Structure of the synapse. In: ER Kandel (ed). *Handbook of Physiology: A Critical, Comprehensive Presentation of Physiological Knowledge and Concepts*, Sect. 1, *The Nervous System*. Vol. 1, *Cellular Biology of Neurons*, Part 1, pp. 261–294. Bethesda, MD: American Physiological Society.

Heuser JE, Reese TS. 1981. Structural changes in transmitter release at the frog neuromuscular junction. J Cell Biol 88:564–580.

Hille B. 1992. *Ionic Channels of Excitable Membranes*, 2nd ed. Sunderland, MA: Sinauer.

Hirning LD, Fox AP, McCleskey EW, Olivera BM, Thayer SA, Miller RJ, Tsien RW. 1988. Dominant role of N-type Ca^{2+} channels in evoked release of norepinephrine from sympathetic neurons. Science 239(4835):57–61.

Jones SW. 1998. Overview of voltage-dependent Ca channels. J Bionerg Biomembr 30(4):299–312.

Kandel ER. 1976. *The Cellular Basis of Behavior: An Introduction to Behavioral Neurobiology*. San Francisco: Freeman.

Kandel ER. 1981. Calcium and the control of synaptic strength by learning. Nature 293:697–700.

Katz B, Miledi R. 1967a. The study of synaptic transmission in the absence of nerve impulses. J Physiol (Lond) 192:407–436.

Katz B, Miledi R. 1967b. The timing of calcium action during neuromuscular transmission. J Physiol (Lond) 189:535–544.

Kelly RB. 1993. Storage and release of neurotransmitters. Cell 72:43–53.

Klein M, Shapiro E, Kandel ER. 1980. Synaptic plasticity and the modulation of the Ca^{2+} current. J Exp Biol 89:117–157.

Kretz R, Shapiro E, Connor J, Kandel ER. 1984. Post-tetanic potentiation, presynaptic inhibition, and the modulation of the free Ca^{2+} level in the presynaptic terminals. Exp Brain Res Suppl 9:240–283.

Kuffler SW, Nicholls JG, Martin AR. 1984. *From Neuron to Brain: A Cellular Approach to the Function of the Nervous System*, 2nd ed. Sunderland, MA: Sinauer.

Lawson D, Raff MC, Gomperts B, Fewtrell C, Gilula NB. 1977. Molecular events during membrane fusion. A study of exocytosis in rat peritoneal mast cells. Cell Biol 72:242–59.

Liley AW. 1956. The quantal components of the mammalian end-plate potential. J Physiol (Lond) 133:571–587.

Llinás RR. 1982. Calcium in synaptic transmission. Sci Am 247(4):56–65.

Llinás RR, Heuser JE. 1977. Depolarization-release coupling systems in neurons. Neurosci Res Progr Bull 15:555–687.

Llinás R, Steinberg IZ, Walton K. 1981. Relationship between presynaptic calcium current and postsynaptic potential in squid giant synapse. Biophys J 33:323–351.

Martin AR. 1977. Junctional transmission. II. Presynaptic mechanisms. In: ER Kandel (ed). *Handbook of Physiology: A Critical, Comprehensive Presentation of Physiological Knowledge and Concepts*, Sect. 1, *The Nervous System*. Vol. 1, *Cellular Biology of Neurons*, Part 1, pp. 329–355. Bethesda, MD: American Physiological Society.

Monck JR, Fernandez JM. 1992. The exocytotic fusion pore. J Cell Biol 119:1395–1404.

Neher E. 1993. Cell physiology. Secretion without full fusion. Nature 363:497–498.

Nicoll RA. 1982. Neurotransmitters can say more than "yes" or "no." Trends Neurosci 5:369–374.

Peters A, Palay SL, Webster H deF. 1991. *The Fine Structure of the Nervous System: Neurons and Supporting Cells*, 3rd ed. Philadelphia: Saunders.

Redman S. 1990. Quantal analysis of synaptic potentials in neurons of the central nervous system. Physiol Rev 70:165–198.

Robitaille R, Adler EM, Charlton MP. 1990. Strategic location of calcium channels at transmitter release sites of frog neuromuscular synapses. Neuron 5:773–779.

Scheller RH. 1995. Membrane trafficking in the presynaptic nerve terminal. Neuron 14:893–897.

Smith SJ, Augustine GJ, Charlton MP. 1985. Transmission at voltage-clamped giant synapse of the squid: evidence for cooperativity of presynaptic calcium action. Proc Natl Acad Sci U S A 82:622–625.

Söllner T, Whiteheart SW, Brunner M, Erdjument-Bromage H, Geromanos S, Tempest P, Rothman JE. 1993. SNAP receptors implicated in vesicle targeting and fusion. Nature 362:318–324.

Spruce AE, Breckenridge LJ, Lee AK, Almers W. 1990. Properties of the fusion pore that forms during exocytosis of a mast cell secretory vesicle. Neuron 4:643–654.

Südhof TC, Czernik AJ, Kao H-T, Takei K, Johnston PA, Horiuchi A, Kanazir SD, Wagner MA, Perin MS, De Camilli P, Greengard P. 1989. Synapsins: mosaics of shared and individual domains in a family of synaptic vesicle phosphoproteins. Science 245:1474–1480.

Sutton RB, Fasshauer D, Jahn R, Brunger AT. 1998. Crystal structure of a SNARE complex involved in synaptic exocytosis at 2.4 A resolution. Nature 395(6700):347–353.

von Gersdorff H, Matthews G. 1994. Dynamics of synaptic vesicle fusion and membrane retrieval in synaptic terminals. Nature 367:735–739.

Weber T, Zemelman BV, McNew JA, Westermann B, Gmachl M, Parlati F, Sollner TH, Rothman JE. 1998. SNAREpins: minimal machinery for membrane fusion. Cell 92(6): 759–772.

Wernig A. 1972. Changes in statistical parameters during facilitation at the crayfish neuromuscular junction. J Physiol (Lond) 226:751–759.

Zucker RS. 1973. Changes in the statistics of transmitter release during facilitation. J Physiol (Lond) 229:787–810.

Increased inwardly rectifying potassium currents in HEK-293 cells expressing murine transient receptor potential 4

Zongming ZHANG, Yufang TANG and Michael Xi ZHU[1]

Neurobiotechnology Center and Department of Neuroscience, Ohio State University, 168 Rightmire Hall, 1060 Carmack Road, Columbus, OH 43210, U.S.A.

Drosophila transient receptor potential (Trp) and its mammalian homologues are postulated to form capacitative Ca^{2+} entry or store-operated channels. Here we show that expression of murine Trp4 in HEK 293 cells also leads to an increase in inwardly rectifying K^+ currents. No similar increase was found in cell lines expressing Trp1, Trp3 or Trp6. Consistent with typical characteristics of inward rectifiers, the K^+ currents in Trp4-expressing cells were blocked by low millimolar concentrations of Cs^+ and Ba^{2+}, but not by 1.2 mM Ca^{2+}, and were only slightly inhibited by 5 mM tetraethylammonium. Single channel recordings of excised inside-out patches revealed the presence of two conducting states of 51 pS and 94 pS in Trp4-expressing cells. The outward current in the excised patches was blocked by 1 mM spermine, but not by 1 mM Mg^{2+}. How Trp4 expression causes the increase in the K^+ currents is not known. We propose that Trp4 either participates in the formation of a novel K^+ channel or up-regulates the expression or activity of endogenous inwardly rectifying K^+ channels.

Key words: capacitative Ca^{2+} entry, K^+ channel, Kir, store-operated channel, Trp4.

INTRODUCTION

In the compound eyes of *Drosophila melanogaster*, transient receptor potential (Trp) and its two homologues, TrpL and Trpγ, form channels that conduct light-induced currents resulting from the activation of G-protein-coupled rhodopsin and the subsequent stimulation of phospholipase C [1–3]. It had long been speculated that, in mammalian cells, capacitative Ca^{2+} entry (CCE), which occurs as a consequence of Ca^{2+} store depletion following the activation of phospholipase C [4,5], might be mediated by channels that share sequence similarity with the *Drosophila* Trp proteins. Indeed, seven Trp homologues have been isolated from mammalian species in recent years, and heterologous expression has revealed a great degree of complexity as to the mode of activation, single-channel conductance and ion selectivity of different Trp homologues [6–14].

Among the seven mammalian Trps, Trp4 has slightly more sequence similarity to the *Drosophila* Trp and TrpL and hence was the first one to be identified by several groups independently using reverse transcriptase coupled to a PCR method. A partial sequence from mouse was first reported [15], which was followed by the full-length cloning of the bovine, rat, mouse and human sequences [7,8,16,17]. The bovine *trp4* was shown to encode a relatively Ca^{2+}-selective channel that was activated in response to Ca^{2+} store depletion when expressed in HEK-293 cells, CHO cells and RBL cells [8,18]. A more recent study indicated that Trp4 participates in the formation of Ca^{2+}-release-activated Ca^{2+}-like channels in bovine adrenal cortex cells [19]. In *Xenopus* oocytes injected with rat *trp4* cRNA, Ca^{2+}-activated Cl^- current was significantly increased after 2 h incubation with a high concentration of thapsigargin (TG) [20]. Thus Trp4 appears to be a component of store-operated channels. However, this view was challenged by a recent study that showed that murine Trp4 (mTrp4), as well as the closely related Trp5, did not respond to store depletion, but rather to the activation of phospholipase C by cell-surface receptors [21]. In addition, the study also suggested that mTrp4 and mTrp5 form non-selective cation channels instead of Ca^{2+}-selective channels, when expressed in HEK-293 cells. Furthermore, expression of human Trp4 in HEK and in CHO cells led to constitutive Ba^{2+} influx and a non-selective cation conductance without affecting either the store-operated or the receptor-activated Ca^{2+} influx and channel activity [17].

It is unclear why the effect of Trp4 on store-operated Ca^{2+} influx or conductance could be observed in some systems but not in others. Perhaps the differences in the DNA constructs, the cellular environment of the expression systems and the experimental protocols used all contribute to the disparities. More importantly, the overexpression of Trp4 may affect the normal function and expression of a number of other proteins in the host cells, such as the up-regulation of Ins(1,4,5)P_3 receptor expression in cells expressing Trp3 [12]. In the present study we show that the constitutive and inducible expression of mTrp4 in HEK-293 cells leads to no significant increases in CCE but causes an enhancement of inwardly rectifying K^+ (Kir) currents. Some preliminary data from the present study have appeared in abstract form [22].

EXPERIMENTAL

Materials

Spermine, potassium gluconate, sodium gluconate, calcium gluconate and tetraethylammonium chloride were from Sigma. ^{35}S Express protein labelling mix (10 Ci/l) was purchased from

Abbreviations used: $[Ca^{2+}]_i$, intracellular Ca^{2+} concentration; CCE, capacitative Ca^{2+} entry; $[K^+]_o$, extracellular K^+ concentration; KATP, ATP-sensitive K^+ channel; Kir, inwardly rectifying K^+; P_o, open probability; Trp, transient receptor potential; T4cAb, anti-Trp4 C-terminal antibody; T4nAb, anti-Trp4 N-terminal antibody; TG, thapsigargin; mTrp4, murine Trp4.

[1] To whom correspondence should be addressed (e-mail zhu.55@osu.edu).

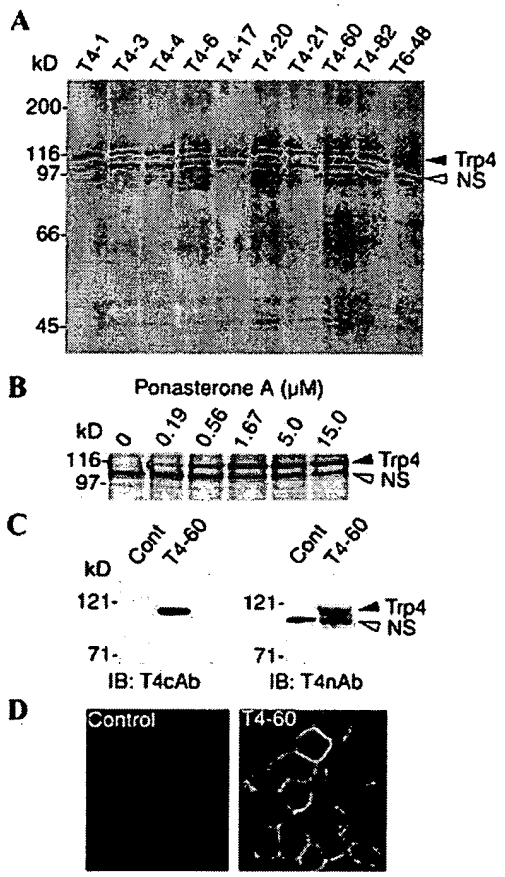

Figure 1 Immunodetection of Trp4 in stable HEK cell lines

(**A**) Immunoprecipitation of [^{35}S]Trp4 from cell lysates prepared from m*trp4* transfected G418-resistant clones using an anti-(Trp4 N-terminus) antibody, T4nAb. The names of the stable clones are indicated on the top. One clone (T4-17) did not express Trp4. A stable HEK cell line expressing murine Trp6 (T6-48) was used as a negative control. The filled arrow indicates the band for Trp4; the open arrow indicates a non-specific (NS) band present in all samples. (**B**) Dose-dependent induction of mTrp4 expression in an inducible cell line by ponasterone A. Equal amount of cells were seeded in wells of a six-well plate. Ponasterone A was added to give the indicated concentrations and cells were incubated at 37 °C for 20 h before [^{35}S]Met/Cys was added. [^{35}S]Trp4 was immunoprecipitated as in (**A**). (**C**) Immunoblotting of Trp4 in control (Cont) and T4-60 cells by the anti-(Trp4 C-terminus) (T4cAb, left) and the anti-(Trp4 N-terminus) (T4nAb, right) antibodies. (**D**) Immunolocalization of Trp4 in control (left) and T4-60 (right) cells by confocal microscopy using T4cAb.

NEN Life Sciences. Protein A–Sepharose (4 Fast Flow) was from Amersham Pharmacia Biotech. Oregon Green-conjugated goat anti-rabbit antibodies were from Molecular Probes. LIPOFECTAMINE® Plus and all tissue-culture reagents were purchased from Life Technologies. EcR 293 cells, ponasterone A and Zeocin were from Invitrogen. Rabbit polyclonal anti-Trp4 N-terminal peptide (Tyr^5–Arg^{17}) antibody (T4nAb) was produced by Quality Controlled Biochemicals (Hopkinton, MA, U.S.A.). Rabbit polyclonal anti-Trp4 C-terminal peptide antibody (T4cAb) was kindly provided by Dr. V. Flockerzi (Universität des Saarlandes, Hamberg, Germany).

cDNA, cell culture, transfection, and cell lines

Full-length cDNA for mTrp4 was isolated from mouse brain as described in [23] and was subcloned into the expression vectors pcDNA3 and pIND (Invitrogen) for constitutive and inducible expression respectively.

Cell-culture conditions and the procedures for the establishment of stable cell lines constitutively expressing mTrp4 in HEK-293 cells were as described in [23]. The expression of mTrp4 in these cell lines was confirmed by immunoprecipitation following the previously described protocol [24] using T4nAb (Figure 1A). To produce stable cell lines for inducible expression of mTrp4, EcR 293 cells were used. These cells are transformed HEK-293 cells that express modified ecdysone receptor and retinoid X receptor required for inducible expression by ecdysone analogues, e.g. ponasterone A. The cells were maintained in Dulbecco's modified Eagle's medium containing 4.5 mg/ml glucose, 10% heat-inactivated fetal-bovine serum, 50 units/ml penicillin and 50 mg/ml streptomycin supplemented with 400 μg/ml Zeocin. m*trp4*/pIND (1 μg) was transfected into 2×10^5 EcR 293 cells seeded in a 35-mm-diameter dish using LIPOFECTAMINE™ Plus reagents following the manufacturer's protocol. Transfected cells were selected by 400 μg/ml G418 in 96-well plates [23], and the expression of mTrp4 was examined by immunoprecipitation after induction by ponasterone A for 20 h. As shown in Figure 1(B), the expression of mTrp4 in one such cell line was dependent on the presence of ponasterone A in a dose-dependent manner, with the maximum induction reached at 5 μM.

For transient expression, 1 μg of m*trp4*/pcDNA3 was co-transfected with 0.2 μg of pEGFPN1 (Clontech) encoding an enhanced green fluorescent protein into 1×10^5 HEK-293 cells seeded on a 35-mm-diameter dish using LIPOFECTAMINE™ Plus reagents. Control cells were transfected with pEGFPN1 only. On the second day, cells were harvested, divided into six portions, plated on 35-mm-diameter dishes, and allowed to grow for an additional 20–30 h. Cells expressing the green fluorescent protein were identified under a Nikon epifluorescence microscope at excitation of 480 nm and emission of 510 mm prior to patch-clamp recording.

Immunoblotting and immunocytochemistry

For immunoblotting, crude membrane preparations from untransfected (control) and the constitutive Trp4 cell line, T4-60, were subjected to SDS/PAGE (8% polyacrylamide) and transferred on to nitrocellulose membrane (Bio-Rad). Western blotting was performed as described in [23], and Trp4 was seen in the preparation from T4-60 by the anti-Trp4 N-terminal antibody, T4nAb (Figure 1C, right) and by the anti-Trp4 C-terminal antibody, T4cAb (Figure 1C, left).

For immunolocalization, formaldehyde-fixed cells were incubated with 1:1000 dilution of T4cAb [19], followed by 1:1000 dilution of Oregon Green-conjugated goat anti-rabbit antibodies. Immunofluorescence signals were examined using a Nikon microscope coupled to a confocal laser scanning unit (Bio-Rad MRC-1024) and were found, to a large extent, to be evenly localized to the periphery of the T4-60 cells (Figure 1D, right), consistent with Trp4 being a plasma-membrane protein. Under the same conditions, untransfected HEK-293 cells (Figure 1D, left) or a stable cell line expressing human Trp3 (not shown) showed no immunostaining.

Intracellular Ca^{2+} imaging

Intracellular Ca^{2+} concentrations ($[Ca^{2+}]_i$) were measured as described previously [6], with the exception that fura 2-loaded cells were examined on a Nikon Eclipse TE200 inverted micro-

scope, a PTI ImageMaster system was used for controlling the excitation wavelengths of 340 nm and 380 nm from a DeltaRAM monochromator, and emitted fluorescence at 510 nm was recorded by an intensified charge coupled device ('CCD') camera (Photon Technology International). The ratio between the emitted fluorescence intensities from 340 nm and 380 nm excitation for individual cells was calculated after experiments using the ImageMaster software. Averages of ratios for cells from 8 to 24 experiments were made using Microsoft Excel.

Electrophysiological studies

Whole-cell recordings

Recording pipettes were pulled from micropipette glass (Drummond Scientific Co., Broomali, PA, U.S.A.) to a resistance of 2–4 MΩ, filled with a pipette solution typically containing, except where indicated otherwise, (in mM): 140 CsCl, 2 $MgCl_2$, 10 Hepes, 10 EGTA, 0.3 $MgATP_2$, and 0.03 GTP, pH 7.20. The normal bath solution contained (in mM): 126 NaCl, 10 $CaCl_2$, 10 glucose, and 15 Hepes, pH 7.40. Isolated HEK cells were voltage-clamped in the whole-cell mode using an Axopatch 200B Amplifier (Axon Instruments, Foster City, CA, U.S.A.). Once the whole-cell configuration was obtained, the recording solution containing (in mM) 140 potassium gluconate/sodium gluconate (either all K^+ or all Na^+, or a mixture of K^+ and Na^+ with a final gluconate concentration of 140), 10 glucose, and 15 Hepes, pH 7.40, was applied through fast bath perfusion. Voltage commands were made from the Clampex program of the pClamp 6.0.4 software and currents were recorded into a Pentium II-based computer through a Digidata 1200 PC interface. A voltage ramp of 210 ms to +80 mV after a brief (25 ms) step to −100 mV from holding potential at 0 mV was applied every 2 s. In some experiments, voltage pulses of 384 ms from −100 mV to 80 mV in 15 mV increments from a holding of 0 mV were also used. All experiments were performed at room temperature. The level of K^+ selective current was determined by subtracting the current recorded in 140 mM sodium gluconate from that recorded in 140 mM potassium gluconate. Data analysis was performed using Clampfit software (Axon Instruments)

Single-channel recordings

The pipettes were pulled from type 7052 glass (Garner Glass Co., Claremont, CA, U.S.A.) to a resistance of 9–11 MΩ and filled with a solution containing (in mM) either 140 sodium gluconate or 140 potassium gluconate, 5 NaCl, 2 $CaCl_2$ and 10 Hepes. Cells were bathed in normal Ringer's solution containing (in mM): 140 NaCl, 10 KCl, 1 $MgCl_2$, 2 $CaCl_2$, and 10 Hepes. Patches were excised to an internal solution containing (in mM) 140 potassium gluconate, 10 Hepes, 2 EGTA and 5 NaCl. $MgCl_2$ or spermine was added to the potassium gluconate internal solution from the concentrated stock and applied through perfusion as needed. The pH was adjusted to 7.40 for all solutions. Currents were recorded at 5 kHz, filtered at 1 kHz for analysis using pClamp 6.0.4 (Axon Instruments). Event lists were generated by Fetchan and used for analysis by the pSTAT program. Open probabilities (P_o) were determined using an interval of 0.5 s and averaged for a given drug treatment.

RESULTS

Expression of mTrp4 in HEK-293 cells leads to no apparent increase in CCE

In order to study its function, we produced stable HEK-293 cell lines expressing mTrp4 in constitutive and inducible ways (Figure 1). To test whether overexpression of Trp4 enhances CCE activity, we measured changes of $[Ca^{2+}]_i$ by fluorescence video imaging in fura 2-loaded cells using the Ca^{2+} free/Ca^{2+} re-addition protocol described previously [6,24]. Although we consistently detected significant increases in agonist-stimulated Ca^{2+} influx in cells expressing human Trp3, we were not able to detect such an increase in stably and transiently transfected cells expressing mTrp4 (results not shown). Cells were also treated with 0.5 μM TG in a nominally Ca^{2+}-free solution, and 1.8 mM Ca^{2+} was added later to reveal store-operated Ca^{2+} influx. However, no change was found in *mtrp4*-transfected cells as compared with the control untransfected cells (results not shown). Thus it is unlikely that expression of mTrp4 in HEK-293 cells is associated with an increase in CCE.

Expression of mTrp4 in HEK-293 cells leads to an increase in Kir whole-cell currents

To test whether mTrp4 expression enhances store-operated cation conductance, we performed whole-cell voltage clamp experiments for the Trp4 cell line, T4-60. Some spontaneous endogenous currents occurred in both control and Trp4 cells and they were prevented by using gluconate instead of Cl^- as the main anion in the bath and using Cs^+ instead of K^+ as the main cation in the pipette solution. Under basal conditions and in an external solution containing 140 mM Na^+, currents were very small at all potentials, as revealed by a voltage-ramp protocol. However, when the Na^+ was replaced by K^+, a significantly larger inward current developed in the Trp4 cells than in control cells at nearly all negative potentials (Figure 2A). The currents were inwardly rectifying and did not inactivate within a period of 384 ms, as shown by a step-pulse protocol (Figure 2B). The K^+ specific current was readily observed when as little as 5 mM K^+ was present in the bath solution (Figure 2C). The reversal potentials under different extracellular K^+ concentrations ($[K^+]_o$) were determined using an internal solution containing 140 mM KCl. The results agreed well with the prediction by the Nernst equation taking K^+ as the sole charge carrier (Figure 2D). Also, the current amplitude was dependent on $[K^+]_o$, following a relationship that g/g_{max} (the fraction of maximal conductance) is proportional to the square root of $[K^+]_o$ (Figure 2E). This relationship has been documented for native and cloned Kir channels [25,26]. Therefore, the expression of Trp4 has led to an increased Kir channel activity in HEK-293 cells.

In order to rule out the possibility that the increase in Kir activity was unique to T4-60 cells, we measured the K^+-selective currents in four other cell lines that constitutively expressed mTrp4 and an inducible cell line after the expression of mTrp4 was induced by 2 μM ponasterone A for 24–48 h. About 2–4-fold significant increase in K^+ conductance at −80 mV was found in all cell lines (Table 1). For the inducible cell line, ponasterone A treatment caused a 2-fold increase in the K^+ current at −80 mV as compared with the uninduced cells, which had the same low level of Kir activity as the untransfected control cells. The K^+-selective currents were also measured in cells transiently expressing mTrp4 and the enhanced green fluorescence protein. These cells also showed a 2-fold increase of Kir activity over control cells (Table 1). Therefore, the increased Kir activity appears to result from the expression of mTrp4, but not a random selection of cell lines.

In contrast with the Trp4-expressing cells, cells expressing Trp1, Trp3 or Trp6 did not show significant increase in K^+-selective currents (Table 1), indicating that the enhancement of Kir activity is not common to the expression of Trps but rather is unique to that of Trp4.

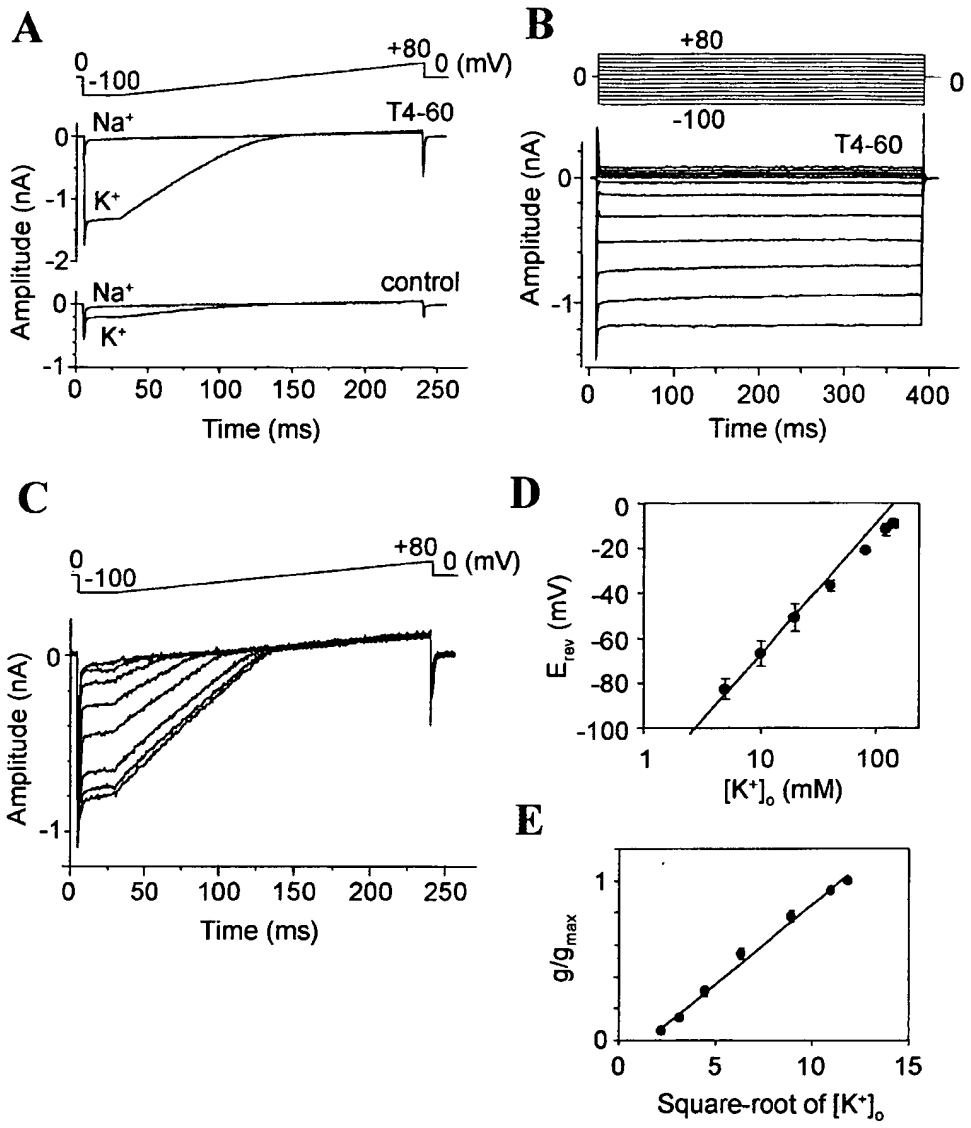

Figure 2 Inwardly rectifying whole-cell K^+ currents in T4-60 cells

(**A**) A voltage ramp to +80 mV after a brief (25 ms) step to −100 mV from holding potential at 0 mV revealed inwardly rectifying currents in T4-60 cells (upper) only in 140 mM potassium gluconate, but not sodium gluconate, bath solution. Non-transfected HEK-293 cells (control) had much smaller K^+ currents (lower). (**B**) Series of voltage steps (−100 mV to 80 mV in 15 mV increments) from 0 mV showed no current inactivation during the 384 ms pulses. (**C**) Effect of $[K^+]_o$ on current sizes and reversal potentials of the inwardly rectifying currents in T4-60 cells. 140 mM KCl was used in the pipette solution in place of CsCl, which was used in all other measurements. $[K^+]_o$ used are from the top to the bottom trace 0, 5, 10, 20, 40, 80, 120 and 140 mM. The solutions were prepared by substituting potassium gluconate with equal concentrations of sodium gluconate and were applied through perfusion. Recordings were made as in (**A**). (**D**) Reversal potential versus log $[K^+]_o$. Currents recorded in 140 mM sodium gluconate were subtracted from all traces, and zero current potential was determined. Data are averages ± range of results obtained from two cells. The continuous line shows the prediction by Nernst equation:

$E_K = 2.303 \cdot [(RT)/F] \cdot \log([K]_o/[K]_i)$

where R (= 8.315 $JK^{-1} \cdot mol^{-1}$) is the gas constant, T (= 295.16 K) is the room temperature, F (= 96480 $C \cdot mol^{-1}$) is the Faraday's constant and E_K is the effect of $[K^+]_o$ on the conductance. g/g_{max} was calculated by dividing the amplitude of K^+ current at −80 mV in a given $[K^+]_o$ by that in 140 mM $[K^+]_o$. The plot shows that the conductance is approximately linear to the square root of $[K^+]_o$. Results are averages ± S.E.M. of results obtained from 10–12 cells. Points were fitted by linear regression.

Further study of the Kir currents in T4-60 cells showed that the currents were relatively insensitive to low millimolar concentration of Ca^{2+} and tetraethylammonium, but highly sensitive to extracellular application of low concentrations of Cs^+ and Ba^{2+} (Figure 3 and Table 2), typical features of most known Kir channels [27–29]. The size of the current was not affected by the holding potential at 60, 0 or −60 mV (not shown), indicating that its activation is not voltage-dependent.

Unlike any store-operated current or any current known to be mediated by Trp channels, the Kir currents found in *mtrp4* transfected cells did not require Ins(1,4,5)P_3 in the pipette. Furthermore, the Trp4 cells displayed similar size of the Kir

Table 1 Summary of inward K^+-selective currents at −80 mV in different HEK-293 cell lines

Whole-cell recordings were made in a bath solution containing 140 mM potassium gluconate as in Figure 2(A). T1, T3, T4 and T6 are stable cell lines expressing human Trp1, human Trp3, murine Trp4 and murine Trp6 respectively. Amplitudes for the K^+-selective currents at −80 mV were determined by subtracting the currents recorded in 140 mM Na^+ from those recorded in 140 mM K^+. For the inducible Trp4 cell line, cells were treated with either carrier only (ethanol) or 2 μM ponasterone A for 24–48 h. Results are averages ± S.E.M. for numbers of cells as indicated. $^*P < 0.0001$ different from control (transiently transfected or a stable cell line expressing a vasopressin receptor [24]); $^{**}P < 0.005$ different from the uninduced as determined by Student's *t* test.

Cell name	K^+ current at −80 mV (nA)	Number of cells
Control	−0.13 ± 0.02	45
mtrp4 transiently transfected	−0.41 ± 0.03*	19
Constitutive cell lines		
T1-28	−0.10 ± 0.02	4
T3-9	−0.11 ± 0.03	5
T4-1	−0.48 ± 0.10*	14
T4-3	−0.41 ± 0.11*	7
T4-20	−0.49 ± 0.10*	7
T4-60	−0.59 ± 0.04*	94
T4-82	−0.48 ± 0.13*	7
T6-48	−0.15 ± 0.03	20
T6-55	−0.15 ± 0.04	10
Inducible Trp4 cell line		
Uninduced	−0.14 ± 0.04	9
Induced	−0.42 ± 0.07**	9

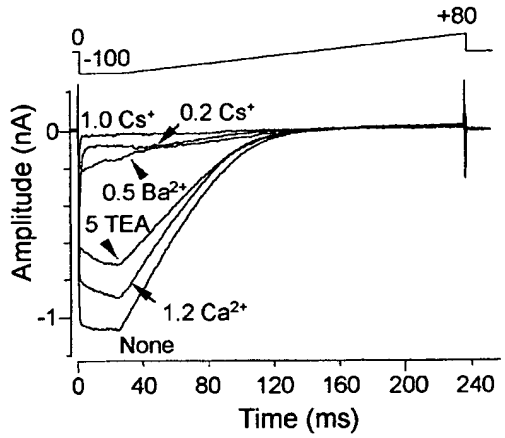

Figure 3 Sensitivity of Kir current in T4-60 cells to bath addition of Ca^{2+}, Ba^{2+}, tetraethylammonium (TEA) and Cs^+

Whole-cell recordings were made in a bath solution containing 140 mM potassium gluconate as in Figure 2(A). Inhibitory ions were applied through fast perfusion of the same solution containing ions (in mM) as indicated. The activity was allowed to recover after wash-out and before the application of the next inhibitory ion. Shown are representative traces of ionic inhibition from a typical cell. Currents recorded in 140 mM sodium gluconate were subtracted.

currents in several different pipette solutions, whether or not they contained ATP, GTP, EGTA or Mg^{2+} (results not shown).

Single-channel analysis of Kir activity in Trp4 cells

The presence of the Kir in Trp4 cells was further demonstrated in single-channel recordings of inside-out patches (Figure 4).

Table 2 Inhibition of Kir current at −80 mV in T4-60 cells by bath addition of Ca^{2+}, Ba^{2+}, tetraethylammonium (TEA^+) and Cs^+

Conditions were the same as in Figure 3. Results are averages ± S.E.M. for the numbers of cells indicated. $^{**}P < 0.0005$; $^*P < 0.0001$ different from 100% as determined by Student's *t* test.

Cation	Concn. (mM)	Inhibition (%)	Number of cells
Ca^{2+}	1.2	5 ± 2	7
Ba^{2+}	0.5	93 ± 2*	7
TEA^+	5.0	26 ± 4**	7
Cs^+	0.2	89 ± 2*	6
Cs^+	1.0	93 ± 2*	6

With transmembrane potential held at +60 mV, current activities were seen upon excision of inside-out membrane patches to an intracellular solution containing potassium. At least two conductance levels were observed for T4-60 cells. Although some patches displayed mostly single conductance as shown in Figure 4(A) for a patch having the higher amplitude and in Figure 4(D), trace i, for another patch having the lower amplitude at +60 mV, many cells showed both conducting states in the same patch (Figure 4D, trace ii). An all-point amplitude histogram analysis also indicated the presence of two conductance levels (Figure 4B). Dwell-time analysis showed that the higher conductance state had a mean open time of 3.3 ms (Figure 4C). The K^+ selectivity of the single channel was demonstrated by the observation that when Na^+ was used in the pipette, only outward currents were recorded at all membrane potentials (Figure 4E, left), whereas when K^+ was used in the pipette, both inward and outward currents were observed (Figure 4E, right). Amplitude analyses at different holding potentials for patches placed in symmetrical K^+ solutions revealed linear current–voltage relationships and slope conductance of 51 and 94 pS for the lower and the higher conducting states respectively. Therefore the channel may have a subconducting state or there may be at least two different channels. Under the same conditions, we have observed single-channel currents in two out of more than 25 patches excised from untransfected control cells. Because of the scarcity of the observation, it is difficult to determine whether the channels are the same as those seen in Trp4 cells. However, if they were the same, then the activity we saw in Trp4 cells would come from the up-regulation of endogenous Kir channels.

The linear current–voltage relationship of the Kir activities seen in inside-out patches of the Trp4 cells is in agreement with the behaviour of a typical Kir channel in this configuration. The presence of Mg^{2+} and polyamines at the cytosolic side of the plasma membrane is mainly responsible for the inwardly rectifying behaviour of Kir in whole-cell configuration [30,31]. We therefore tested the effect of Mg^{2+} and spermine on the outward single-channel current in inside-out patches. Excised patches were held at +60 mV and a potassium gluconate solution containing either 1 mM Mg^{2+} or 0.1 or 1 mM spermine was applied to the cytoplasmic side of the membrane through perfusion. In all cases, we did not observe any decrease in the P_o of the channel by Mg^{2+} (0.39 ± 0.13 and 0.56 ± 0.11 for P_o before and after the application of Mg^{2+} respectively. Average ± S.E.M., $n = 4$). In three out of the four patches, there was a small increase in P_o by Mg^{2+} (Figure 5A). On the other hand, while 0.1 mM spermine caused a small decrease in P_o, application of 1 mM spermine abolished the outward current (Figure 5B; the inhibition of P_o was 98.4 ± 0.7% for 1 mM spermine, $n = 4$).

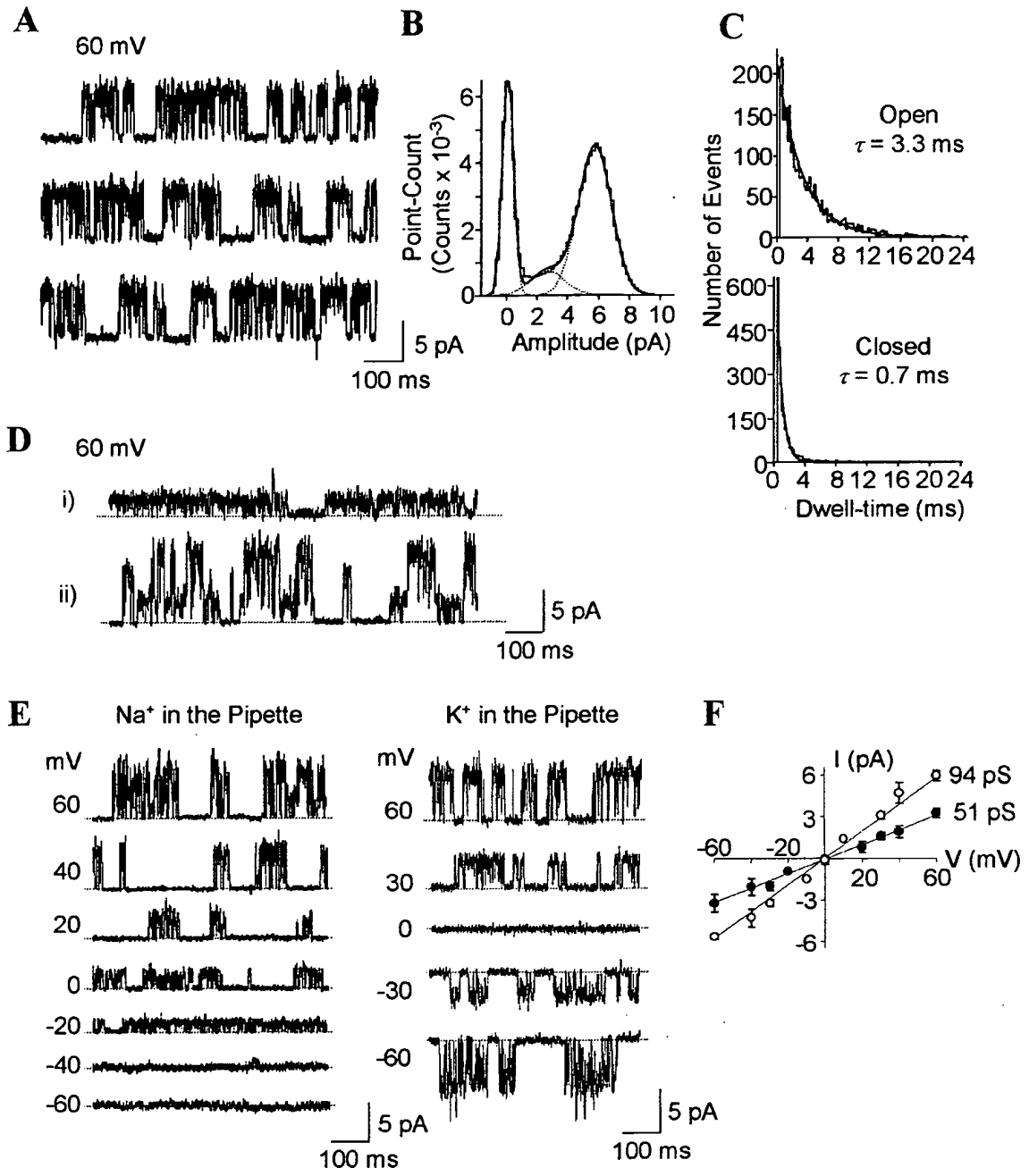

Figure 4 Single-channel Kir currents in inside-out patches excised from T4-60 cells

(**A**) Representative traces of current at +60 mV in symmetrical K^+ solutions of a patch having predominantly the higher conducting state. (**B**) An all-point amplitude histogram analysis for the same patch shown in (**A**) recorded at +60 mV for 20 s. Broken lines show the least-square fits of Gaussian function for zero and two open levels using the Simplex method. (**C**) Dwell-time analysis of open (upper) and closed (lower) states for the same record as in (**B**). Continuous curves are single exponential fits by the Simplex method. (**D**) Representative traces of currents at +60 mV of a patch having predominantly the lower conducting state (trace i) and another patch having both the higher and the lower conducting states (trace ii). (**E**) Representative traces of single-channel activity at different holding potentials recorded in Na^+ outside and K^+ inside configuration (left) or in symmetrical K^+ solutions (**A**). Broken lines indicate the closed state. (**F**) Single-channel current–voltage relationship. Results are averages ± S.E.M. for three to six patches. Points were fitted by linear regression.

DISCUSSION

In an effort to study the electrophysiological properties of heterologously expressed Trp channels, we accidentally found that there is a significant increase in Kir current in all Trp4-expressing cells. The K^+ activities are typical features of Kir channels, including a high sensitivity to extracellular application of Cs^+ and Ba^{2+} and to the intracellular block by polyamines. Because it is insensitive to intracellular application of 1 mM

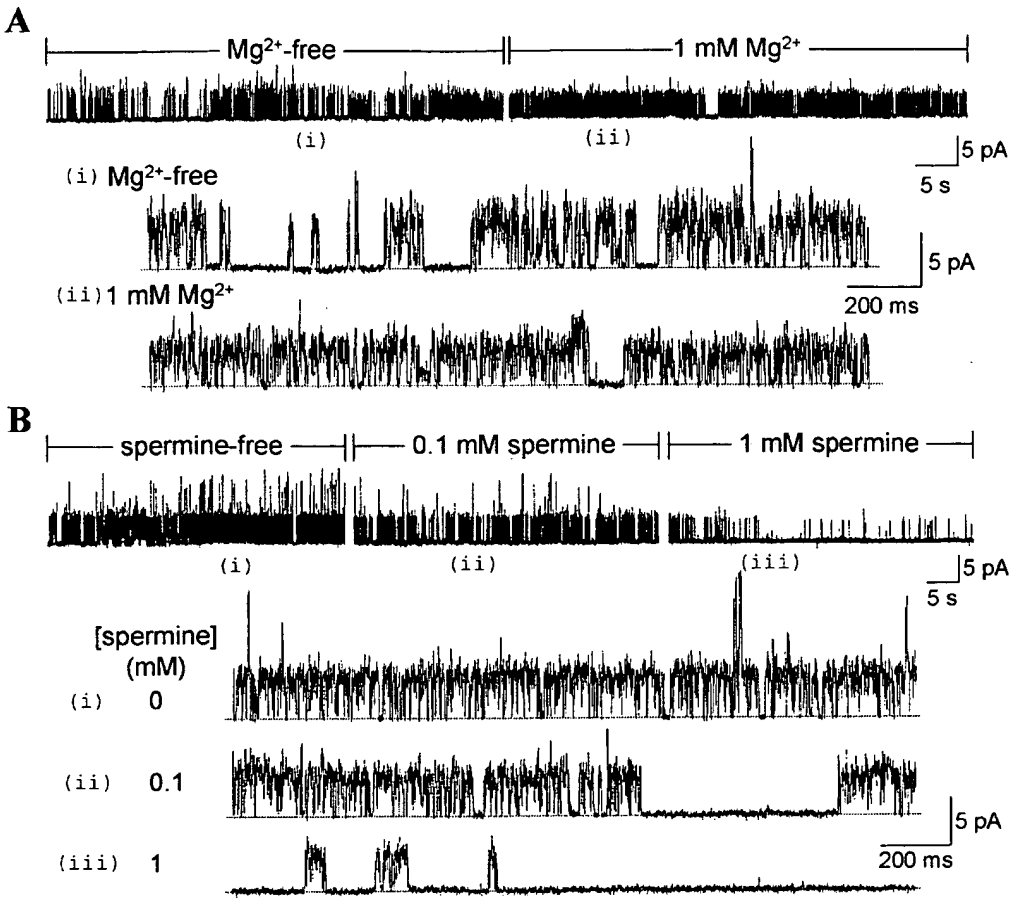

Figure 5 Effect of Mg^{2+} (A) and spermine (B) on the outward current in inside-out patches of T4-60 cells in symmetrical 140 mM K^+

Patches were held at +60 mV. $MgCl_2$ or spermine was added to the potassium gluconate internal solution and perfused to the cytoplasmic side of the inside-out patch as indicated. Upper traces show the single channel activities of the same patch before and after the addition of Mg^{2+} or spermine. Gaps indicate solution changes, which were less than 15 s. Sections marked (i), (ii) and (iii) are expanded and shown below. Broken lines indicate the closed level.

Mg^{2+} and only blocked by high concentrations of spermine, the Kir channel(s) seems to belong to the group of weakly rectifying Kir channels [32–34]. The single-channel conductance of this channel appears to be higher than that of channels formed by Kir1, Kir2 and Kir3 subfamilies [35–37], but is within the range of that of ATP-sensitive K^+ channels (KATP) [38,39].

It remains controversial whether Trp4 is involved in CCE. While two groups have demonstrated TG-stimulated Trp4 activity [8,18,20], another group showed that the channel only responded to receptor agonist but not store-depletion by TG [21]. Using Trp4-specific antibodies, we showed that mTrp4 was expressed and was localized at or near plasma membrane of the transfected HEK 293 cells. However, under the same conditions that Trp3-mediated Ca^{2+} influx was clearly revealed, we failed to detect any increase in agonist- or TG-stimulated Ca^{2+} influx. The difficulty of seeing Trp4 function in CCE was also evident in a recent study, where agonist- and TG-stimulated Ba^{2+} influx was not increased in Trp4-expressing cells [17]. Therefore, either Trp4 cannot form a Ca^{2+} influx channel by itself or its overexpression changes the homoeostasis of the transfected cells and thus alters the expression and activity of other proteins, some of which may undermine its effect on CCE. The increased Kir activity may be an example of the latter possibility. It is important to note that Kir activities are not readily noticeable in whole-cell recordings using standard external solutions that contain low or no K^+. This may be why in previous studies, the effect on Kir activity was not noticed for bovine, human, and rat Trp4 [8,17,18,20]. Moreover, the Kir may not be the only channel affected by Trp4 overexpression. Since the effect of Trp4 on Kir current was only revealed after changing the $[K^+]_o$, it is conceivable that under other specific conditions the effect of Trp4 on additional channels may be discovered.

The reason for the increased Kir activity in Trp4-expressing cells is not known. The Trp channels are structurally different from the Kir channels in that each Trp has six transmembrane segments, whereas a Kir subunit has only two, which together with an intervening P-domain form the conducting pore [32–34]. The putative pore region of Trp4 lacks the Gly-Tyr-Gly (or Gly-Phe-Gly as in the case of KATP channels) motif typically required for K^+ selectivity [34]. Therefore it is unlikely that Trp4 would form a Kir by itself. However, Trp4 might recruit and interact with endogenous Kir subunits in the HEK cells to form

a novel channel, in a manner similar to the octameric structure of KATP, which is made of four Kir (Kir6.1 or Kir6.2) subunits and four sulphonylurea receptor subunits [38,39]. The possibility that Trp4 and Kir6.x co-assemble exists because the cystic-fibrosis transmembrane conductance regulator, which forms a Cl^- channel by itself, could form a Kir with Kir6.1 [40]. Secondly, overexpression of Trp4 could have adverse effects on cellular function, and thus Kir activity may be up-regulated to overcome these effects. The increased basal influx of Na^+ [17] may lead to membrane depolarization, which Kir can correct, and hence stabilize the resting potential of the transfected cells. However, the intrinsic Ca^{2+} and Na^+ influx cannot account solely for the increase in Kir activity, because the increase was not seen in cells expressing Trp1, Trp3 and Trp6, which are partially active under basal conditions [11,24,41,42]. Therefore functions unique to Trp4 must be involved. Thirdly, it could be expected that, during the stabilization process when multiple passages were engaged to allow the selection of transformed cells, the selection pressure could favour the growth of cells with initially higher Kir activity when Trp4 was overexpressed. However, since the Kir activity was readily seen in transiently transfected cells and in induced cells that had expressed Trp4 for less than 48 h, it appears that the enhanced Kir activity is a direct response to Trp4 expression but not a result of selection of cell lines. In transiently transfected CHO cells we also observed 1.5-fold increase in K^+-selective currents in cells expressing mTrp4 (Z. Zhang and M. X. Zhu, unpublished work). Therefore the enhancement of Kir activity due to Trp4 expression is not limited to HEK-293 cells. Lastly, the transcription and/or translation of the Kir, or its regulatory subunit or activator, may be controlled by a factor that is part of Trp4-mediated signalling. Thus the activity of Trp4 may increase the expression of the Kir or the expression of other proteins that modulate the activity of the Kir.

In summary, we have demonstrated for the first time that the expression of mTrp4 in a mammalian cell line leads to increased Kir activity. This unexpected finding adds a new dimension to the studies on cellular responses modulated by Trp homologues. In addition to mediating Ca^{2+} influx, the non-selective cation channels formed by some members of the Trp family also mediate a substantial amount of Na^+ influx, and thereby initiate membrane depolarization in response to the activation of phospholipase C. By enhancing the activity of Kir, Trp4 helps to stabilize the membrane potential, opposing the depolarizing effect of other Trp proteins, but on the other hand prolonging the duration of an action potential if sufficient depolarizing force is exerted. Whether or not Trp4 itself participates in the formation of Kir channel(s) or how it affects the formation of such channels, as well as the physiological significance for the correlation between Trp4 and Kir, remain to be elucidated.

We specially thank Dr Lutz Birnbaumer (University of California, Los Angeles) for continued encouragement and intellectual as well as financial support during the cloning stages for mTpr4. We thank Dr Pappachan Kolattukudy and Dr John Enjeart for critical reading of the manuscript, Dr John Enjeart, Dr Scott Herness and Dr Diana Kunze for technical advice, and Dr Veit Flockerzi for the antiTrp4 C-terminal antibody. This work is supported in part by National Institutes of Health Grant GM54235 to M. X. Z.

REFERENCES

1 Montell, C. and Rubin, G. M. (1989) Molecular characterization of the *Drosophila trp* locus: a putative integral membrane protein required for phototransduction. Neuron **2**, 1313–1323

2 Phillips, A. M., Bull, A. and Kelly, L. E. (1992) Identification of a *Drosophila* gene encoding a calmodulin-binding protein with homology to the *trp* phototransduction gene. Neuron **8**, 631–642

3 Xu, X. Z., Chien, F., Butler, A., Salkoff, L. and Montell, C. (2000) TRPγ, a *Drosophila* TRP-related subunit, forms a regulated cation channel with TRPL. Neuron **26**, 647–657

4 Putney, Jr., J. W. (1990) Capacitative calcium entry revisited. Cell Calcium **11**, 611–624

5 Berridge, M. J. (1995) Capacitative calcium entry. Biochem. J. **312**, 1–11

6 Zhu, X., Jiang, M., Peyton, M., Boulay, G., Hurst, R., Stefani, E. and Birnbaumer, L. (1996) *trp*, a novel mammalian gene family essential for agonist-activated capacitative Ca^{2+} entry. Cell **85**, 661–671

7 Funayama, M., Goto, K. and Kondo, H. (1996) Cloning and expression localization of cDNA for rat homolog of TRP protein, apossible store-operated calcium (Ca^{2+}) channel. Mol. Brain. Res. **43**, 259–266

8 Philipp, S., Cavalie, A., Freichel, M., Wissenbach, U., Zimmer, S., Trost, C., Marquart, A., Murakami, M. and Flockerzi, V. (1996) A mammalian capacitative calcium entry channel homologous to Drosophila TRP and TRPL. EMBO J. **15**, 6166–6171

9 Boulay, G., Zhu, X., Peyton, M., Jiang, M., Hurst, R., Stefani, E. and Birnbaumer, L. (1997) Cloning and expression of a novel mammalian homolog of *Drosophila* transient receptor potential (Trp) involved in calcium entry secondary to activation of receptor coupled by the G_q class of G protein. J. Biol. Chem. **272**, 29672–29680

10 Okada, T., Inoue, R., Yamazaki, K., Maeda, A., Kurosaki, T., Yamakuni, T., Tanaka, I., Shimizu, S., Ikenaka, K., Imoto, K. and Mori, Y. (1999) Molecular and functional characterization of a novel mouse transient receptor potential protein homologue TRP7. Ca^{2+}-permeable cation channel that is constitutively activated and enhanced by stimulation of G protein-coupled receptor. J. Biol. Chem. **274**, 27359–27370

11 Hofmann, T., Obukhov, A. G., Schaefer, M., Harteneck, C., Gudermann, T. and Schultz, G. (1999) Direct activation of human TRPC6 and TRPC3 channels by diacylglycerol. Nature (London) **397**, 259–263

12 Kiselyov, K., Xu, X., Kuo, T. H., Mozhayeva, G., Pessah, I., Mignery, G., Zhu, X., Birnbaumer, L. and Muallem, S. (1998) Functional interaction between *HTRP3* channel and IP_3 receptors. Nature (London) **396**, 478–482

13 Hofmann, T., Schaefer, M., Schultz, G. and Gudermann, T. (2000) Transient receptor potential channels as molecular substrates of receptor-mediated cation entry. J. Mol. Med. **78**, 14–25

14 Zhu, X. and Birnbaumer, L. (1998) Calcium channels formed by mammalian TRP homologues. News Physiol. Sci. **13**, 211–217

15 Petersen, C. C. H., Berridge, M. J., Borgese, F. and Bennet, D. L. (1995) Putative capacitative calcium entry channels: expression of *Drosophila* trp and evidence for the existence of vertebrate homologues. Biochem. J. **311**, 41–44

16 Mori, Y., Takada, N., Okada, T., Wakamori, M., Imoto, K., Wanifuchi, H., Oka, H., Oba, A., Ikenaka, K. and Kurosaki, T. (1998) Differential distribution of TRP Ca^{2+} channel isoforms in mouse brain. Neuroreport **9**, 507–515

17 McKay, R. R., Szymeczek-Seay, C. L., Lievremont, J.-P., Bird, G. St. J., Zitt, C., Jüngling, E., Lückhoff, A. and Putney, Jr., J. W. (2000) Cloning and expression of the human transient receptor potential 4 (TRP4) gene: localization and functional expression of human TRP4 and TRP3. Biochem. J. **351**, 735–746

18 Warnat, J., Philipp, S., Zimmer, S., Flockerzi, V. and Cavalie, A. (1999) Phenotype of a recombinant store-operated channel: highly selective permeation of Ca^{2+}. J. Physiol. **518**, 631–638

19 Philipp, S., Trost, C., Warnat, J., Rautmann, J., Himmerkus, N., Schroth, G., Kretz, O., Nastainczyk, W., Cavalie, A., Hoth, M. and Flockerzi, V. (2000) TRP4 (CCE1) protein is part of native calcium release-activated Ca^{2+}-like channels in adrenal cells. J. Biol. Chem. **275**, 23965–23972

20 Tomita, Y., Kaneko, S., Funayama, M., Kondo, H., Satoh, M. and Akaike, A. (1998) Intracellular Ca^{2+} store-operated influx of Ca^{2+} through TRP-R, a rat homolog of TRP, expressed in *Xenopus* oocytes. Neurosci. Lett. **248**, 195–198

21 Schaefer, M., Plant, T. D., Obukhov, A. G., Hofmann, T., Gudermann, T. and Schultz, G. (2000) Receptor-mediated regulation of the nonselective cation channels TRPC4 and TRPC5. J. Biol. Chem. **275**, 17517–17526

22 Zhang, Z. and Zhu, M. X. (1999) Appearance of an inwardly rectifying potassium current in stable HEK 293 cell lines expressing murine Trp4. Biophys. J. **76**, A210, (abstr. M-Pos330)

23 Tang, Y., Tang, J., Chen, Z., Trost, C., Flockerzi, V., Li, M., Ramesh, V. and Zhu, M. X. (2000) Association of mammalian Trp4 and phospholipase C isozymes with a PDZ domain protein, NHERF. J. Biol. Chem. **275**, 37559–37564

24 Zhu, X., Jiang, M. and Birnbaumer, L. (1998) Receptor-activated Ca^{2+} influx via human Trp3 stably expressed in HEK293 cells: evidence for a non-capacitative Ca^{2+} entry. J. Biol. Chem. **273**, 133–142

25 Kubo, Y., Reuveny, E., Slesinger, PA., Jan, Y. N. and Jan, L. Y. (1993) Primary structure and functional expression of a rat G-protein-coupled muscarinic potassium channel. Nature (London) **364**, 802–806

26 Wischmeyer, E., Lentes, K. U. and Karschin, A. (1995) Physiological and molecular characterization of an IRK-type inward rectifier K^+ channel in a tumour mast cell line. Pflügers Arch. **429**, 809–819

27 Hagiwara, S., Miyazaki, S. and Rosenthal, N. P. (1976) Potassium current and the effect of cesium on this current during anomalous rectification of the egg cell membrane of a starfish. J. Gen. Physiol. **67**, 621–638
28 Hagiwara, S., Miyazaki, S., Moody, W. and Patlak, J. (1978) Blocking effects of barium and hydrogen ions on the potassium current during anomalous rectification in the starfish egg. J. Physiol. (London) **279**, 167–185
29 Loffler, K. and Hunter, M. (1997) Cation permeation and blockade of ROMK1, a cloned renal potassium channel. Pflügers Arch. **434**, 151–158
30 Kubo, Y. (1996) Two aspects of the inward rectification mechanism. Effects of cytoplasmic blockers and extracellular K^+ on the inward rectifier K^+ channel. Jpn. Heart J. **37**, 631–641
31 Williams, K. (1997) Interactions of polyamines with ion channels. Biochem. J. **325**, 289–297
32 Nichols, C. G. and Lopatin, A. N. (1997) Inward rectifier potassium channels. Annu. Rev. Physiol. **59**, 171–191
33 Jan, L. Y. and Jan, Y. N. (1997) Voltage-gated and inwardly rectifying potassium channels. J. Physiol. (London) **505**, 267–282
34 Isomoto, S., Kondo, C. and Kurachi, Y. (1997) Inwardly rectifying potassium channels: their molecular heterogeneity and function. Jpn. J. Physiol. **47**, 11–39
35 Lu, Z. and MacKinnon, R. (1994) A conductance maximum observed in an inward-rectifier potassium channel. J. Gen. Physiol. **104**, 477–486
36 Doupnik, C. A., Davidson, N. and Lester, H. A. (1995) The inward rectifier potassium channel family. Curr. Opin. Neurobiol. **5**, 268–277
37 Dascal, N. (1997) Signalling via the G protein-activated K^+ channels. Cell Signalling **9**, 551–573
38 Isomoto, S. and Kurachi, Y. (1997) Function, regulation, pharmacology, and molecular structure of ATP-sensitive K^+ channels in the cardiovascular system. J. Cardiovasc. Electrophysiol. **8**, 1431–1446
39 Aguilar-Bryan, L., Clement, J. P. 4th, Gonzalez, G., Kunjilwar, K., Babenko, A. and Bryan, J. (1998) Toward understanding the assembly and structure of K_{ATP} channels. Physiol. Rev. **78**, 227–245
40 Ishida-Takahashi, A., Otani, H., Takahashi, C., Washizuka, T., Tsuji, K., Noda, M., Horie, M. and Sasayama, S. (1998) Cystic fibrosis transmembrane conductance regulator mediates sulphonylurea block of the inwardly rectifying K^+ channel Kir6.1. J. Physiol. (London) **508**, 23–30
41 Sinkins, W. G., Estacion, M. and Schilling, W. P. (1998) Functional expression of TrpC1: a human homologue of the *Drosophila* Trp channel. Biochem. J. **331**, 331–339
42 Hurst, R. S., Zhu, X., Boulay, G., Birnbaumer, L. and Stefani, E. (1998) Ionic currents underlying hTRP3 mediated agonist-dependent Ca^{2+} influx in stably transfected HEK293 cells. FEBS Lett. **422**, 333–338

Received 5 October 2000/4 December 2000; accepted 17 January 2001